The
THEORY, CONSTRUCTION, AND FIELD USE
of a
DIRECT CURRENT POTENTIOMETER
for
MEASURING EARTH RESISTIVITY

by

Russell Carter Doolittle

Thesis Submitted in Partial Fulfilment of the
Requirements for the Master of Science Degree

Division of Geological Sciences
California Institute of Technology
Pasadena, California

June 1, 1940

CONTENTS

CONTENTS

continued

TABLES

I

Abstract

The fundamental theory underlying direct current methods of measuring "apparent" earth resistivity and of interpreting these field measurements to obtain the actual resistivities of the parts of a composite earth is extensively reviewed. The three main types of apparatus used in making the field measurements, the Gish-Rooney, "Megger", and "porous pot" instruments are briefly outlined. Considerations involved in making a general design for a "porous pot" outfit are briefly discussed, and a detailed description of the apparatus used by the writer is given. Field data obtained with this apparatus is interpreted by the several methods discussed in the literature.

Acknowledgements

The subject of this thesis was suggested by Dr. R. A. Peterson of the California Institute Division of Geological Sciences, whose supervision and helpful suggestions have been of great value. Funds for buying parts for the apparatus and for paying field expenses were kindly furnished by the Division of Geological Sciences together with the use of its 1931 Ford station wagon. The Institute Physics Department allowed the use of electrical instruments borrowed from its stock room which afforded a considerable saving of expense. The writer is grateful that his problem and that of Martin Eichelberger required in part the use of the same equipment as the energy and skill of the latter were invaluable in assembling the battery and potentiometer units, constructing an amplifier, and cooperating in some of the field tests. Mr. R. W. Lohman of South Pasadena generously suggested the location of the test near Sierra Madre and upon its completion allowed the writer to compare results with some he had previously obtained. Permission to run the profile at the point suggested on the Hastings Ranch was kindly given by Mr. Christy, and the carrying out of field operations was made possible through the assistance of Messrs. Wm. Bonell, Robert Hull, and Wm. Morris. The second test made near Delano, Cal. was suggested by Dr. Peterson

and carried out with the assistance of Mr. Eichelberger. The United Geophysical Company kindly allowed the use of a truck and cable in the field. Dr. Maxson of the Institute Geology Department spent a day in the field outlining the work at Victorville which was financed by the department and carried out with the help of Dr. Robert Dreyer and Mr. Ellis Roberts. Finally, the writer is greatly indebted to Dr. Potapenko for valuable advice and criticism, especially on interpreting field curves with the Paletca method.

TABLE I

Some Resistivities of Common Rocks and Rock Materials

This table indicates the wide range of resistivities commonly found for different rock types, and for the same rock type under different conditions by different observers. It is by no means complete and in most cases is of value only in suggesting the order of magnitude to be expected. The values are taken from the following sources:

(a) Eve and Keys, Applied Geophysics, 2nd. edition, p. 94, Table I. Taken from Ambronn-Lehrbuch der Angewandten Geophysik p. 110; Sundberg, Lundberg, and Eklund--Electrical Prospecting in Sweden pp. 11-12; Gutenberg-Lehrbuch der Geophysik p. 571

(b) Eve and Keys, Loc. Cit. Footnote--Taken from Koenigsberger, AIME Tech. Paper #125, 1928

(c) Sherwin Kelley--A Uniform Expression for Resistivity AIME Geophysical Prospecting, 1932, p. 142.

(d) Karl Sundberg--Effect of Impregnating Waters on Electrical Conductivity of Soils and Rocks, AIME Geophysical Prospecting, 1932, p. 388.

(e) Potapenko--C.I.T., Lecture in Course on Electrical Methods of Geophysical Prospecting, 1940.

(f) Edge and Laby--I.G.E.S. p. 11, Table II.

A. Electrolytes

Material	Resistivity (ohm-cm.)	Source
Surface waters:		
Areas of volcanic rocks and crystalline schists	3×10^3--5×10^4	d
Areas of younger sediments	10^3--10^4	d
Sea water	About 25	e
Salt water	25--10^3	e
Ground waters:	10^3--10^4	e
Normal (potable)	10^3--10^5	f
Areas of volcanics and schists	3×10^3--1.5×10^4	d
Areas of younger sediments	100 and greater	d
Saline (1% NaCl)	75.0	f
(5% NaCl)	15.0	f
(10% NaCl)	8.25	f
(20% NaCl)	5.10	f
Connate waters:		
Areas of younger sediments	10 and greater	d

B. Metallic Ore Minerals

Zinc blende, hematite, limonite, stibnite, wolframite	10^3--10^6	f
Zinc blende	1.5×10^8	a
Molybdenite	1--50	f

TABLE I (Cont'd)

Material	Resistivity (ohm-cm.)	Source
Chalcopyrite, bornite, chalcocite, pyrite, pyrrhotite, galena, magnetite, specular hematite	10^{-4}--1	f
Chalcopyrite	1.0	a
Pyrite	0.005--0.5	e
Pyrrhotite	0.01	a
Galena	0.003--5.0	e
Magnetite	0.6	a
Cuprite	0.2--1.0	e
Copper	1.7×10^{-6}	a
Lead	2.1×10^{-5}	a
Mercury	0.96×10^{-4}	a
Silver	1.6×10^{-6}	a

C. Dielectrics

Coal	About 10^9	e
Gypsum	10^{11}	e
Vein quartz	10^{10}--10^{12}	e
Calcites (chalk, marble)	10^6--10^{14}	e
Mica (biotite muscovite)	10^{10}--10^{15}	e
Rocksalt (mineral)	10^{17}	e
Sulphur	10^{17}--10^{18}	e
Crude oil	10^{10}--10^{18}	e

D. Ores and Rocks

Formation with about 5% sulphides	10^9	e
5% to 20%	10^6	e
20% to 50%	10^3	e
50% or more	10^2	e
Blende-galena ore (Illinois, U.S.A., dry)	1.6×10^4	a
(Illinois, U.S.A., moist)	1.5×10^3	a
(Sweden, dry)	1.3×10^3	a
(Sweden, moist)	3.0×10^2	a
Pyrite ore, dry	1.0×10^4	a
Pyrite ore, moist	6.0×10^3	a
Rocksalt (in ground)	10^6--10^7	b
Igneous rocks, gneiss, schist	2×10^7-10^6	f
Igneous rocks	10^7--10^9	e
Granite	10^9--10^{11}	a
porphyry	10^9	a
Diabase, dry	3.0×10^5	a
Diabase, moist	2.0×10^4	a
Lavas	Greater than 10^6	c
Volcanic rocks and crystalline schists	Much greater than 10^5	d
Serpentine	3.0×10^5--2×10^6	a
Sedimentary	10^4--10^6	e
Compact sandstone, quartzite, recrystallized limestone	About 10^5	f

TABLE I (Cont'd)

Material	Resistivity (ohm-cm.)	Source
Sedimentary (Cont'd)		
Shale, mudstone, sandstone, limestone, slates	10^3--5 x 10^4	f
Conglomerates	up to 1.3 x 10^5	b
Shales	up to 1.5 x 10^3	c
Sandstone	5 x 10^9--10^{11}	a
Sandstone	5.1 x 10^4--4 x 10^5	b
Sandstone (dry)	up to 10^6	c
Sandstone (moist)	3 x 10^3--4 x 10^4	c
Limestone	2.5 x 10^5--3.5 x 10^5	b
Limestone (dry)	6.8 x 10^4	a
Limestone (moist)	4.0 x 10^4	a
Normal limestone and sandstone saturated with surface waters	10^3--10^6	d
saturated with connate waters	5 x 10^2--10^3	d
Marls, clays, sands, alluvium (non arid)	50--10^4	f
Most oil sands	10^7-10^9	e
Yellow river sand 86% water	830	a
Yellow river sand 1.52% water	380	a
Yellow river sand 9.5% water	95	a
Glacial drift	5 x 10^2--4 x 10^5	c
Clay 4.4% water	1450	a
Clay 16.8% water	50	a
Clay 28.0% water	16	a
Clays and sands saturated with surface waters	4 x 10^4--4 x 10^5	d
Porous sands and clays saturated with surface waters	6 x 10^3--2 x 10^5	d
Clays and sands saturated with connate waters	2 x 10^2--4 x 10^2	d
Porous sands and clays saturated with connate waters	30--200	d
Limestone, dolomite, marl, loess saturated with surface waters	3 x 10^3--2 x 10^4	d
with connate waters	15--40	d
Garden soil, 3.3% water	1670	a
Garden soil, 17.3% water	60	a

III

Introduction

Geophysics or "physics of the earth" is a branch of science which investigates the physical properties of the earth. In its broadest sense it is concerned with the constitution and physical environment of the whole earth including the atmosphere.

In Applied Geophysics, a knowledge of local anomalies in the physical properties of the earth is used as a basis for solving geological problems. Thus variations in the earth's magnetic and gravitational fields, local differences in the speed of propagation of seismic waves, and anomalous accumulations of radioactive substances have all been measured in the search for subterranean structures geologically favorable for the accumulation of oil.

Variations in the electrical resistivity of the earth have been used to detect potable water in arid regions, and metallic ore-bodies, to locate faults, and to determine geological structure where conditions make surface geologic studies useless. The great range of resistivity in rocks is illustrated in table I.

A method for measuring the resistivity of an electrically homogeneous terrain was suggested by Wenner as early as 1915, and various methods of interpreting variations of "apparent resistivity" with electrode spacing or location have been described. The porous

pot, direct-current method of measuring apparent resistivities requires relatively simple apparatus and was chosen as most suitable for illustrating the principles of resistivity investigations to students.

This paper is divided into five parts, as follows:

1. The theory underlying direct current methods of earth resistivity investigation. Chapter IV.

2. Direct current methods of measuring earth resistivity and the principle instruments used. Chapter V.

3. Details of construction of the apparatus used. Chapter V.

4. Field use of the apparatus. Chapter VI.

5. Interpretation of the field data obtained with it. Chapter VII.

Of these parts, 1 and 2 are common knowledge, and based on the literature. Part 3 is original insofar as small changes dictated by expediency are concerned, and in part 5, methods of interpretation in common use are applied to data obtained by the writer in the field.

A large and varied literature has arisen on earth-resistivity prospecting due to its commercial application. It consists in part of a few books combining theoretical discussion with the results of experimental investigation, but mainly of short articles on special phases of the subject in several languages scattered through a great number of diverse periodicals. An extensive bibliography is included at the end of the paper.

IV

The Theory of Direct Current Methods of Measuring Earth Resistivity

The methods of measuring resistivity, and of interpreting measurements obtained in the field are based on the theory of flow of direct currents in homogeneous media, and in such special cases of ordered heterogeneity as horizontal conducting layers and regions separated by vertical faults. The following pages present a review of this theory. Definitions and fundamental concepts involved in this review are given in single-spaced type for the benefit of readers unfamiliar with the subject.

1. An electric current is now commonly accepted to be a flow of small units of matter called electrons. These have a mass of about 9.00×10^{-28} grams, a radius of about 2×10^{-13} centimeters, and a negative charge of 4.774×10^{-10} electrostatic units. A gram of electrons in close cubic piling would occupy about 7×10^{-11} cubic centimeters, and two grams at a distance of a meter would repel each other with a force of 3×10^{22} tons, a force greater than that due to gravitation in the ratio of 4.2×10^{42} to 1.[a] Electrically neutral matter is composed of positively charged neuclei surrounded by negatively charged electrons, and positive charges characterize particles of matter from which part of the normal number of electrons has been removed.

2. The force of repulsion between any two point charges is expressed by Coulomb's Law

$$F = k \frac{q_1 q_2}{r^2} \qquad (1)$$

where q_1, q_2 are the charges, r is the distance between them, and k is a constant depending on the units used. When k is unity for F in dynes and r in centimeters, the equation defines the c.g.s. unit of electrostatic charge.

(a) Jeans - Electricity and Magnetism. p. 20

If the two charges are of opposite sign, the force is attractive.

3. The force acting on an electric charge is the vector sum of forces acting due to the presence of all other charges distributed throughout space, and at every point of space a vector may be drawn indicating the direction and magnitude of the electric force which a unit positive charge would experience if it were placed at that point without changing the pre-existing charge distribution. This force is called the electric intensity and is represented by the vector $\bar{E}$.

4. A quantity useful in solving problems of electrostatics and of steady current flow is the potential which is defined as the work required to bring a unit positive charge to a point in space by any path, against the forces exerted on it by the other charges in the field. For a given charge distribution the potential varies only with the location of the point and each point in Euclidian space is characterized by a single value of potential. The potential is defined as zero at an infinite distance from a charge. Points having the same potential lie on equipotential surfaces and no work is required to move a charge from one point on an equipotential surface to another. The gradient of this scalar potential field is a vector field giving the magnitude and direction of fastest increase of potential and this direction is perpendicular to the equipotential surfaces.

5. A charge at a point of given potential is acted upon by a force directed toward points of lower potential, and if the charge is free to move it will take a path normal to the equipotential surfaces so that the direction of the lines of force (or line of flow if motion takes place) is opposite to that of the gradient. Thus the electric intensity at any point is the negative of the gradient of the potential at the point, or in vector notation

$$\bar{E} = -\nabla \bar{V} \qquad (2)$$

Electromotive force is a force which produces an electric current and is measured in terms of the potential difference of points between which the current flows. The volt is that potential difference against which one joule of work is done in the transfer of one coulomb. $\bar{E}$ is commonly expressed in volts per centimeter.

6. The quantity of the c.g.s. unit of electric charge is derived from equation (1), but the practical unit of electric charge is the coulomb, and is defined as the quantity of electricity required to liberate .001118 grams of silver from a solution of silver nitrate according to certain specifications. A coulomb is equal to 3.0×10^9 e.s.u. and each is made up of an integral multiple of the charge on a single electron. The practical unit of current, the ampere, is a flow of

one coulomb per second, and corresponds to the motion of 6.3×10^{18} electrons per second.

7. The direction of the electric current is taken by convention to be opposite to the motion of electrons and corresponds to the direction of motion of equivalent positive charges. At any point in space the motion of electrons will be in a given direction and the current will be in the opposite direction. The current is a vector quantity having direction and magnitude, and if at any point a coordinate system is set up it can be resolved into components parallel to the coordinate axes. The direction of the current is normal to the plane through which the greatest number of electrons pass at a given point, and the current density is a vector quantity in the direction of the current with magnitude equal to the number of amperes which pass through unit cross section area; e.g. the number of coulombs which pass through a square centimeter in a second. The relation between current and current density is expressed by the equation

$$I = \int \bar{i} \cdot d\bar{s} = \int i \cos(n,i)\, ds \qquad (3)$$

where I is the current, $\bar{i}$ the current density of magnitude i, and (n,i) the angle between the direction of the current density and the normal to the surface through which the current flow is taken.

8. Electric currents will flow only through electric circuits. Electrons travel in closed paths, from points of one potential to those of lower potential, and back to the original point, the electrical energy required to reach the original points of higher potential being furnished by chemical or other means. An electron will be driven by an applied electromotive force to a point in a solid conductor only when other electrons formerly at that point have been driven to yet another point by the same force.

9. A conductor is a body through which motion of electrons can take place. A dielectric is a substance through which no motion of electrons is possible. In nature, all materials will permit some flow of electrons if under a sufficiently large electric intensity so that in practice, distinction is between good conductors and poor, rather than between conductors and dielectrics.

10. A line of flow is a line drawn in a conductor such that at every point it is tangent to the direction of the current at that point. A tube of flow is a tubular region of infinitely small cross-section bounded by lines of flow. No current can cross the boundaries of a tube of flow, and the aggregate current flowing across all sections of the tube is constant, and a measure of the strength of the tube of flow.

11. Resistance is the property of conductors, depending upon their dimensions, materials, and temperature, which determines the current produced by a given difference of potential. The practical unit of resistance, the ohm, is that resistance through which a difference of potential of one volt will produce a current of one ampere. It is defined by the Ohm's Law equation:

$$R = E/I \qquad (4)$$

R is in ohms when E is in volts, I in amperes. Conductance is the reciprocal of resistance and is expressed by the reciprocal of the same equation and is measured in mhos for E in volts and I in amperes. In linear conductors the resistance is proportional directly to the length and inversely to the cross section of the conductor.

$$R = \rho L/A \qquad (5)$$

and this equation defines the resistivity as resistance of a body of unit cross section and unit length at 0°C.

$$\rho = RA/L \qquad (5a)$$

When R is in ohms, A in square centimeters, and L in centimeters, ρ is expressed in ohm-centimeters. Other units in use are the ohm-meter equal to 100 ohm-centimeters, and the ohm-foot equal to 30.48 ohm-centimeters. Conductivity, σ, is the reciprocal of resistivity. A three dimensional body may be considered as made up of linear conductors or tubes of flow and Ohm's Law takes the form

$$\bar{i} = \sigma \bar{E}, \text{ or } \bar{E} = \rho \bar{i} \qquad (6)$$

Derivation of the Potential Functions and Expressions for Earth Resistivity

It is not possible to measure earth resistivity directly, and it is necessary to express the resistivity in terms of measurable quantities, so that it can be computed from measurements feasible in the field.

Infinite Homogeneous Medium

We will first consider the case of an infinite, homogeneous medium of uniform resistivity ρ into which

a current I is introduced at a point source and from which the same current flows by a point sink. (Figure 1) The potential at any point other than the source or sink may be derived from the following conditions:

(1) The electricity must flow in continuous paths. This may be expressed

$$\text{div } \bar{I} = 0 \quad \text{or} \quad \nabla \cdot \bar{I} = 0 \tag{7}$$

or since $\bar{I} = \sigma \bar{E}$ and $\sigma = 1/\rho$ is constant,

$$\sigma \nabla \cdot \bar{E} = 0 \tag{8}$$

and since $\bar{E} = -\nabla V$ (2)

$$-\sigma \nabla \cdot \nabla V = 0 \quad \text{or} \quad \nabla^2 V = 0 \tag{9}$$

which is Laplace's equation.

(2) The current diverges radially from the point source and converges radially toward the point sink. The actual current density $\bar{I}$ is subject to the condition $\nabla \cdot \bar{I} = 0$, and may be considered as composed of two current densities i_1 and i_2 due to current issuing from the source, and that leaving at the sink respectively provided that

$$\nabla \cdot (\bar{I}_1 + \bar{I}_2) = \nabla \cdot \bar{I}_1 + \nabla \cdot \bar{I}_2 = 0 \tag{10}$$

This will be true provided $\nabla \cdot \bar{I}_1 = 0$ and $\nabla \cdot \bar{I}_2 = 0$. The actual potential V is the sum of potentials V_1 and V_2 which may be defined by the equations $\bar{I}_1 = -\sigma \nabla V_1$, $\bar{I}_2 = -\sigma \nabla V_2$.

(3) The potential must vanish at infinity at least as fast as $1/r$ where r is the distance from the source or sink to the point where the potential is measured.

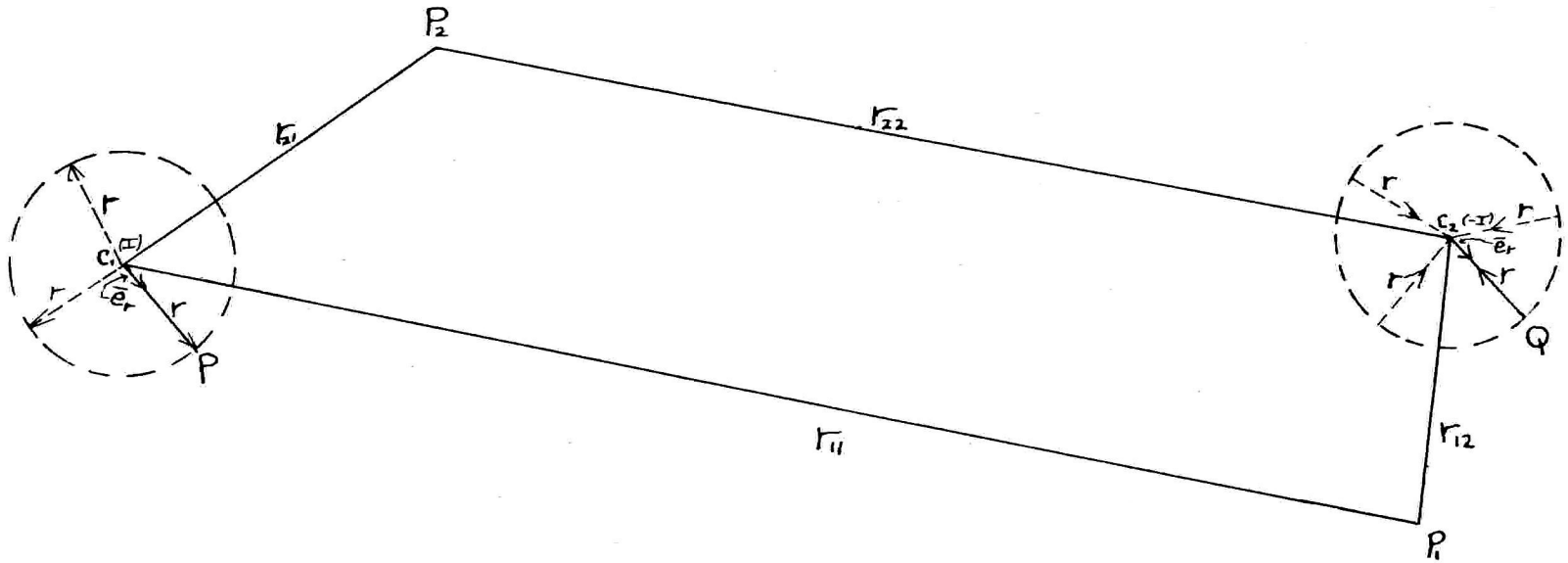

Figure 1 Diagram explaining symbols used in deriving potential in an infinite homogeneous medium

If we consider the source shown at C_1 in Figure 1 as an origin, then at a point P on a spherical surface of radius r from C_1 the current density of entering current will have a magnitude $I/4\pi r^2$ and the direction of the unit vector $\bar{e}_r$.

$$\bar{i}_1 = (I/4\pi r^2)\ \bar{e}_r \qquad (11)$$

If the sink shown as C_2 is taken as origin, the current density at a similar point Q due to leaving current will have magnitude $I/4\pi r^2$, and direction $-\bar{e}_r$.

$$\bar{i}_2 = -(I/4\pi r^2)\ \bar{e}_r \qquad (12)$$

Substituting $\bar{E}_1/\rho$ for $\bar{i}_1$ in (11), and $-\nabla V_1$ for $\bar{E}_1$, we have

$$-\nabla V_1/\rho = (I/4\pi r^2)\ \bar{e}_r \qquad (13)$$

or in spherical coordinates after multiplying through by $(-\rho)$

$$\frac{\partial V_1}{\partial r}\bar{e}_r + \frac{1}{r}\frac{\partial V_1}{\partial \theta}\bar{e}_\theta + \frac{1}{r\sin\theta}\frac{\partial V_1}{\partial \phi}\bar{e}_\phi = -\frac{\rho I}{4\pi r^2}\bar{e}_r \qquad (14)$$

From this it follows that $\frac{\partial V_1}{\partial \theta} = \frac{\partial V_1}{\partial \phi} = 0$ and equating coefficients of $\bar{e}_r$

$$\frac{\partial V_1}{\partial r} = -\frac{\rho I}{4\pi r^2} \qquad (15)$$

from which $V_1 = \rho I/4\pi r + C \qquad (16)$

Since the potential is defined to be zero as r becomes infinitely great, C = 0. By the same process,

$$V_2 = -\rho I/4\pi r \qquad (17)$$

Differentiation shows that $\nabla^2 V_1 = \nabla^2 V_2 = 0$ satisfying condition (1) so that at a point P_1, r_{11} distant from C_1 and r_{12} distant from C_2

$$V_{p_1} = \rho I/4\pi r_{11} - \rho I/4\pi r_{12} = (\rho I/4\pi)(1/r_{11} - 1/r_{12}) \qquad (18)$$

That this is the required potential is guaranteed (since it satisfies Laplace's equation and the boundary conditions) by the Uniqueness Theorem which says that two solutions of Laplace's equation that satisfy the boundary conditions can differ only by an additive constant and this can be set to zero. Similarly at P_2

$$V_{p_2} = (\rho I/4\pi)(1/r_{21} - 1/r_{22}) \qquad (19)$$

Subtracting (19) from (18) we have

$$V_{p_1} - V_{p_2} = (\rho I/4\pi)\,(1/r_{11} - 1/r_{12} - 1/r_{21} + 1/r_{22}) \qquad (20)$$

This is an expression relating the resistivity to the current, potential difference, and various distances.

Semi Infinite Medium

However, in order to gain access to points C_1, C_2, P_1 and P_2 for measurement it is necessary to consider the case of a homogeneous medium extending infinitely in all directions below a bounding plane. Above this plane we postulate a medium of infinite resistivity which is well approximated in practice by the air. If the point source and sink are located in the bounding plane, since all current enters the semi infinite medium through hemi-spherical surfaces,

$$\bar{i}_1 = (I/2\pi r^2)\,\bar{e}_r, \qquad \bar{i}_2 = -(I/2\pi r^2)\,\bar{e}_r$$

and equation (20) becomes[(a)]

$$V_{p_1} - V_{p_2} = (\rho I/2\pi)(1/r_{11} - 1/r_{12} - 1/r_{21} + 1/r_{22}) \qquad (21)$$

(a) For another derivation see Wenner, F. - U.S. Bureau of Standards Bulletin #258, 1916 - A Method of Measuring Earth Resistivity - Vol. 12, No. 4.

If we consider the points C_1, P_1, P_2, C_2 to lie on a straight line separated by equal intervals of length a, as shown in Fig. (2a), $r_{11} = a$, $r_{12} = 2a$, $r_{21} = 2a$, $r_{22} = a$, and (21) becomes

$$V_{p_1} - V_{p_2} = (\rho I/2\pi)(1/a - 1/2a - 1/2a + 1/a)$$
$$= (\rho I/2\pi)(1/a) = \rho I/2\pi a \qquad (22)$$

This is Wenner's Formula, and when solved for the resistivity takes the form

$$\rho = 2\pi a\,(V_{p_1} - V_{p_2})/I = 2\pi aE/I = 2\pi aR \qquad (22a)$$

where a, $V_{p_1} - V_{p_2}$, and I are all measurable and in practice C_1 is the current anode, C_2 the current cathode, and points P_1, P_2 are occupied by potential electrodes. In the Lee-Partition method, (Fig. 2b) a third potential electrode P_3 is inserted half way between P_1 and P_2 so that

$$V_{p_1} - V_{p_3} = (\rho I/2\pi)(1/a - 1/2a - 2/3a + 2/3a) = \rho I/4\pi a \qquad (23)$$

and
$$\rho = 4\pi a\,(V_{p_1} - V_{p_3})/I \qquad (23a)$$

and similarly
$$\rho = 4\pi a\,(V_{p_3} - V_{p_2})/I \qquad (23b)$$

The equation for the resistivity when one of the current electrodes is moved to a great distance (single electrode probe method - Fig. 2c) may be obtained from equation (21). When $r_{11} = a$, $r_{12} = \infty$, $r_{21} = b$, $r_{22} = \infty$,

$$E = (\rho I/2\pi)(1/a - 1/2b) = \rho I(b-a)/2\pi ab \qquad (24)$$
$$\rho = 2\pi baR/(b - a) \qquad (24a)$$

It should be noted that in the above derivation ρ is assumed constant in all directions throughout the medium.

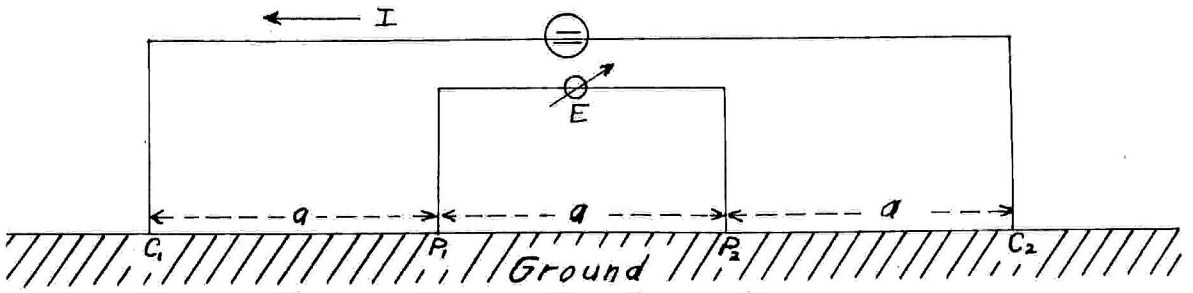

a. Wenner's Configuration

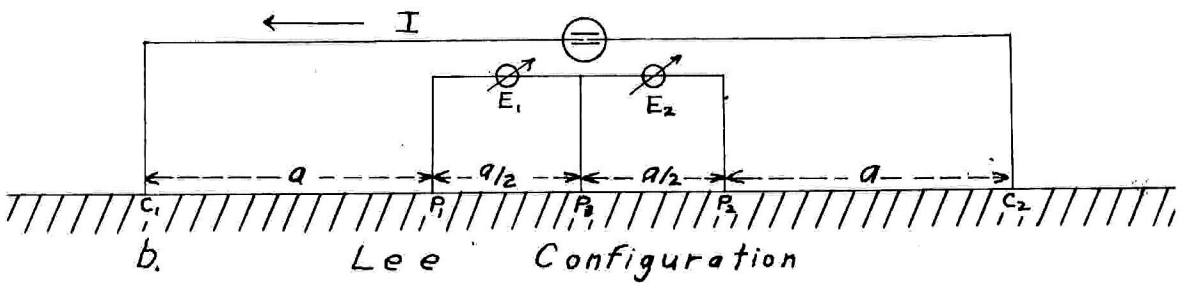

b. Lee Configuration

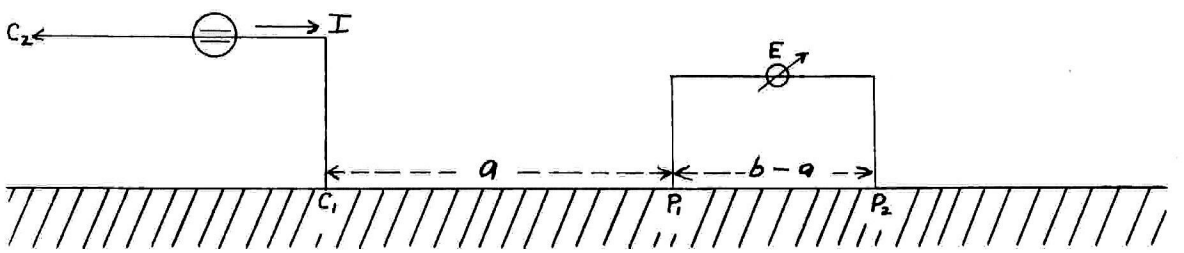

C. Single electrode Configuration

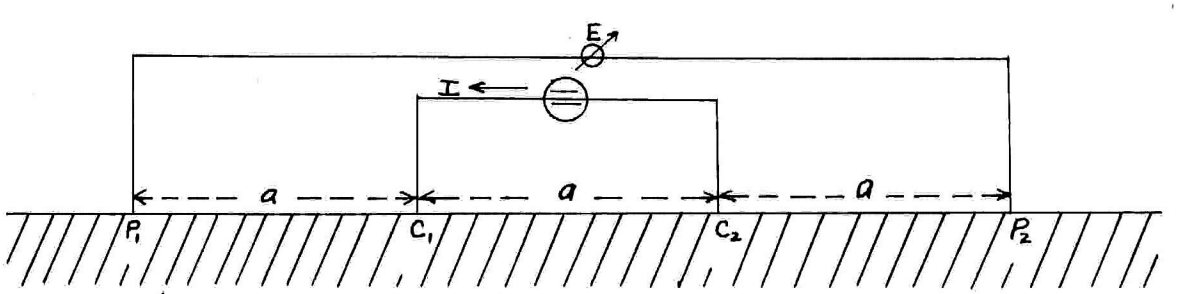

d. Inverted Wenner Configuration

Figure 2

The current and potential electrodes are assumed to be infinitely small and on the plane boundary surface between the two media, and the air is assumed to have infinite resistivity. Furthermore, it is assumed that the medium acts as a metallic conductor being unchanged by the passage of current, that no current is drawn from the potential electrodes in measuring their potential difference, and finally that no other currents or potentials than those postulated are present.

Characteristics of the Potential and Force Fields in a Semi-infinite Medium

Before considering some of the effects of variations from these assumptions which occur in field practice, it is instructive to consider certain characteristics of the potential in a semi-infinite medium.

(1) If the current and potential electrodes in the Wenner configuration are interchanged (Fig. 2d), the difference of potential for a given current between the inner electrodes is the same as would be set up between the inner electrodes by the same current in the normal configuration. This follows from Green's reciprocation theorem[a] and holds for any distribution of resistivities in space. It may be seen for homogeneous media by substituting the new values $r_{11} = a$, $r_{12} = 2a$, $r_{21} = 2a$, $r_{22} = a$ in equation (21)

$$V_{p_1} - V_{p_2} = (\rho I/2\pi)(1/a - 1/2a - 1/2a - 1/a) = \rho I/2\pi a$$

which is equation (22), so that the resistivity for both the Wenner and inverted Wenner configurations is given

(a) Jeans, Electricity and Magnetism - p. 92.
Schlumberger, C. and Schlumberger, M., A.I.M.E. Geophysical Prospecting 1932, p. 134, footnote 1.

by equation (22a).

(2) The potential can have a maximum value only at a current source, and a minimum only at a current sink, Laplace's equation prohibiting the condition for an extremum--that the second partials be all negative, or all positive. This will hold for any distribution of the resistivity in the ground as it follows from $\nabla \cdot \vec{I} = 0$ which holds for a steady current in any type of medium.

(3) It is instructive to investigate the equipotential surfaces and lines of flow in the case of a semi-infinite medium given above. The equipotential surfaces may be found by putting the expression for potential equal to a constant

$$V = (\rho I/2\pi)(1/r_1 - 1/r_2) = K \qquad (25)$$

or since $\rho I/2\pi$ is a constant,

$$1/r_1 - 1/r_2 = C \qquad (26)$$

From Figure (3) it is evident that the potential is symmetrical about the X axis, as the point P can be rotated about the axis without changing the values of r_1 or r_2, and as equipotential surfaces are therefore surfaces of revolution about the X axis, they may be visualized from their trace on the X-Z plane. The slope of the tangent to the equipotential lines is given by

$$\frac{dz}{dx} = \frac{x\left[(x-d)^2 + z^2\right]^{3/2} - (x-d)(x^2+z^2)^{3/2}}{z\left\{(x^2+z^2)^{3/2} - \left[(x-d)^2 + z^2\right]^{3/2}\right\}} \qquad (27)$$

obtained by differentiating (26a) (below) with respect to x, and for $z = 0$, and finite $x \neq 0$ or d, the lines

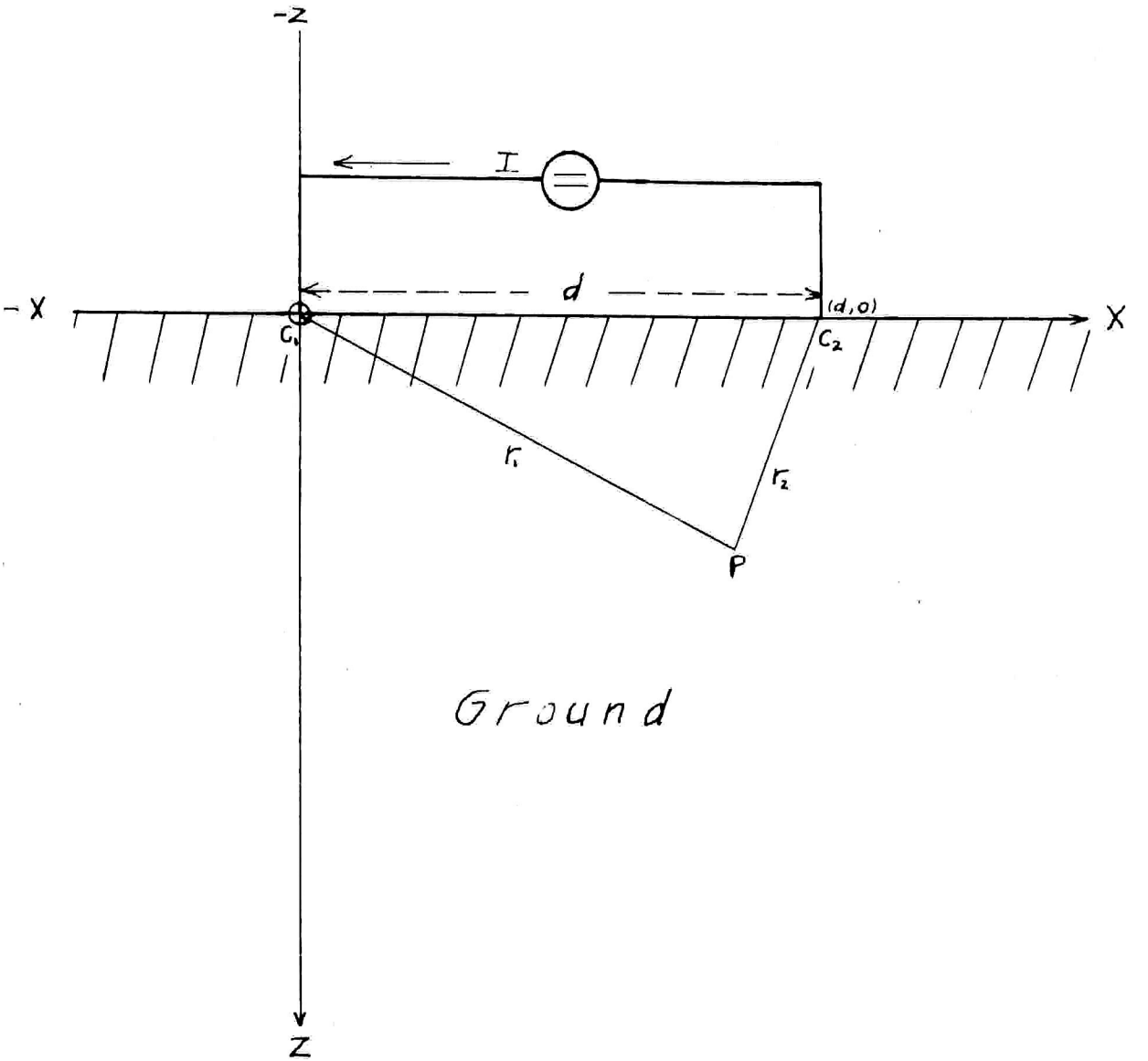

Figure 3. Diagram of symbols used in discussing potential and current distribution in a semi-infinite homogeneous medium

approach the x axis perpendicularly. The slope of the tangent to the lines of force or lines of flow at a point in the X-Z plane may be found by substituting the coordinates of the point into the equation

$$\frac{E_z}{E_x} = \frac{\frac{\partial V}{\partial z}}{\frac{\partial V}{\partial x}} = \frac{z\left\{\left[(x-d)^2+z^2\right]^{3/2} - (x^2+z^2)^{3/2}\right\}}{x\left[(x-d)^2+z^2\right]^{3/2} - (x-d)(x^2+z^2)^{3/2}} \qquad (28)$$

This shows for z = 0, and x any finite value other than 0 or d that one line of flow is along the X axis. It will be seen from a comparison of equations (27) and (28) that the lines of flow, and of equal potential are perpendicular as their slopes are negative reciprocals of each other. Figure (4) showing the nature of the equipotential lines in the X-Z plane for the case when the distance d between the source and sink was taken as 10 units is sketched from the values of C computed by substituting values for x and z in formula (26a).

$$C = 1/(x^2+z^2)^{\frac{1}{2}} - 1/\left[(x-d)^2+z^2\right]^{\frac{1}{2}} \qquad (26a)$$

The lines of force were then drawn perpendicular to the equipotential lines. From the closeness of the spacing of the equipotential contour lines one can get an impression of the spacial variation of the field strength and of the current density which is proportional to it. The distribution of current in the ground is of fundamental importance in determining depth of penetration and resolving power of resistivity methods. These problems are discussed in some detail at the end of the chapter, but a few conclusions which may be reached after an examination

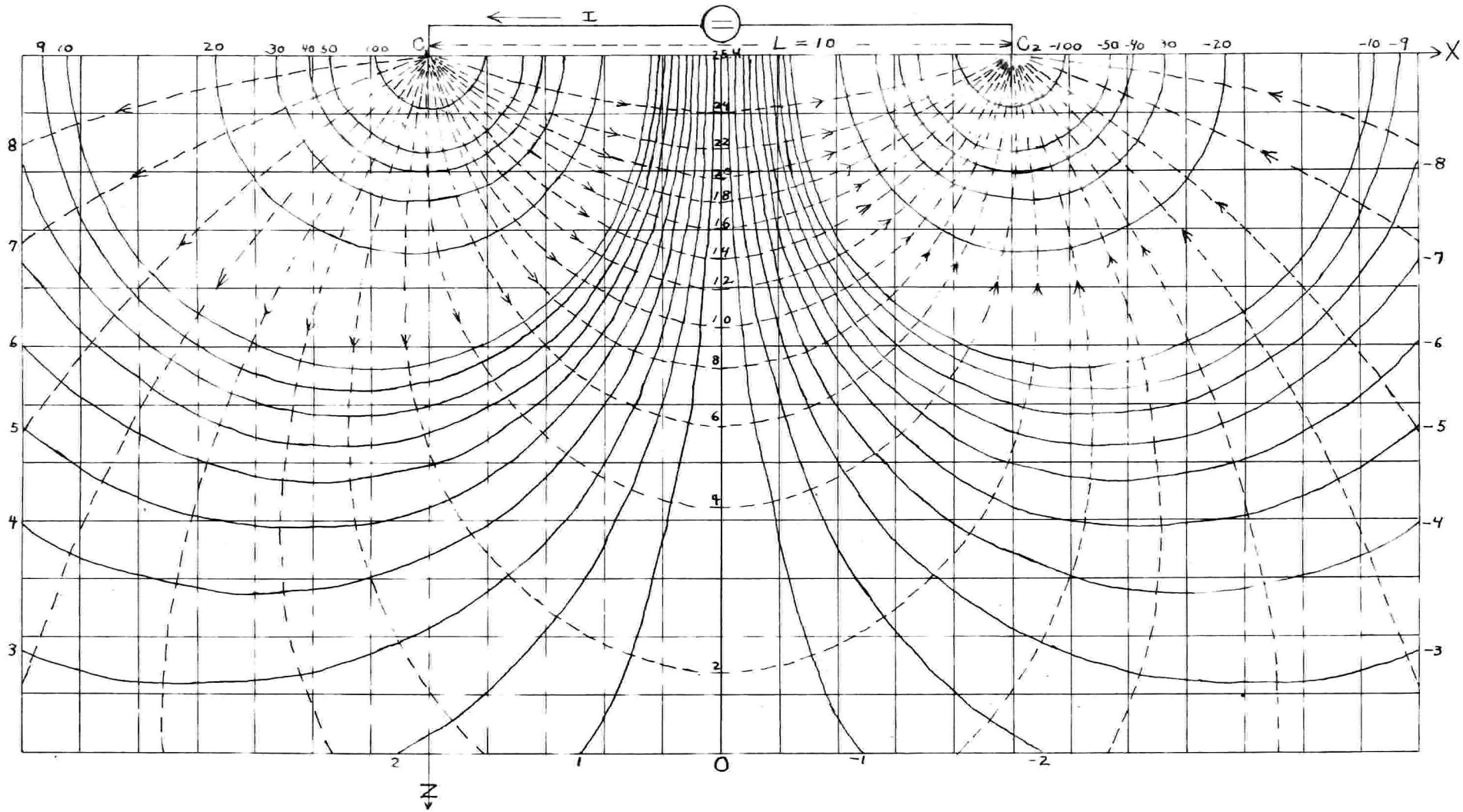

Figure 4. Current and equipotential lines in a semi-infinite homogeneous medium.

Solid line: lines of constant potential Numbers at margins give potential $V = \frac{\rho I}{2\pi}\{(X^2+Z^2)^{-\frac{1}{2}} - [(10-X)^2+Z^2]^{-\frac{1}{2}}\}$ in volts when X, Z, and L are in meters, $\rho = \pi \times 10^5$ ohm-centimeters, and $I = 0.2$ amperes.

Broken line: lines with direction of current flow. Numbers along central line of zero potential give current density through median plane $X = 5$ in microamperes per square meter for same case.

of Figure 4 may be mentioned here. First, the equipotential lines are crowded together near the current source and sink. This is one reason for not using the two-electrode method, which measures the potential and resulting current between a single pair of electrodes in the ground as the greatest part of the voltage drop for a given current takes place very near the electrodes so that the resistivity measured is that of the small region at the surface directly surrounding the current stakes. The depth of penetration is therefore negligible whatever the amount of separation of the stakes. Secondly, the field varies almost linearly along the part of the line between the current electrodes from 3/10 to 7/10 of the distance from one to the other. Placing the potential electrodes in the central 2/5 of the current spread as in the Wenner configuration is therefore desirable as it reduces the error introduced into the calculation of the resistivity when they are shifted somewhat from their normal position. If they were nearer to the current electrodes a shift in position would result in a larger difference between the measured potential difference and that which would be measured with the electrode position assumed in the resistivity formulae. It is also apparent that the field becomes rapidly uniform but very weak with increasing distance from the source and sink.

To return to the problem of experimentally determining elec rical resistivity of the ground from surface measurements, we have found that

$$\rho = 2\pi a \ E/I \qquad (22a)$$

for the Wenner configuration when it is assumed that

1. The electrodes are on a plane surface bounding the semi-infinite medium.

2. Current and potential electrodes are infinitely small.

3. The resistivity of the air is infinite.

4. ρ is constant throughout a semi-infinite medium.

5. The conduction through the medium is metallic.

6. No current is drawn from the potential electrodes in measuring their potential difference.

7. There are no potentials set up by other charge accumulations or currents.

Effect of Error in Assumptions

In practice it usually happens that none of the seven assumptions is strictly true.

(1) As it is difficult to make proper correction for topography, lines should be made as level as possible in rough country. The effect of small topographic irregularities in even country is not serious.

(2) Finite size of the electrodes is not a serious cause of error if they are small with respect to the electrode separation a. In earlier methods of interpreting

field data it was necessary to use very small electrode separations to determine the surface resistivity and much difficulty was experienced in getting reliable values, but with the now universally used superposition methods the use of small spreads is not necessary. It is common practice to water the electrodes in planting them to expedite the digging of holes, and to cut down contact resistance if the surface material is hard or dry. This increases the effective diameter of the electrodes to a foot or more, and for that reason it is desirable to have the electrode interval "a" at least ten feet.

(3) As no appreciable ionization of the air takes place, its resistivity is so great that no appreciable error is found from the fact that it is finite. It occurs in the formulae in the form

$$\frac{\rho_{air} - \rho_{earth}}{\rho_{air} + \rho_{earth}}$$

which is assumed unity. If $\rho_{air} = 1000\ \rho_{earth}$, the ratio is 999/1001 and the error is only one part in 1000.

(4) The ground is not homogeneous, and even in the simplest geological case of two rock layers such as crystalline bed rock and overburden there are commonly

irregularities in the resistivity which may take the form of several parallel layers, or be so irregular that no theoretical interpretation is possible. In non-homogeneous ground, the measured value $2\pi a\, E/I$ no longer is a true resistivity but a complexly and irregularly weighted average of the actual resistivities. It is therefore termed the apparent resistivity and denoted by ρ_a. The mathematical problem then arises of expressing the actual resistivities in terms of the measurable apparent resistivity. This has been worked out for various cases including the case of any number of parallel layers and the case of a vertical fault. The cases of two and three rock layers will be treated here as they have been quite largely used in interpretation of field data and have received much attention in the literature.

Method of Images in a Semi-Infinite Medium

Before turning to the case of two rock layers (which because of the air is a three layer physical problem) it is instructive to rework the case of the semi-infinite medium to illustrate the general method of attack. Consider all space to be divided into two regions of resistivity ρ_1 and ρ_2 respectively by a horizontal plane boundary surface (Figure 5). Take X and Y axes in the plane and a Z axis positive downward. The potential at any point in the first region is denoted by $V_1 = V_1(x_1, y_1, z_1 < 0)$, that at a point in the second region by $V_2 = V_2(x_2, y_2, z_2 > 0)$. Postulate a point current source of strength I at $C_1(0,0,z_0)$ and a corresponding sink at $C\,(x_0,0,z_0)$. The potential V_1 must now satisfy three

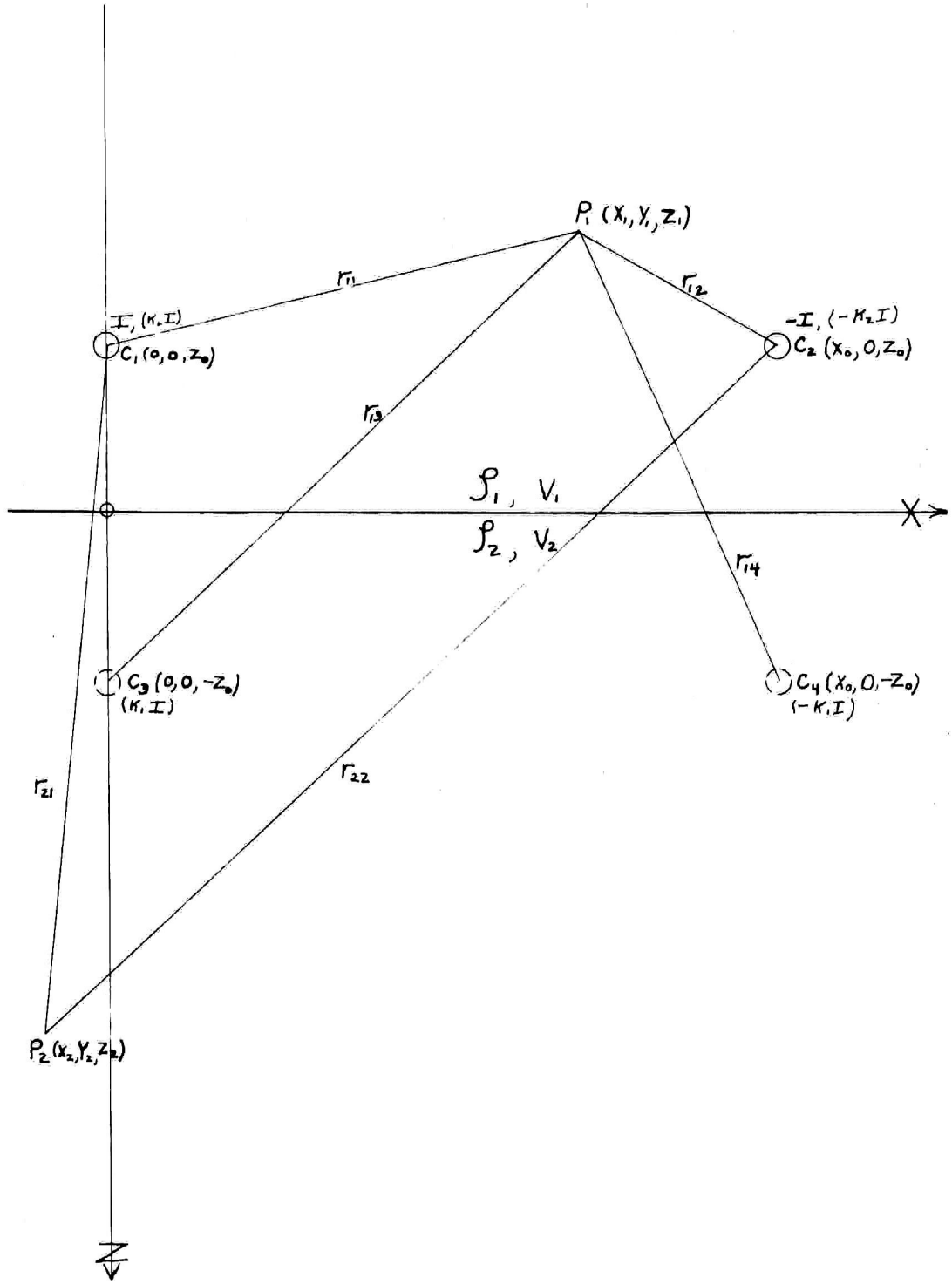

Figure 5. Diagram explaining symbols used in deriving expressions for potential and resistivity in a semi-infinite homogeneous medium by the method of images.

boundary conditions as well as Laplace's equation $\nabla^2 V_1 = 0$. These are

1. At two infinitely close points on opposite sides of the interface the potential must be the same as no finite work is done in moving electricity an infinitely small distance from one point to the other. Therefore, at $z = 0$

$$V_1 = V_2$$

2. All the current which passes through one side of unit area of the interface must emerge from the other, or at $x_1 = x_2$, $y_1 = y_2$, $z = 0$, $i_{1z} = i_{2z}$ where i_{1z} denotes the component of current density in the direction of the positive Z axis in the first medium, and i_{2z} that in the second medium(a) or

$$-\sigma_1 \frac{\partial V_1}{\partial z} = -\sigma_2 \frac{\partial V_2}{\partial z}$$

or

$$\rho_2 \frac{\partial V_1}{\partial z} = \rho_1 \frac{\partial V_2}{\partial z} \qquad \text{when } z = 0.$$

3. The potential must vanish at infinity at least as fast as $1/r$.

The problem of finding the potential which will satisfy Laplace's equation and the two boundary conditions

- -

(a)

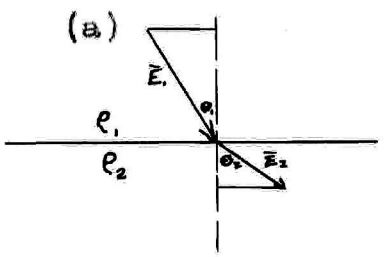

From these two laws may be derived the laws of refraction for lines of force at the interface. From (1)

$$\frac{\partial V_1}{\partial s} = \frac{\partial V_2}{\partial s}$$

where s is any direction in the boundary plane.

$$E_1 \sin\theta_1 = E_2 \sin\theta_2 \qquad (29)$$

From (2), $\rho_2 E_1 \cos\theta_1 = \rho_1 E_2 \cos\theta_2$ (30)

Dividing, $\tan\theta_1/\rho_2 = \tan\theta_2/\rho_1$ or $\tan\theta_1/\tan\theta_2 = \rho_2/\rho_1$ (31)

is solved by the method of images.(a) The material of resistivity ρ_2 is replaced by material of resistivity ρ_1, and a current source of unknown strength $k_1 I$ is placed at C_3, as far below the interface on a line C_1C_3 perpendicular to it as C_1 is above it, and a sink image of C_2 is placed similarly at C_4. The potential V_1 at any point $P_1(x_1, y_1, z_1)$ in the first region is then thought of as due to the combined currents of the real and image sources and sinks in a single infinite homogeneous medium of resistivity ρ_1. V_2 at any point $P_2(x_2, y_2, z_2)$ in the second region is thought of as due to a single source at C_1 of strength $k_2 I$ and sink at C_2 of strength $-k_2 I$ in the same infinite medium. The unknown constants k_1 and k_2 are then determined so as to satisfy the two boundary conditions, while the form of the potential is that known to satisfy Laplace's equation in a homogeneous infinite medium.

$$V_1 = (\rho_1 I/4\pi)(1/r_{11} - 1/r_{12}) + (\rho_1 k_1 I/4\pi)(1/r_{13} - 1/r_{14}) \qquad (32)$$

$$V_2 = (\rho_1 k_2 I/4\pi)(1/r_{21} - 1/r_{22}) \qquad (33)$$

or in cartesian coordinates

$$V_1 = \frac{\rho_1 I}{4\pi}\left(\frac{1}{\sqrt{x_1^2+y_1^2+(z_1-z_0)^2}} - \frac{1}{\sqrt{(x_1-x_0)^2+y_1^2+(z_1-z_0)^2}}\right) + \frac{\rho_1 k_1 I}{4\pi}\left(\frac{1}{\sqrt{x_1^2+y_1^2+(z_1+z_0)^2}} - \frac{1}{\sqrt{(x_1-x_0)^2+y_1^2+(z_1+z_0)^2}}\right) \qquad (32a)$$

$$V_2 = \frac{\rho_1 k_2 I}{4\pi}\left(\frac{1}{\sqrt{x_2^2+y_2^2+(z_2-z_0)^2}} - \frac{1}{\sqrt{(x_2-x_0)^2+y_2^2+(z_2-z_0)^2}}\right) \qquad (33a)$$

To satisfy condition 1, at $z = 0$, $V_1 = V_2$

$$(\rho_1 I/4\pi)(1 + k_1) = \rho_1 k_2 I/4\pi \quad \text{or} \quad k_2 = 1 + k_1 \qquad (34)$$

(a) See Jeans, Electricity and Magnetism p. 208.
Maxwell, Electricity and Magnetism, 2nd ed. Vol. I, pp. 228, 404.
or 3rd ed. Vol. I, p. 435.
Ehrenburg and Watson, A.I.M.E. Geophysical Prospecting, 1932, p. 420.

To satisfy the second condition differentiating $\rho_2 V_1$ and $\rho_1 V_2$ with respect to z and equating gives

$$\frac{\rho_2 \rho_1 I}{4\pi}\left[(z_1 - z_0)\left(\frac{1}{r_{12}^3} - \frac{1}{r_{11}^3}\right) + K_1 (z_1 + z_0)\left(\frac{1}{r_{14}^3} - \frac{1}{r_{13}^3}\right)\right] = \frac{\rho_1^2 K_2 I}{4\pi}(z - z_0)\left(\frac{1}{r_{22}^3} - \frac{1}{r_{21}^3}\right) \tag{35}$$

Putting $x_1 = x_2$, $y_1 = y_2$, $z_1 = z_2 = 0$, we have, since

$r_{11} = r_{13} = r_{21}$ AND $r_{12} = r_{14} = r_{22}$

$$\rho_2(K_1 - 1) = -\rho_1 K_2 \quad \text{OR} \quad K_1(\rho_2 + \rho_1) = \rho_2 - \rho_1 \quad \text{SINCE } K_2 = 1 + K_1 \tag{36}$$

so that

$$k_1 = \frac{\rho_2 - \rho_1}{\rho_2 + \rho_1} \tag{36a}$$

$$k_2 = \frac{2\rho_2}{\rho_2 + \rho_1} \tag{37}$$

For a point A in the interface,

$$V_A = \frac{2\rho_1 \rho_2}{\rho_1 + \rho_2} \frac{I}{4\pi}\left(\frac{1}{\sqrt{x_A^2 + y_A^2 + z_0^2}} - \frac{1}{\sqrt{(x_A - x_0)^2 + y_A^2 + z_0^2}}\right) \tag{38}$$

If in particular we take two points, $P_1(a,0,0,)$ and $P_2(2a,0,0,)$ and put $\rho_1 = \infty$, $z_0 = 0$, $x_0 = 3a$

$$V_{p1} - V_{p2} = (\rho_2 I/2\pi)(1/a - 1/2a - 1/2a - 1/a) = \rho_2 I/2\pi a \tag{22}$$

as found before.

METHOD OF IMAGES IN THE CASE OF TWO HORIZONTAL LAYERS

In the case of two rock layers(a) the process of finding the potential is complicated by the presence of two bounding planes, and two sets of boundary conditions, so that the image which will satisfy one set disturbs the potential at the other boundary.

In the physical case shown in Figure 6 it is convenient to take as origin of coordinates the real current source, a Z axis positive downward, and an X-Y axis parallel to the beds. The whole space is again regarded

(a) This case has been worked out using images by
Edge and Laby I.G.E.S. p. 255, 1931
Hummell - Zeitschrift fur Geophysik, Vol. 5, p. 89, 1929.
or A.I.M.E. Geophysical Prospecting, 1932, p. 400.
Lancaster-Jones--The Mining Magazine, Vol. 43, July, 1930, p. 19.

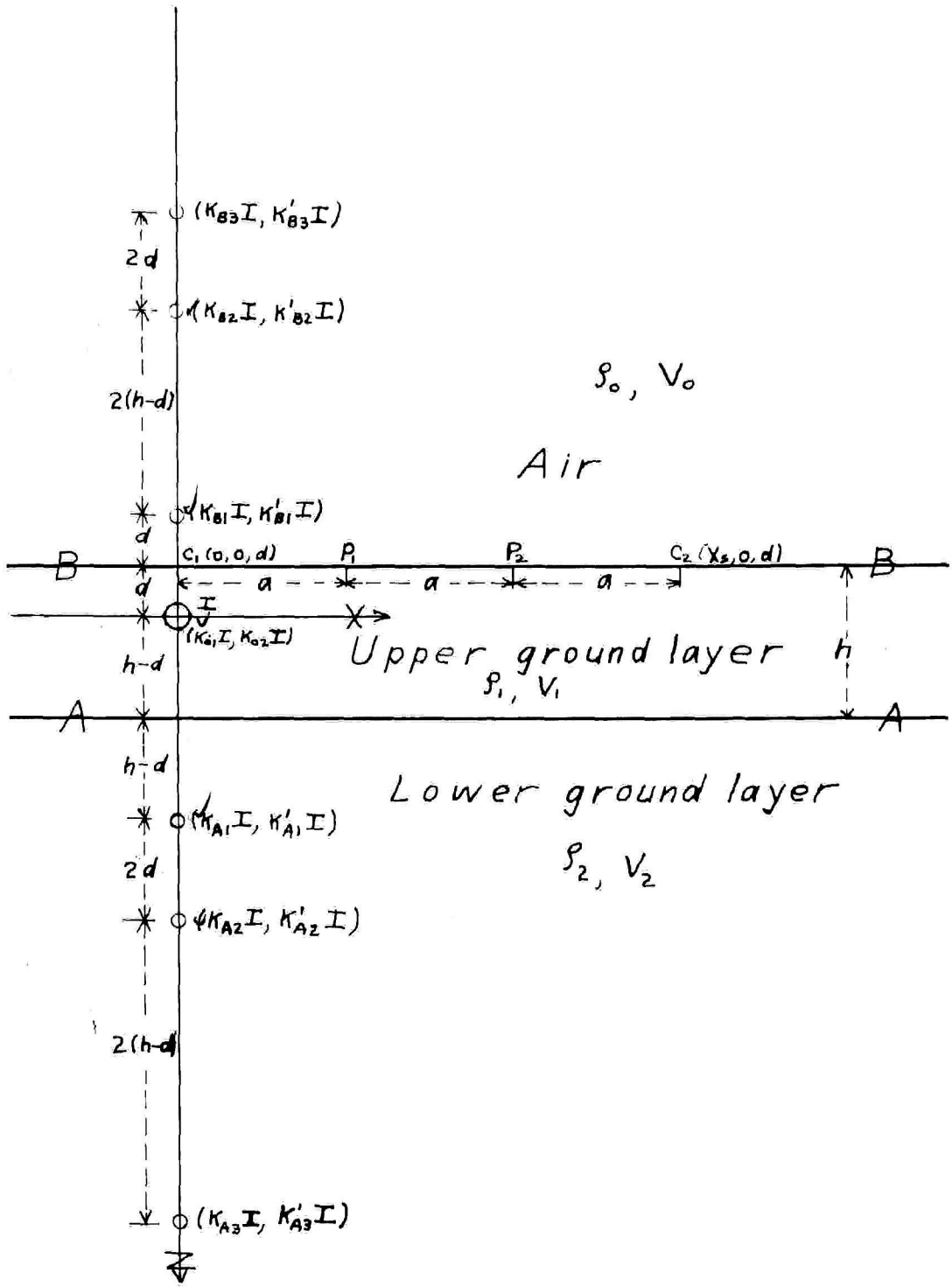

Figure 6. Diagram explaining symbols used in deriving expressions for potential and resistivity in a two-layer ground by the method of images.

as of resistivity ρ_1, and the potential is modified by a series of images to satisfy the boundary conditions.

If an image of strength $k_{A_1}I$ is placed as shown to satisfy conditions at the A boundary, and an image of $k_{B_1}I$ to satisfy the B boundary conditions, other images k_{B_2} and k_{A_2} must be used to nullify the undesired distortion of the A boundary by k_{B_1} and of the B boundary by k_{A_1}. These in turn disturb the conditions at the boundaries, and so on. The potential, however, is approximated more and more closely by successive sets of images, and is accurately given by an infinite series.

The potential in the three regions is expressed as

$$V_0 = \frac{\rho_1 I}{4\pi}\left[\frac{1}{\sqrt{x_0^2+y_0^2+z_0^2}} + \frac{K_{B_1}}{\sqrt{x_0^2+y_0^2+(z_0-2h+2d)^2}} + \frac{K_{A_2}}{\sqrt{x_0^2+y_0^2+(z_0-2h)^2}} + \cdots\right] \quad (39)$$

$$V_1 = \frac{\rho_1 I}{4\pi}\left[\frac{1}{\sqrt{x_1^2+y_1^2+z_1^2}} + \frac{K'_{A_1}}{\sqrt{x_1^2+y_1^2+(z_1-2h+2d)^2}} + \frac{K'_{A_2}}{\sqrt{x_1^2+y_1^2+(z_1-2h)^2}} + \cdots + \frac{K'_{B_1}}{\sqrt{x_1^2+y_1^2+(z_1+2d)^2}} + \frac{K'_{B_2}}{\sqrt{x_1^2+y_1^2+(z_1+2h)^2}} + \cdots\right] \quad (40)$$

$$V_2 = \frac{\rho_1 I}{4\pi}\left[\frac{K_{1_2}}{\sqrt{x_2^2+y_2^2+z_2^2}} + \frac{K_{B_1}}{\sqrt{x_2^2+y_2^2+(z_2+2d)^2}} + \frac{K_{B_2}}{\sqrt{x_2^2+y_2^2+(z_2+2h)^2}} + \cdots\right] \quad (41)$$

where x_0, y_0, z_0 are the coordinates of any point in the region of resistivity ρ_0 and the constants are chosen to satisfy the boundary conditions

1. $V_0 = V_1$
2. $\rho_1 \frac{\partial V_0}{\partial z_0} = \rho_0 \frac{\partial V_1}{\partial z_1}$

when $z_1 = z_0 = -d$, $x_1 = x_0$, $y_1 = y_0$.

3. $V_1 = V_2$
4. $\rho_2 \frac{\partial V_1}{\partial z_1} = \rho_1 \frac{\partial V_2}{\partial z_2}$

when $z_2 = z_1 = h - d$, $y_1 = y_2$, $x_1 = x_2$.

1. $$V_0 = \frac{\rho_1 I}{4\pi}\left[\frac{K_{0_1}}{\sqrt{x_0^2+y_0^2+d^2}} + \frac{K_{A_1}}{\sqrt{x_0^2+y_0^2+(d-2h)^2}} + \frac{K_{A_2}}{\sqrt{x_0^2+y_0^2+(d+2h)^2}} + \cdots\right] \quad (39a)$$

$$V_1 = \frac{\rho_1 I}{4\pi}\left[\frac{1+K'_{B_1}}{\sqrt{x_0^2+y_0^2+d^2}} + \frac{K'_{A_1}+K'_{B_2}}{\sqrt{x_0^2+y_0^2+(d-2h)^2}} + \frac{K_{A_2}}{\sqrt{x_0^2+y_0^2+(d+2h)^2}} + \cdots\right] \quad (40a)$$

Equating coefficients of like terms,

$$k_{0_1} = 1 + k'_{B_1} \qquad (41a)$$

$$k_{A_1} = k'_{A_1} + k'_{B_2} \qquad (41b)$$

$$k_{A_2} = k'_{A_2} + k'_{B_3} \qquad (41c)$$

2. $$\rho_1 \frac{\partial V_0}{\partial z_0} = \frac{\rho_1 I}{4\pi}\left[\frac{-K_{01}(-d)}{[x_0^2+y_0^2+d^2]^{3/2}} + \frac{-K_{A1}(d-2h)}{[x_0^2+y_0^2+(d-2h)^2]^{3/2}} + \frac{-K_{A_2}(-d-2h)}{[x_0^2+y_0^2+(d+2h)^2]^{3/2}} + \cdots\right] \qquad (42a)$$

$$\rho_0 \frac{\partial V_1}{\partial z_1} = \frac{\rho_0 \rho_1 I}{4\pi}\left[\frac{+d(1-K'_{01})}{[x_0^2+y_0^2+d^2]^{3/2}} + \frac{-(d-2h)(K'_{A1}-K'_{B2})}{[x_0^2+y_0^2+(d-2h)^2]^{3/2}} + \frac{-(-d-2h)(K'_{A2}-K'_{B3})}{[x_0^2+y_0^2+(d+2h)^2]^{3/2}} + \cdots\right] \qquad (43a)$$

Again equating coefficients,

$$k_{0_1} = \frac{\rho_0}{\rho_1}(1 - k'_{B_1}) \qquad (44a)$$

$$k_{A_1} = \frac{\rho_0}{\rho_1}(k'_{A_1} - k'_{B_2}) \qquad (44b)$$

$$k_{A_2} = \frac{\rho_0}{\rho_1}(k'_{A_2} - k'_{B_3}) \qquad (44c)$$

3. $$V_1 = \frac{\rho_1 I}{4\pi}\left[\frac{1+K'_{A1}}{\sqrt{x_1^2+y_1^2+(h-d)^2}} + \frac{K'_{A2}+K'_{B1}}{\sqrt{x_1^2+y_1^2+(h+d)^2}} + \frac{K'_{A3}+K'_{B2}}{\sqrt{x_1^2+y_1^2+(d-3h)^2}} + \cdots\right] \qquad (40b)$$

$$V_2 = \frac{\rho_1 I}{4\pi}\left[\frac{K_{12}}{\sqrt{x_2^2+y_2^2+(h-d)^2}} + \frac{K_{B1}}{\sqrt{x_2^2+y_2^2+(h+d)^2}} + \frac{K_{B2}}{\sqrt{x_2^2+y_2^2+(d-3h)^2}} + \cdots\right] \qquad (41a)$$

Equating coefficients,

$$k_{12} = 1 + k'_{A_1} \qquad (45a)$$

$$k_{B_1} = k'_{A_2} + k'_{B_1} \qquad (45b)$$

$$k_{B_2} = k'_{A_3} + k'_{B_2} \qquad (45c)$$

4. $$\rho_2 \frac{\partial V_1}{\partial z_1} = \frac{\rho_1 \rho_2 I}{4\pi}\left[\frac{-(h-d)(1-K'_{A1})}{[x_2^2+y_2^2+(h-d)^2]^{3/2}} + \frac{-(-h-d)(K'_{A2}-K'_{B1})}{[x_2^2+y_2^2+(h+d)^2]^{3/2}} + \frac{-(d-3h)(K'_{A3}-K'_{B2})}{[x_2^2+y_2^2+(d-3h)^2]^{3/2}} + \cdots\right] \qquad (46a)$$

$$\rho_1 \frac{\partial V_2}{\partial z_2} = \frac{\rho_1^2 I}{4\pi}\left[\frac{-(h-d)K_{12}}{[x_2^2+y_2^2+(h-d)^2]^{3/2}} + \frac{-(-h-d)(-K_{B1})}{[x_2^2+y_2^2+(h+d)^2]^{3/2}} + \frac{-(d-3h)(-K_{B2})}{[x_2^2+y_2^2+(d-3h)^2]^{3/2}} + \cdots\right] \qquad (47a)$$

Equating Coefficients,

$$k_{12} = \frac{\rho_2}{\rho_1}(1 - k'_{A_1}) \qquad (48a)$$

$$k_{B_1} = \frac{\rho_2}{\rho_1}(k'_{B_1} - k'_{A_2}) \qquad (48b)$$

$$k_{B_2} = \frac{\rho_2}{\rho_1}(k'_{B_2} - k'_{A_3}) \qquad (48c)$$

From 41a and 44a we have

$$k_{01} = \frac{2\rho_0}{\rho_0+\rho_1} \equiv k_1 + 1$$

$$k'_{B_1} = \frac{\rho_0 - \rho_1}{\rho_0 + \rho_1} \equiv k_1$$

From 41b and 44b

$$k'_{B_2} = k_1 k_2 \qquad k_{A_1} = k_2(1 + k_1)$$

From 41c and 44c

$$k'_{B_3} = k_1^2 k_2 \qquad k_{A_2} = k_2 k_1 (1 + k_1)$$

From 45a and 48a we have

$$k_{12} = \frac{2\rho_2}{\rho_1 + \rho_2} \equiv k_2 + 1$$

$$k'_{A_1} = \frac{\rho_2 - \rho_1}{\rho_2 + \rho_1} \equiv k_2$$

From 45b and 48b

$$k'_{A_2} = k_1 k_2 \qquad k_{B_1} = k_1(1 + k_2)$$

From 45c and 48c

$$k'_{A_3} = k_1 k_2^2 \qquad k_{B_2} = k_1 k_2 (1 + k_2)$$

The expressions for the potential then become

$$V_0 = \frac{\rho_1 I}{4\pi}(1+K_1)\left[\frac{1}{\sqrt{x_0^2+y_0^2+z_0^2}} + \frac{K_2}{\sqrt{x_0^2+y_0^2+(z_0-2h+2d)^2}} + \frac{K_2 K_1}{\sqrt{x_0^2+y_0^2+(z_0-2h)^2}} + \cdots\right]$$

$$V_1 = \frac{\rho_1 I}{4\pi}\left[\frac{1}{\sqrt{x_1^2+y_1^2+z_1^2}} + \frac{K_2}{\sqrt{x_1^2+y_1^2+(z_1-2h+2d)^2}} + \frac{K_1 K_2}{\sqrt{x_1^2+y_1^2+(z_1-2h)^2}} + \frac{K_1 K_2^2}{\sqrt{x_1^2+y_1^2+(z_1-4h+2d)^2}} + \right.$$

$$\left. + \frac{K_1}{\sqrt{x_1^2+y_1^2+(z_1+2d)^2}} + \frac{K_1 K_2}{\sqrt{x_1^2+y_1^2+(z_1+2h)^2}} + \frac{K_1^2 K_2}{\sqrt{x_1^2+y_1^2+(z_1+2h+2d)^2}} + \right] \qquad (39b)$$

$$V_2 = \frac{\rho_1 I}{4\pi}(1+K_2)\left[\frac{1}{\sqrt{x_2^2+y_2^2+z_2^2}} + \frac{K_1}{\sqrt{x_2^2+y_2^2+(z_2+2d)^2}} + \frac{K_1 K_2}{\sqrt{x_2^2+y_2^2+(z_2+2h)^2}} + \cdots\right] \qquad (40c)$$

These series can be summed in the form

$$V_0 = \frac{\rho_1 I}{4\pi}(1+K_1)\left\{\sum_{m=0}^{\infty}\frac{K_1^m K_2^m}{\sqrt{x_0^2+y_0^2+(z_0-2mh)^2}} + \sum_{m=1}^{\infty}\frac{K_2^m K_1^{m-1}}{\sqrt{x_0^2+y_0^2+(z_0-2mh+2d)^2}}\right\} \qquad (41b)$$

$$V_1 = \frac{\rho_1 I}{4\pi}\left\{\sum_{m=0}^{\infty}\left[\frac{K_1^m K_2^m}{\sqrt{x_1^2+y_1^2+(z_1-2mh)^2}} + \frac{K_2^m K_1^{m+1}}{\sqrt{x_1^2+y_1^2+(z_1+2mh+2d)^2}}\right]\right.$$

$$\left. + \sum_{m=1}^{\infty}\left[\frac{K_2^m K_1^{m-1}}{\sqrt{x_1^2+y_1^2+(z_1-2mh+2d)^2}} + \frac{K_2^m K_1^m}{\sqrt{x_1^2+y_1^2+(z_1+2mh)^2}}\right]\right\} \qquad (39c)$$

$$V_2 = \frac{\rho_1 I}{4\pi}(1+K_2)\sum_{m=0}^{\infty}\left[\frac{K_1^m K_2^m}{\sqrt{x_2^2+y_2^2+(z_2+2mh)^2}} + \frac{K_2^m K_1^{m+1}}{\sqrt{x_2^2+y_2^2+(z_2+2mh+2d)^2}}\right] \qquad (40d)$$

(41c)

If we now include the effect due to a sink at C_2, we must add a term of the form:

$$V_1' = \frac{-\rho_1 I}{4\pi}\left\{\sum_{m=0}^{\infty}\left[\frac{K_1^m K_2^m}{\sqrt{(x_1-x_s)^2+y_1^2+(z_1-2mh)^2}} + \frac{K_2^m K_1^{m+1}}{\sqrt{(x_1-x_s)^2+y_1^2+(z_1+2mh+2d)^2}}\right] + \sum_{m=1}^{\infty}\left[\frac{K_2^m K_1^{m-1}}{\sqrt{(x_1-x_s)^2+y_1^2+(z_1-2mh+2d)^2}} + \frac{K_1^m K_2^m}{\sqrt{(x_1-x_s)^2+y_1^2+(z_1+2mh)^2}}\right]\right\} \quad (49)$$

If we now put $\rho_0 = \infty$, d = 0, then $k_1 = +1$, and the origin moves to C_1, $k_2 = k = \frac{\rho_2-\rho_1}{\rho_2+\rho_1}$, and at a point P (a,0,0) in the B interface distant a from C_1,

$$V_{P_1} = \frac{\rho_1 I}{2\pi}\left\{\sum_{m=0}^{\infty}\frac{K^m}{\sqrt{a^2+(2mh)^2}} + \sum_{m=1}^{\infty}\frac{K^m}{\sqrt{a^2+(2mh)^2}} - \sum_{m=0}^{\infty}\frac{K^m}{\sqrt{4a^2+(2mh)^2}} - \sum_{m=1}^{\infty}\frac{K^m}{\sqrt{4a^2+(2m\frac{h}{a})^2}}\right\} \quad (50)$$

$$= \frac{\rho_1 I}{2\pi}\left\{\frac{1}{a} + 2\sum_{m=1}^{\infty}\frac{K^m}{\sqrt{a^2+(2mh)^2}} - \frac{1}{2a} - 2\sum_{m=1}^{\infty}\frac{K^m}{\sqrt{4a^2+(2mh)^2}}\right\} \quad (50a)$$

$$= \frac{\rho_1 I}{4\pi a}\left\{1 + 4\sum_{m=1}^{\infty}K^m\left[\frac{1}{\sqrt{1+(2m\frac{h}{a})^2}} - \frac{1}{\sqrt{4+(2m\frac{h}{a})^2}}\right]\right\} \quad (50b)$$

and at point P_2(2a,0,0)

$$V_{P_2} = \frac{\rho_1 I}{2\pi}\left\{\sum_{m=0}^{\infty}\frac{K^m}{\sqrt{4a^2+(2mh)^2}} + \sum_{m=1}^{\infty}\frac{K^m}{\sqrt{4a^2+(2mh)^2}} - \sum_{m=0}^{\infty}\frac{K^m}{\sqrt{a^2+(2mh)^2}} - \sum_{m=1}^{\infty}\frac{K^m}{\sqrt{a^2+(2mh)^2}}\right\} \quad (51)$$

$$= \frac{\rho_1 I}{2\pi}\left\{\frac{1}{2a} - \frac{1}{a} + 2\sum_{m=1}^{\infty}\left[\frac{K^m}{\sqrt{4a^2+(2mh)^2}} - \frac{K^m}{\sqrt{a^2+(2mh)^2}}\right]\right\} \quad (51a)$$

$$= \frac{\rho_1 I}{4\pi a}\left\{-1 - 4\sum_{m=1}^{\infty}K^m\left[\frac{1}{\sqrt{1+(2m\frac{h}{a})^2}} - \frac{1}{\sqrt{4+(2m\frac{h}{a})^2}}\right]\right\} \quad (51b)$$

$$V_{P_1} - V_{P_2} = \frac{\rho_1 I}{2\pi a}\left\{1 + 4\sum_{m=1}^{\infty}K^m\left[\frac{1}{\sqrt{1+(2m\frac{h}{a})^2}} - \frac{1}{\sqrt{4+(2m\frac{h}{a})^2}}\right]\right\} \quad (51c)$$

$$V_{p_1} - V_{p_2} = \rho_1 I/2\pi a\,(1 + 4F) \quad (51d)$$

$$\rho_a = \rho_1\,(1 + 4F) \quad (51e)$$

The series

$$\rho_a/\rho_1 = 1 + 4\sum_{m=1}^{\infty}K^m\left(\frac{1}{\sqrt{1+(2m\frac{h}{a})^2}} - \frac{1}{\sqrt{4+(2m\frac{h}{a})^2}}\right)$$

where $k = \frac{\rho_2-\rho_1}{\rho_2+\rho_1}$ converges, and has been evaluated for assumed values of h/a and k. The variation of ρ_a/ρ_1 with h/a for different values of k is used in the interpretation of field data discussed in a later section of this paper. The convergence is slow, and the evaluation(a) is tedious, so that it is instructive to consider an

(a) Roman--U.S. Bureau of Mines, Tech, Paper #502, 1931

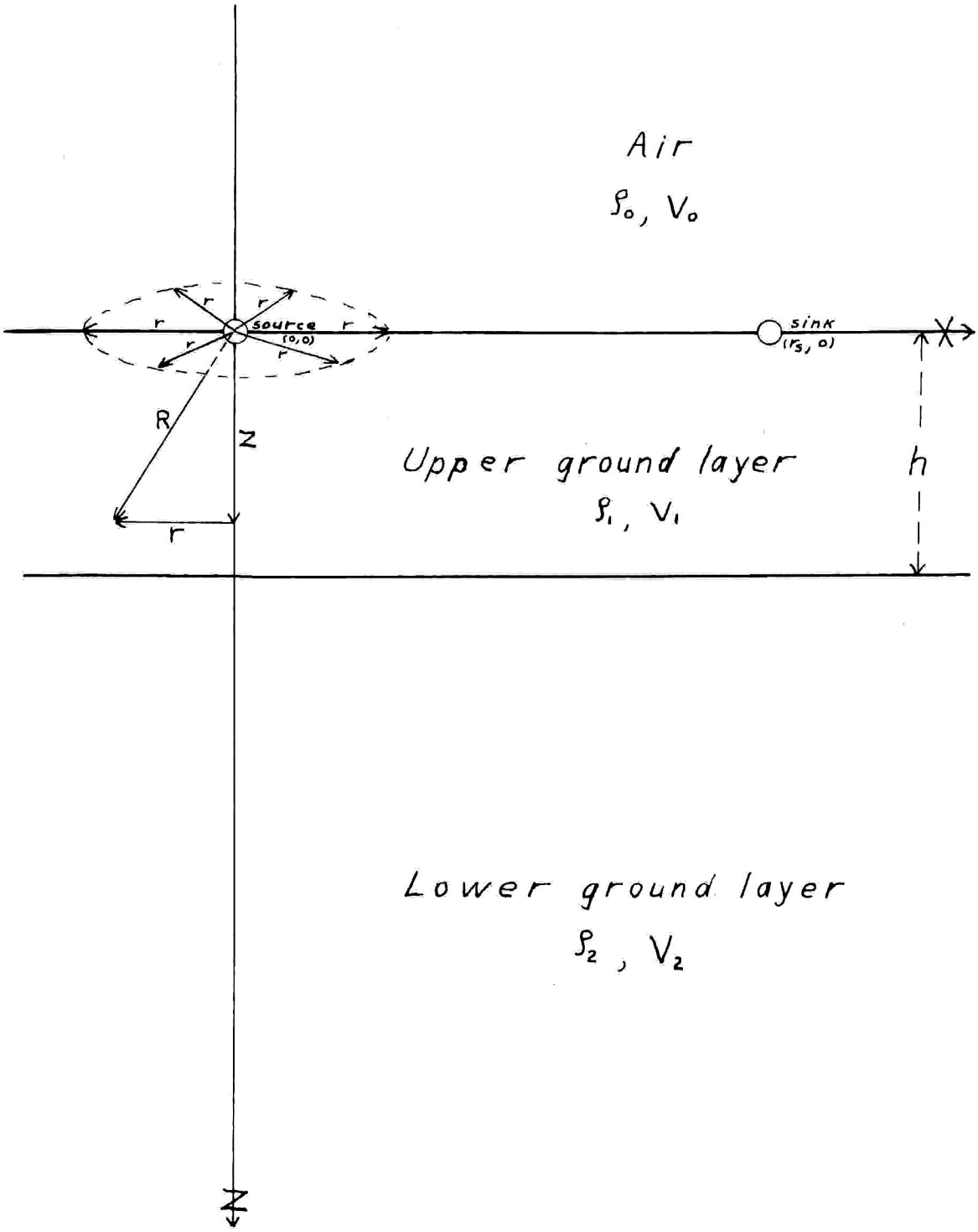

Figure 7. Diagram explaining symbols used in deriving expressions for potential and resistivity in a two-layer ground by the integral method.

alternative type of solution[a] which makes mechanical evaluation possible. This is especially important for three and more rock layers for which the series solution is more complicated. We will rework the case of two layers with this method for the sake of comparison.

INTEGRAL METHOD IN THE CASE OF TWO HORIZONTAL LAYERS

Cylindrical coordinates are set up (Figure 7) with origin at the source, a Z axis positive downward, and an r ($=(x^2 + y^2)^{\frac{1}{2}}$) axis in the boundary plane. As the potential is symmetrical about the Z axis, Laplace's equation in cylindrical coordinates takes the form

$$\frac{\partial^2 V}{\partial r^2} + \frac{1}{r}\frac{\partial V}{\partial r} + \frac{\partial^2 V}{\partial z^2} = 0 \qquad (9a)$$

A solution is sought of the form

$$V = U(r)\, e^{\lambda z} \qquad z < 0$$

$$= U(r)\, e^{-\lambda z} \qquad z > 0 \qquad (52)$$

where λ is a positive real number

as the potential must vanish for z infinitely large. If the value of V in equation (52) is substituted in equation (9a), there results

$$\frac{\partial^2 U}{\partial r^2} + \frac{1}{r}\frac{\partial U}{\partial r} + \lambda^2 U = 0 \qquad (53)$$

the Bessel's equation of zero order, whose solutions are two kinds of Bessel function series denoted by $J_0(\lambda r)$ and $Y_0(\lambda r)$. In this case we are concerned only with the series

$$J_0(\lambda r) \equiv \sum_{s=0}^{\infty} \frac{(-1)^s \left(\frac{\lambda r}{2}\right)^{2s}}{[s!]^2} \qquad (54)$$

We now have particular solutions of the type

$$V = J_0(\lambda r)\, e^{-\lambda z} \qquad z > 0$$

$$V = J_0(\lambda r)\, e^{\lambda z} \qquad z < 0 \qquad (52a)$$

A general solution is found by summing particular solutions multiplied by arbitrary functions of , and the

(a) This case is treated by Ollendorf, Erdstrome, p. 69

infinite sum of solutions with different values of λ may be replaced with the integral forms (Hankel's or Bessel-Fourier integrals)

$$V = C\int_0^\infty \Theta(\lambda) J_0(\lambda r) e^{-\lambda z} d\lambda \qquad z > 0$$

$$V = C\int_0^\infty \phi(\lambda) J_0(\lambda r) e^{\lambda z} d\lambda \qquad z < 0 \qquad (55)$$

where C, $\Theta(\lambda)$, $\phi(\lambda)$ are to be evaluated to fit the boundary conditions.

Weber(a) has shown that

$$\int_0^\infty J_0(\lambda r) e^{-\lambda z} d\lambda = \frac{1}{\sqrt{z^2+r^2}} = \frac{1}{R} \qquad (z > 0)$$

$$\int_0^\infty J_0(\lambda r) e^{\lambda z} d\lambda = \frac{1}{\sqrt{z^2+r^2}} = \frac{1}{R} \qquad (z \quad 0)$$

so that in the case of a semi-infinite medium where $V = \frac{\rho I}{2\pi R}$

$$C = \frac{\rho I}{2\pi} \quad \text{AND} \quad \Theta(\lambda) = 1$$

In the two layer case, the potential is regarded as made up of a primary part (that set up in an infinite medium) modified by a secondary potential due to the boundaries.

$$V_0 = \frac{\rho_1 I}{2\pi}\left\{\int_0^\infty J_0(\lambda r) e^{\lambda z} d\lambda + \int_0^\infty \Theta_0(\lambda) J_0(\lambda r) e^{-\lambda z} d\lambda + \int_0^\infty \phi_0(\lambda) J_0(\lambda r) e^{\lambda z} d\lambda\right\} \quad (56)$$

$$V_1 = \frac{\rho_1 I}{2\pi}\left\{\int_0^\infty J_0(\lambda r) e^{-\lambda z} d\lambda + \int_0^\infty \Theta_1(\lambda) J_0(\lambda r) e^{-\lambda z} d\lambda + \int_0^\infty \phi_1(\lambda) J_0(\lambda r) e^{\lambda z} d\lambda\right\} \quad (57)$$

$$V_2 = \frac{\rho_1 I}{2\pi}\left\{\int_0^\infty J_0(\lambda r) e^{-\lambda z} d\lambda + \int_0^\infty \Theta_2(\lambda) J_0(\lambda r) e^{-\lambda z} d\lambda + \int_0^\infty \phi_2(\lambda) J_0(\lambda r) e^{\lambda z} d\lambda\right\} \quad (58)$$

Since the potential must approach zero as z becomes infinitely large, V_0 cannot contain a term of the form $\int_0^\infty \Theta_0(\lambda) J_0(\lambda r) e^{-\lambda z} dz$ as z is negative. Therefore $\Theta_0 = 0$.

Similarly $\phi_2 = 0$

When $z = 0$, $V_1 = V_0$ or $\phi_0 = \phi_1 + \Theta_1$ (a)

$\rho_1 \frac{\partial V_0}{\partial z} = \rho_0 \frac{\partial V_1}{\partial z}$ and since $\frac{\partial}{\partial z}\int_0^\infty J_0(\lambda r) e^{\lambda z} d\lambda = \frac{\partial}{\partial z}\left(\frac{1}{\sqrt{z^2+r^2}}\right) = 0$ for $z = 0$,

$$\lambda \rho_1 \phi_0 = -\lambda \rho_0 \Theta_1 + \lambda \rho_0 \phi_1 \qquad \text{or} \qquad \phi_0 = \frac{\rho_0}{\rho_1}(\phi_1 - \Theta_1) \qquad (b)$$

(a) See Webster, Partial Differential Equations of Mathematical Physics - p. 120.

When $z = h$, $V_1 = V_2$, $\theta_1 e^{-\lambda h} + \phi_1 e^{\lambda h} = \theta_2 e^{-\lambda h}$

$\rho_1 \frac{\partial V_2}{\partial z} = \rho_2 \frac{\partial V_1}{\partial z}$, or $\theta_2 = \theta_1 + \phi_1 e^{2\lambda h}$

$\rho_2 (e^{-\lambda h} + \theta_1 e^{-\lambda h} - \phi_1 e^{\lambda h}) = \rho_1 [e^{-\lambda h} + \theta_2 e^{-\lambda h}]$ (c)

$$\theta_2 = \frac{\rho_2}{\rho_1}(1 + \theta_1 + \phi_1 e^{2\lambda h}) - 1 \qquad (d)$$

Equating (a) and (b) gives $\phi_1 = \theta_1 \frac{\rho_1 + \rho_0}{\rho_0 - \rho_1}$ (e)

Equating (c) and (d) gives $\phi_1 = \theta_1 \frac{\rho_2 - \rho_1}{\rho_2 + \rho_1} e^{-2\lambda h} + \frac{\rho_2 - \rho_1}{\rho_2 + \rho_1} e^{-2\lambda h}$ (f)

Equating (e) and (f) gives

$$\theta_1 = \frac{\frac{\rho_2 - \rho_1}{\rho_2 + \rho_1} e^{-2\lambda h}}{\frac{\rho_1 + \rho_0}{\rho_0 - \rho_1} - \frac{\rho_2 - \rho_1}{\rho_2 + \rho_1} e^{-2\lambda h}}$$

If we now put $\rho_0 = \infty$, θ_1 becomes $\frac{\kappa e^{-2\lambda h}}{1 - \kappa e^{-2\lambda h}}$

where $\kappa = \frac{\rho_2 - \rho_1}{\rho_2 + \rho_1}$

$\phi_1 = \theta_1$ by (e) $\qquad \phi_0 = 2\theta_1$ by (a)

$\theta_2 = \theta_1 (1 + e^{2\lambda h})$ by (c)

$$\therefore V_1 = \frac{\rho_1 I}{2\pi}\left\{\int_0^\infty J_0(\lambda r) e^{-\lambda z} d\lambda + \int_0^\infty J_0(\lambda r) \frac{\kappa e^{-2\lambda h}}{1 - \kappa e^{-2\lambda h}} (e^{\lambda z} + e^{-\lambda z})\, d\lambda\right\}$$

For the potential due to the sink, a term must be added of the form

$$V_1' = -\frac{\rho_1 I}{2\pi}\left\{\int_0^\infty J_0(\lambda[r_s - r]) e^{-\lambda z} d\lambda + \int_0^\infty J_0(\lambda(r_s - r)) \frac{\kappa e^{-2\lambda h}}{1 - \kappa e^{-2\lambda h}} (e^{\lambda z} + e^{-\lambda z})\, d\lambda\right\}$$

where r_s is the distance from source to sink

Thus at P, ($r = a$, $z = 0$), with $r_s = 3a$,

$$V_{P_1} = \frac{\rho_1 I}{2\pi}\left\{\int_0^\infty [J_0(\lambda a) - J_0(2\lambda a)]\, d\lambda + 2\int_0^\infty [J_0(\lambda a) - J_0(2\lambda a)] \frac{\kappa e^{-2\lambda h}}{1 - \kappa e^{-2\lambda h}}\, d\lambda\right\}$$

The series form may be gotten from the integral form by expanding $\frac{\kappa e^{-2\lambda h}}{1 - \kappa e^{-2\lambda h}} = \kappa e^{-2\lambda h} + \kappa^2 e^{-4\lambda h} + \kappa^3 e^{-6\lambda h} + \cdots$

$$V_{P_1} = \frac{\rho_1 I}{2\pi}\left\{\frac{1}{a} - \frac{1}{2a} + 2\int_0^\infty J_0(\lambda a)[\kappa e^{-2\lambda h} + \kappa^2 e^{-4\lambda h} + \cdots] d\lambda - 2\int_0^\infty J_0(2\lambda a)[\kappa e^{-2\lambda h} + \kappa^2 e^{-4\lambda h} + \cdots] d\lambda\right\}$$

$$V_{P_1} = \frac{\rho_1 I}{2\pi}\left\{\frac{1}{a} - \frac{1}{2a} + 2\left[\frac{K}{\sqrt{a^2+(2h)^2}} + \frac{K^2}{\sqrt{a^2+(4h)^2}} + \cdots\right] - 2\left[\frac{K}{\sqrt{4a^2+(2h)^2}} + \frac{K^2}{\sqrt{4a^2+(4h)^2}} + \cdots\right]\right\}$$

$$V_{P_1} = \frac{\rho_1 I}{2\pi a}\left\{\frac{1}{2} + 2\sum_{n=1}^{\infty}\left(\frac{K^n}{\sqrt{1+(2n\frac{h}{a})^2}} - \frac{K^n}{\sqrt{4+(2n\frac{h}{a})^2}}\right)\right\} \qquad (52)$$

The case for n layers has been worked out by both the image and integral methods(a) and in particular, the integral form worked out by Schlichter for the case of three rock layers has been evaluated by Wetzel and McMurray(b) on the differential analyzer(c). Equations for the apparent resistivity have also been worked out for the case of anisotropic layers(d), a vertical fault(e), and numerous others which will not be considered here. These expressions for the potential are also fundamental to other surface potential methods such as the potential-drop-ratio(f) and potential gradient methods(g).

(5) The fifth assumption made in deriving Wenner's formula that conduction is metallic is not generally true as in most cases the current is carried through the ground

---

(a) Stefanesco and Schlumberger--Jour. De Physique et Le Radium, Vol. 1, series 7, 1930, p. 132.
Schlichter, L.B.--Physics 4, p. 307 (1931)
Ehrenburg and Watson--A.I.M.E. Geophysical Prospecting, 1932, p. 423
(b) Geophysics, Vol. 2, 1937, p. 329.
(c) V. Bush--Journal, Franklin Institute, 212 (1931) p. 447.
(d) Pirson, Bull. A.A. P.E. (1935) Vol. 19, #1, 37-57
Schlumberger, C.&M., Leonarden, A.I.M.E., Geophysical Prospecting, 1934, p. 159.
(e) Edge & Laby, I.G.E.S., p. 252
Tagg--Mining Mag., Sept. 1930, p. 155.
(f) Lundberg & Zuschlag, A.I.M.E., Geophysical Prospecting (1932) p. 47.
Hedstrom--Mining Magazine, April, 1932, Vol. XLVI p. 201.
(g) Heiland--N.R.C. Pt. II, 1937, p. 581.

by salts dissolved in the ground water, and obeys the rules of electrolytic conduction. The conductivity of the rocks is therefore a function of their porosity and permeability, and of the presence or absence of soluble salts within the rocks which may increase locally the number of ions in the ground water and consequently the conductivity.(a) Electrochemical studies have shown that when metal stake electrodes are used with applied voltage above a certain value (of the order of magnitude of a volt) further increase in voltage will result in proportionate current increase, so that Ohm's law holds. The failure of Ohm's law for voltages less than the critical value, is due to the development of a back e.m.f. due to accumulation of ions at the electrodes. There is also an increase in contact resistance at the electrode due to formation of gas films, etc. This phenomenon of a back or polarization voltage has negligible effect on the current and potential distribution set up by the applied e.m.f. which is large compared to the critical voltage. It has a large effect on the difference of potential measured between the potential electrodes, as the polarization voltage often amounts to several hundred millivolts, and is of the order of magnitude of the potential difference set up between the potential electrodes by the applied current.

(a) Sundberg--A.I.M.E., Geophysical Prospecting, 1932-p. 367.
Fritsch--Electrotechnische Zeitschrift, Vol. 58, 1937, Pt. I, p. 319.
(These theoretical and experimental studies show that the problem is quite complicated.)

To eliminate this effect, as well as that of the galvanic potential commonly set up between the two potential stakes because of difference of the character of the electrolyte at the two points, it is customary to commutate both the applied and resulting voltages, or to replace the metal potential stakes with non-polarizing potential electrodes. Carl Barus[a] encountered this trouble in 1882, in the Comstock Lode, and remedied it by using zinc electrodes in a solution of zinc sulphate in a semi permeable goatskin bag.

Most workers have used copper rods and a saturated solution of copper sulphate in porous clay pots as originated by Schlumberger. The saturated solution ensures both potential pots being at the same concentration after a current has passed. This is the method used by the writer.

According to Dr. Potapenko[b], the use of zinc and zinc sulphate in place of copper and copper sulphate may be more satisfactory in some types of soil. He also has found that if a high input resistance is put in the potential circuit so that current flow between the potential electrodes is very small, it is possible to use a more dilute solution of about 1/7 saturation concentration of zinc sulphate. This low concentration avoids the clogging of the porous walls of the clay pot with sulphate crystals which would block the interchange of ions between the pot and the ground and prevent equalizing of the

(a) U.S.G.S. Monograph #3, Chapter X.
(b) C.I.T.--Lecture course in electrical methods of Geophysical Prospecting.

potentials of the pots in the ground. Unfortunately the writer was not aware of this until after the field work had been completed.

(6) If much current is drawn from the potential electrodes, the flow will reduce their potential difference and a low reading will result. This effect is more serious when the potential electrodes have a large contact resistance as the potential difference between the two contacts in the instrument where it is measured will be smaller than that in the actual ground by an IR drop, most of which is in the contact resistance.

(7) The final source of error is the presence of potentials not considered in the theory. These may be classified for our purpose as due to (A) spontaneous polarization, (B) instrumental leakage between circuits, and (C) other causes, both natural and artificial.

(A) Spontaneous polarization is known to occur in sulphide ores of a pyritic nature, in anthracitic coals and graphite bearing ores, pyrrothite deposits, and in peat bogs[a]. In the case of the sulphide ore bodies, the upper end undergoes oxidation because of the ground water and becomes the negative end of the body, while the lower end is reduced becoming positive. A current is thus set up from bottom to top of the ore body through the ground, and sets up a potential field similar to that artificially produced by an applied current.

(a) For a discussion of spontaneous polarization, see
R.C. Wells--Electric Activity in Ore Deposits, U.S.G.S. Bull. 548, 1914 and
Poldini--Geophysical Exploration by Spontaneous Polarization Methods, Mining Magazine, 1938-1939 LIX p. 278ff, and p. 347ff and LX, p.22 and p. 90

Although this has a disturbing effect on resistivity measurements which may be serious unless the applied current is large, it has also the advantage that if no current is applied, the potential gradient due to the polarization (which may be as large as 25 millivolts per 100 feet) can be measured, and a "negative center" of potential will be found over the ore body.

(B) Leakage between the applied voltages and the separate circuit which measures the e.m.f. between the potential electrodes will be serious according to the magnitude of the leakage, but is negligible with proper construction of the apparatus.

(C) Other potentials[a] will have an effect depending upon their magnitude. To eliminate the effect of unidirectional direct currents, the applied current may be sent through the ground in both directions. In any case it is well to use large applied voltages so that the effect of undesired potentials will be relatively small.

Depth of Penetration and Resolving Power

In concluding a discussion of the theory underlying earth resistivity measurements it is well to consider the question of the depth of penetration and the resolving power of restivity-depth profiles. In general, the greater the electrode separation is made, the deeper the current penetration and the deeper are the regions

(a) Gish and Rooney have made extended studies of natural earth potentials, and interested readers are referred to the bibliography at the end of the paper.

which contribute to the value of the apparent resistivity. Gish and Rooney[a] have found empirically that for a Wenner configuration the depth at which a discontinuity occurs is equal to the electrode separation at which a turning point occurs on the apparent resistivity-electrode separation curve. This has been frequently substantiated in the course of resistivity prospecting, but very often is greatly in error. Tagg and others have developed theoretical methods of determining the depth to an interface in the case of two, three, or more layers in terms of the electrode separation, and it may be seen from equation 51c above to depend upon the values of the resistivities. The Schlumbergers[b] have found that for many practical applications it is sufficiently accurate to consider the apparent resistivity to represent a layer of earth to a depth about equal to $\frac{1}{2}$ the separation between the current electrodes, or 3/4 the Wenner configuration separation "a". Lancaster Jones[c] estimates the depth to a horizontal discontinuity as 2/3 of the electrode separation at which an inflection point between points of maximum curvature occurs on the electrode separation-apparent resistivity curve. An explanation for the validity in many cases of the approximation that the depth to a discontinuity is roughly 1/3 the distance between the current electrodes may be

(a) A.I.M.E., Geophysical Prospecting, 1929, p. 53.
(b) A.I.M.E., Geophysical Prospecting, 1932, p. 134.
(c) Mining Magazine, Vol. 43, p. 22.

seen from the following analysis.(a)

The magnitude of the field at a point r_1 distant from a current source of strength I on the surface of a semi-infinite medium is $E_1 = \frac{\rho I}{2\pi r_1^2}$ and that from a corresponding sink r_2 distant from the point is $E_2 = \frac{\rho I}{2\pi r_2^2}$. The magnitude of the resultant field is $E = \sqrt{E_1^2 + E_2^2 - 2E_1E_2\cos(E_1,E_2)}$. Since $\cos(E_1,E_2) = \frac{r_1^2+r_2^2-L^2}{2r_1r_2}$ where L is the distance between source and sink, $E = \frac{\rho I}{2\pi}\sqrt{\frac{1}{r_1^4}+\frac{1}{r_2^4}-\frac{r_1^2+r_2^2-L^2}{r_1^3r_2^3}}$ and the corresponding current density is $i = \frac{I}{2\pi}\sqrt{\frac{1}{r_1^4}+\frac{1}{r_2^4}-\frac{r_1^2+r_2^2-L^2}{r_1^3r_2^3}}$. The current density in the median plane perpendicular to the line joining source and sink at its midpoint m is found by putting $r_1 = r_2 = \sqrt{(\frac{L}{2})^2+h^2}$ where h is the distance in the median plane from the midpoint m to the point at which the current density is desired. The equation then reduces to the form $i_h = \frac{4I}{\pi L^2(1+4\frac{h^2}{L^2})^{3/2}}$. The total amount of current flowing through a semi-circle of radius h in the median plane with m as a center is then given by the integral $I_h = \int_0^h i_h \pi h\, dh$ which gives the expression $I_h = I\left(1 - \frac{1}{\sqrt{1+4\frac{h^2}{L^2}}}\right)$. This current is about 1/10 the total current when h = L/4 and increases to more than $\frac{1}{2}$ the total current when h = L and to about 3/4 the total current for h = 2L. The ratio increases fastest for an increase in h/L at the point of inflection found by putting $\frac{d^2}{dh^2}\left(\frac{I_h}{I}\right) = \frac{4}{L^2}\left(1+4\frac{h^2}{L^2}\right)^{-3/2} - 48\frac{h^2}{L^4}\left(1+4\frac{h^2}{L^2}\right)^{-5/2} = 0$ from which h/L is found to be 0.354. If now a discontinuity at a certain depth h is considered it follows that the spread length L at which a change in L will cause the greatest change in

(a) Dr. Potapenko, Lecture Course in electrical methods of prospecting.

the amount of the current down to the depth of the discontinuity is h/0.354 or about 3h, and the break in the ρ-L curve is to be expected at this ratio of L/h. This is only approximate as the presence of a resistivity discontinuity was not postulated in deriving the expression for the current density and also because the formula holds exactly only in the median plane. However it is found to be of great value in determining the best of several possible interpretations in case of ambiguous data as discussed in Chapter VII. When the ratio of resistivities at a discontinuity is very much different from unity, the break in the resistivity-electrode spread curve tends to come at values of L corresponding to larger values of L/h, so that the values of h given by the approximation are too large.

Evjen[a] has considered the case of n horizontal layers, defining the depth of penetration as the depth to or below which exactly $\frac{1}{2}$ of the total current penetrates. In the case of a semi-infinite homogeneous earth, this

(a) Geophysics, Vol. 3, #2, March, 1938., p. 78.

depth is equal to $\frac{1}{2}$ the distance between the current electrodes. He undertakes to find a theoretical value for the depth factor (ratio of depth to a discontinuity to the electrode separation) for various types of electrode configuration assuming a horizontally layered earth, and a point source of current (Figure 8).

He considers the function

$$\frac{I}{2\pi}(\rho_2 - \rho_1) = W(r) \equiv r\,V(r) - \frac{\rho_1 I}{2\pi} = 2r\sum_{n=1}^{\infty}\frac{e_n}{\sqrt{r^2 + h_n^2}}$$

where V(r) is the potential on the surface of the ground due to the point source, and h_n is the depth of the image of strength e_n.

The series is then transformed into an integral by means of the definitions

$$\text{Image density}\quad g(z) = 0 \quad \text{for } z \neq h_n$$

$$\lim_{\Delta \to 0} g(z) = \infty \quad \text{for } z = h_n$$

$$\int_{h_n-\Delta}^{h_n+\Delta} g(z)\,dz = 2e_n$$

so that

$$W(r) = \int_0^{\infty} \frac{r\,g(z)}{\sqrt{r^2 + z^2}}\,dz$$

and by defining the sum of image densities to a depth z by

$$G(z) = \int_0^z g(z)\,dz$$

he obtains

$$W(r) = \int_0^{\infty} \frac{r\,z\,G(z)}{(r^2 + z^2)^{3/2}}\,dz$$

W(r) is now regarded as a weighted average of the sum of image densities G(z), greatest weight being given to the depth given by making

$$\frac{rz}{(r^2+z^2)^{3/2}}$$

a maximum. This is found by setting

$$\frac{\partial}{\partial z}\left(\frac{rz}{(r^2+z^2)^{3/2}}\right) = 0 \qquad \text{to be } z_m = r/\sqrt{2}$$

and since images appear at twice the depth of the interface to which they are due, the depth factor is taken as

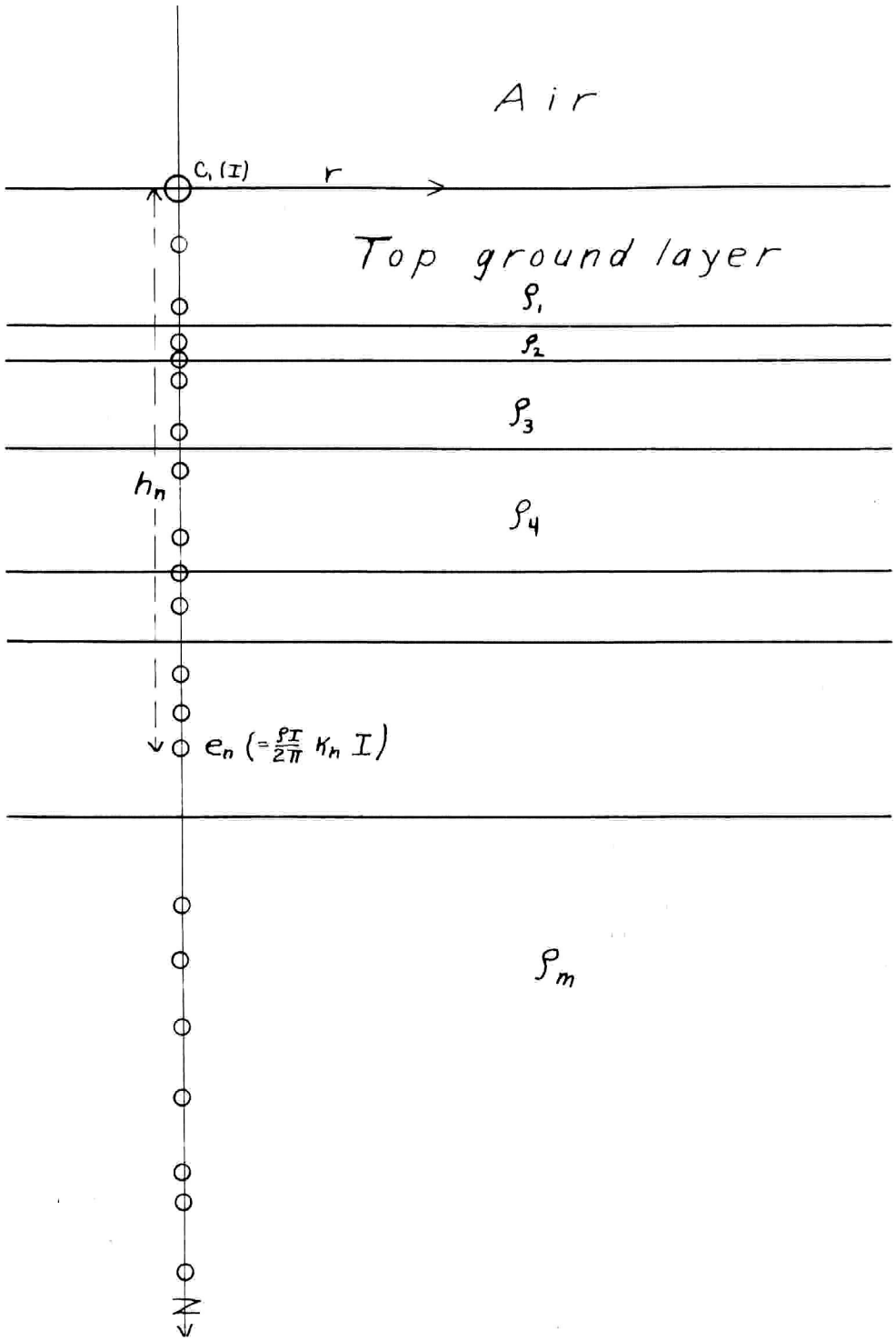

Figure 8. Diagram explaining symbols used in review of Evjen discussion of depth of penetration of d.c. resistivity method in a ground of many horizontal layers.

a first approximation to be $1/2\sqrt{2}$. By replacing the weight function

$$Q_0 = \frac{r z}{(r^2+z^2)^{3/2}}$$

with more sharply peaked functions formed from higher derivatives of Q_0 with respect to r it is possible to increase the resolving power. In particular for a Wenner configuration he finds a depth factor of about 1/3, i.e. "when a layer is present in the ground such that the surface log of apparent resistivity has a maximum or minimum, this maximum or minimum usually will come at a total electrode spread which is about nine times the depth to the upper interface."

In general the vertical resolving power will be greater, the greater the discontinuity in resistivites, and the shallower its depth. The depth factor will depend both upon the magnitude of the image density sums and the weight functions, which in turn will depend upon the magnitude of the resistivity discontinuities and their depths.

The resistivity method has a much greater resolving power for horizontal changes in resistivity which may be found by moving the set-up along the surface, and is especially useful in engineering foundation problems, and in seeking the surface trace of buried faults.

The resolving power will also depend on the location of the electrodes. If the potential electrodes are too far from the current electrodes their potential difference will be very small, and changes in potential difference due to change in their location will be very difficult to measure accurately. For example, in the Wenner configuration, the potential difference for constant current is inversely proportional to the separation "a". If a single current electrode is used and the potential electrodes are kept a constant distance apart and moved farther and farther away from it, the voltage between them is inversely proportional to the square of the distance to the current electrode. If the potential electrodes are too far from each other, the volume of ground whose resistivity is measured (the volume between the equipotential surfaces on which the potential electrodes are located to a depth of about the distance between the current electrodes) will be so large that the measured apparent resistivity will be insensitive to a small increase of electrode separation to include a small volume of material of different resistivity.

V

Design and Construction of the Apparatus

As shown in Part IV, the "apparent resistivity" from which the true distribution of resistivity in the ground is obtained requires the measurement of (1) the strength of a direct current, I, applied to the ground, (2) the resulting potential difference, E, which the applied current sets up between two potential electrodes, and (3) various distances between electrodes.

Two separate circuits are thus necessary, of which one applies a voltage of desired magnitude to the current electrodes, and measures the strength of current resulting, and the other measures the potential difference, E. Because of the necessity of eliminating the adverse effects of polarization, galvanic, and other potentials present in the ground, and of taking as small a current as possible from the potential electrodes, several modifications of each circuit are in use.(a) The Gish-

(a) In addition to the instruments mentioned in the text, there is the new more complicated equipment designed by Jakosky for continuous profiling. Only one electrode is moved and this, one of the two current electrodes, is a radially projecting blade on the rim of the rear wheel of a truck which is driven at speeds up to several miles an hour while a continuous record of the resistivity is made. (Jakosky, J.J. Geophysics III, #2, March 1938, p. 130.)

Somewhat different types of apparatus used in two other surface-potential methods are the "racom" which measures potential-drop-ratios from which resistivity ratios are obtained, (Lundberg and Zuschlag, AIME "Geophysical Prospecting" 1932 p47, Hedstrom, The Mining Magazine, April 1932), and the 'resistance-gradiometer' by which a "higher derivative of the surface-potential function is measured in such a manner that the depths to formation boundaries are read directly from the instrument without conversion." (Heiland, Trans. Am. Geoph. Union, N.R.C. 1937, Pt. II, p. 581.)

Rooney[a] apparatus uses "B" batteries as a current source, and to reduce the effects of polarization, reverses the direction of the applied current through the ground at a desired frequency of the order of 30 times per second. This is accomplished by putting one half of a double commutator in the circuit between the battery and current meter, and the current electrodes. In the secondary circuit, the potential difference to be measured is opposed by the e.m.f. of a potentiometer through a galvanometer used as a null instrument. The potentiometer is adjusted until the meter shows that no current is flowing in the circuit and the potentiometer reading then gives the desired voltage. The measured potential difference must be applied to the circuit always in the same direction, and for this reason, since it reverses direction with the applied current, its polarity is kept correct.with the other half of the double commutator. A condenser is inserted in the potential circuit to eliminate stray direct currents.

In the Megger[b], an instrument commonly used to determine insulation resistance in electrical machinery, the source of applied current is a hand driven direct current generator and the current is reversed with a double commutator as before.

(a) Further details of the design of this apparatus are given in U.S. Patent # 1,813,895, July 7, 1931. Accounts of its field use are given in papers by Gish and Rooney and others listed in the Bibliography.

(b) A more detailed description of the 'megger' is given by Drysdale and Jolley in their "Electrical Measuring Instruments" Part II, pp. 385-388 and 398, 399. Accounts of field use of the instrument may be found among the papers listed in the bibliography.

The current and voltage are not measured separately but are passed through the current and voltage coils of a galvanometer which records the ratio directly in ohms. Originally no potentiometer was used, and potential electrode stakes as much as 12 feet long were sometimes necessary to reduce the contact-resistance voltage drop between the ground and the instrument.

When non polarizing electrodes (described below) are used, it is no longer necessary to commutate the current, and the electrical apparatus is simplified by replacing the double commutator with reversing switches.

General Considerations

In designing apparatus for measuring resistivity, the following factors are to be considered,

1. Range of values which will be encountered.
2. Accuracy desirable.
3. Convenience for field use--ruggedness
4. Expense.

In this case, low expense and ruggedness were considered most important, because, as the apparatus is to be used only occasionally and then for student instruction there is no demand for extreme accuracy or great range of values. As it worked out, stock instruments borrowed from the Physics department were used to avoid unnecessary duplication by the institute, and the range, accuracy, and field convenience of the apparatus were controlled by what was available.

The quantities whose range should be considered are

the electrode separation a, the applied current I, and the potential difference E.

The value of a is governed by the depth of penetration desired, and the only requirement placed on the apparatus by larger values is the necessity for longer cables connecting the electrodes to the instrument. The California Institute of Technology Division of Geological Sciences kindly made available the use of its 1931 Model A Ford station wagon (Fig. 15) originally outfitted for Seismograph use, and this was equipped with four cable reels making possible Wenner separations of 350 feet. In the field tests made it was not deemed worth while to increase this separation, and the considerable expense of buying cable was saved.

The values of E and I occur in the ratio E/I = R. Most values of R found from the great amount of resistivity prospecting that has been done fall in a range of from 0 to 300 ohms. The instrumental value of E was limited above, by the use of a Leeds and Northrup student potentiometer, to 1.6 volts, and below, to a large enough value (from about .010 to .200 volts depending on local conditions) so that polarization and other disturbing potentials would not cause too large a relative error. The value of current should be limited to 200 milliamps(a) to avoid excessive drain on B batteries, but in the limited amount of field work done, no appreciable wear on the batteries was noticed with occasional currents of .7 amps. The lower limit of current is flexible, and

(a) Hawkins--A.I.M.E. Geophysical Prospecting, 1934, p. 117.

should be large enough to overshadow the effects of natural potentials. In the variety of places at which measurements were made, the extreme values encountered were

a = 200'; R = 0.07Ω; E = .046 volts; I = .646 Amp. Near Delano
.020 volts .318 Amp. Calif.

a = 2'; R = 1500Ω; E = .9 volts, I = .0006 Amp. Near Victorville on granite

No determination of the accuracy of measurement was made, but the error was probably not greater than ten percent, and because of the inacuracies inherent in making theoretical interpretations of data obtained from a heterogeneous terrain it is likely that increased accuracy in measurements would be of no real value.

Detailed Design and Construction

The design used is taken in outline from an article by E.R. Sheperd[a], but the details have been dictated by expedience, and the ideas of other writers have been used occasionally. The reader will be aided in following the ensuing description by consulting Plate I at the end of the paper.

The Primary Circuit

For a current source, 8 22.5-45 volt Burgess heavy duty B batteries (B_1, Plate I) were connected in series. The negative terminal was connected to the moving contact of a 17 point non-shorting type yaxley selector switch, (S_1) and a wire from each of the positive terminals was soldered to one of the stationary contacts making possible a range of applied voltage from 22½ to 360 volts at 22½ volt steps.

(a) Trans. Am. Geoph. Union--N.R.C., 1935, Pt. I, p. 78.

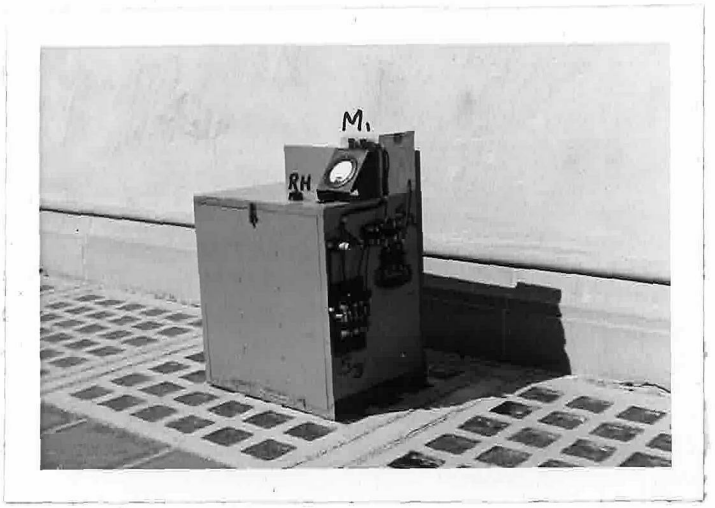

Figure 9. Primary circuit unit: battery box with current meter (M_1, Plate I) and controls on top, switch S_2 on side above handle, and reversing switch S_3 to which current electrodes are connected when in use below and to the left.

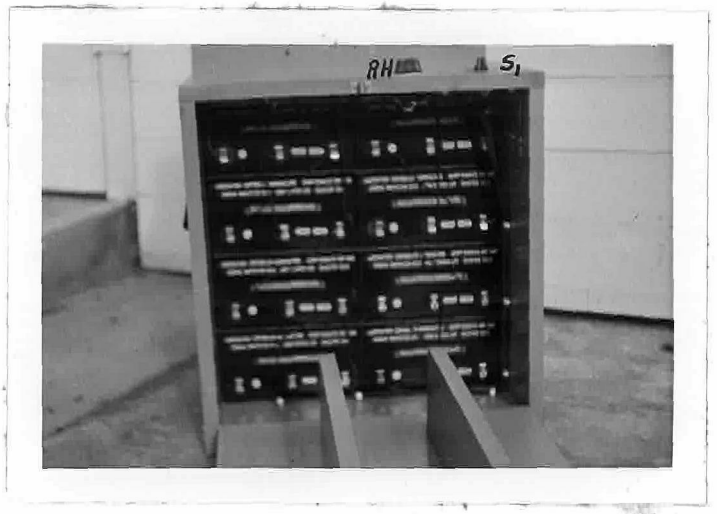

Figure 10. Open battery box showing heavy duty B batteries, voltage selector switch S_1 at right, and rheostat RH at left, on top.

In addition the negative terminal was connected to the off position of the selector switch so that natural earth currents could be measured on the milliammeter(M_1) in the circuit. However it was found that with the high stake contact resistance in the circuit the current resulting from natural potentials was too small to measure on a meter with 1 milliampere full range.

As a precaution against too great a current at 22½ volts in case contact and ground resistance should fall to a value of a few ohms, a 500 ohm rheostat(RH) was placed in series with the batteries. This proved convenient for making small adjustments of current when the resulting P.D. had such a value that the balance point came at one end of the potentiometer slide wire.

For measuring the value of applied current it was originally intended to use a multirange instrument with ranges of 10, 50, 100, 500, and 1000 milliamperes. The extension of range by a series of external shunt resistors of accuracy as high as called for by that of the meter is not expensive, and the cost of meter and shunts with 2% guaranteed accuracy should run about $15.00. However, it was found expedient to use two borrowed meters with .150 and .750 amperes full scale deflection. These were wired to a switch (S_2) so that either one could be put into the circuit at will. When small currents were to be measured, one or the other meter was replaced by the 10 milliampere meter used in the conditioning circuit described below.

The two ends of the part of the circuit described (battery, selector switch, rheostat, meter) were then connected to the two center poles of a double pole, double throw porcelain base copper knife switch(S_3). Cross connections were made so that the polarity of the two end poles connected to the current electrode cables could be reversed.

No. 18 Tirex portable S.J. cord two conductor rubber insulated cable was used. The two conductors were shorted together where they were connected to the reversing switch, and at the opposite end were attached to the female part of an ordinary domestic attachment plug.

The male counterpart was then attached to one end of a few feet of cable whose opposite end was fastened to a current electrode stake (C_1,C_2).

The stakes were of two types, one of 1½ x 1½ x 3/16 T section iron, the other of 1½ x 1½ x 3/16 angle iron. The two types were made because of the desire to see which type would have the least contact resistance. Although, unfortunately, no comparative tests were made, whatever small difference may have existed was of no practical importance in the course of field work. Two stakes of each type were made enabling two stakes to be connected in parallel at each electrode position. The stakes were about 18 inches long pointed at one end. The other ends were cut to the proper size so that the three end points of the angle or tee would lie on the

circumference of a circle a little larger than the inner edge of a 2 inch steel cap. The caps were then hammered on, the edges of the stake cutting through the soft lining material containing the threads. The caps formed a solid surface large enough to hit solidly with the 6 pound sledge used for driving the stakes. In the course of field operations several of the cap tops split where the top of the stake cut into them, and one was replaced. However, it was found that the iron ring left when the cap top broke off served sufficiently to keep the stake tops from spreading, and no difficulty arose from pounding on the stake tops themselves.

A hole was cut in each side of the angle or in the stem of the T below the cap, and a 3-foot piece of clothes line was passed through the holes and tied. The rope was looped at the other end to form a handle, and proved a convenient means of pulling out the stakes once they had been loosened by tapping their sides with the sledge.

Some trouble was at first experienced with the manner in which the short length of cable was connected to the stakes. A brass bolt was placed through a hole in the stake below the cap, and the cable wire was wound around the bolt between two washers and tightened with a nut. This connection came loose every time a stake was driven. This was remedied by applying a thick coat of solder with a hot gas flame. This kept the washers, nut, and cable firm indefinitely, but trouble now arose from snapping of the cable where it was

Figure 11. Angle iron current electrode stake with steel cap for driving, and rope for removing from the ground.

Figure 12. Potential electrode: asphault coated porous clay pot with paper cap to keep the cable from twisting and to keep dust from the copper electrode and sulphate solution.

weakened just outside the connection by removal of the insulation, heating from the solder, and the continual twisting. This was fixed by soldering the cable ends to a thin steel lug which kept the cable from twisting. The lug was then soldered firmly to the stake, and strengthened with a bridge of solder about the size of the cable.

These stakes worked well, but had a high contact resistance in dry ground. This was reduced by soaking the ground around the stakes with a solution of salt water. In one case, where the set up was on solid granite, a satisfactory contact was obtained by laying the stakes on cloths soaked with salt water and weighting them down with slabs of rock.

Potential Circuit

The The potential circuit consisted of non polarizing electrodes, switches for selecting (when a Lee Configuration was used) the electrodes whose potential difference was to be measured, a switch for reversing the direction in which it was applied to the circuit, a potentiometer circuit to produce an opposing voltage of known value, a null indicator to show when the two e.m.f.'s were in balance, and a key to make and break the circuit so that current would only flow instantaneously when the system was out of balance

The non-polarizing potential electrodes (P_1,P_2,P_3) consisted of porous pots containing pure copper pipe in a saturated solution of C.P. cupric sulphate with an excess of crystals. The pots were of unglazed porcelain 76 mm. in diameter, 3/16 of an inch thick in the

walls, and 177 mm. in height. To avoid excessive loss of solution by evaporation the outside walls were saturated with a solution of asphalt in xylone so that the outside was dry except for the untreated base which was wetted by the copper sulphate solution inside.(a) The coat of asphalt penetrated perhaps only a fifth of the way through the walls, and several pots split when excess pressure was placed on the solution because of hydraulic action by the fluid in the pores of the walls. The pots were greatly strengthened by coating the inner walls with the asphalt, thus keeping the solution out of their pores. The presence of the inner coating of asphalt did not noticeably increase the size of the polarization potential. It was found in working in dry areas that contact resistance was too high with only the bottom of the cup wet. New pots were assembled with only the upper half of the pot coated with asphalt so that when the pots were planted in holes liberally sprinkled with a solution of technical powdered copper sulphate the increased contact area greatly reduced the resistance. This method of waterproofing the walls proved very convenient. The asphalt dissolved rapidly in the xylone, and when applied to the pots with a paint brush dried so rapidly that a thick coating could be applied and dry within an hour.

The copper electrodes were cut from a single piece of ½ inch i.p.s. electrolytic copper pipe, the commercial

(a) Partly glazed pots for electrodes are available commercially from Geophysical Instrument Company in Washington, D.C. and from Coors in Boulder, Colorado.

grade being fortunately more than 99% pure, so that no special treatment was needed to avoid "local action" potentials between the copper and metallic impurities such as zinc. All electrodes were cut from the same piece of pipe to insure uniformity. They were about 9 inches long, with holes cut near the end immersed in the solution to obtain the increased electrochemical stability of having an almost doubly large contact surface of solution and metal with the solution filling the interior of the pipe too. The bottom of the pipe was raised above the bottom of the pot by plugging it with a cork. This was to prevent the possibility of having the copper in direct contact with the solutions of dissolved salts in the ground.

The solution was made up by dissolving C.P. copper sulphate crystals in distilled water until it was saturated and an excess of crystals remained. This ensured the pots being at the same concentration of solution and avoided the potentials set up by a concentration cell.

The pipe was kept vertical in the middle of the pot by passing its top through a tight hole bored in the flat cork which fitted into the top of the pot and sealed in the solution. To further prevent evaporation and leakage, the cork was dipped in a bath of melted paraffin to seal up its pores, and a thick coating of "air-tite" auto-top sealer was placed over the cork, especially at its junctions with the pot walls, and with the outside of the pipe. This inexpensive substance

has the desirable properties of staying fluid in a tube indefinitely, and of drying to a smooth-surfaced, rubbery consistency after about 24 hours exposure to the air. It will form a water and air-tight seal indefinitely and yet the cork was easily removed by a gentle pull when the pot was to be recoated with asphalt.

The upper end of the pipe was sealed with a cork when it was not used for filling the pot with solution.

The upper end of the pipe above the pot was grooved and a hole bored through it. The two strands of copper cable were passed through the hole and wrapped in the groove to form the contact. In later pots a thin-walled copper tubing was used, and the cable was attached to a brass bolt passed through a hole in the tubing. The contact potential between the brass and copper was negligibly small. To keep out dust and to keep the cable from twisting, a tin can was placed over the upper end of the pipe bottom end up, so that the cork in the upper end of the pipe was fastened to the bottom of the can with a small woodscrew, and the top border of the can was pressed against the top of the clay pot with a flexible collar of 20 guage copper drawn together and tightened with a brass bolt. The cable was passed through a rubber grommet in a hole in the top of the can wall. This proved unsatisfactory both because the solution of copper sulphate in which the pots were kept would splash against the tin cover, with danger of galvanic action disturbing the potential equilibrium of the pots, and because the copper collar put too great a pressure

on the clay pot.

The can was then replaced with a large inverted tapered paper cup which was held in place sufficiently well by the cable passing through a grommet near its bottom, and by the friction where it slid over the top of the porous pot.

To the other end of the cable attached to the pipe was attached the male part of an attachment plug.

The pots when not in use were kept in a saturated solution of copper sulphate with excess of crystals in a 2 gallon stone jar, and the terminals were shorted together with a double socket to keep the pots at the same potential. The pots were kept tight in the jar by wedging in pieces of paper and cloth so that they would not jostle and break in transit. To prevent splashing, a piece of 16 ounce canvas folded to four thicknesses was placed over the jar and secured by a piece of wire wound around the jar's upper circumference beneath a small projecting rim.

The pots proved very durable, none breaking in the field work, even though two were knocked over by inquisitive calves. It was originally planned to have double chambered pots of the I.G.E.S. type used by Edge and Laby[a], in which the chamber in contact with the ground contains gelatin soaked with the copper sulphate solution so that there is less loss of copper sulphate into the ground, and less chance of leakage. However, no double chambered pots were available, and the problem of cutting

(a) I.G.E.S.--p. 238 (Type B)

a piece of clay for a partition and cementing it was given up after a few attempts as of more bother than use. Fortunately, it was found that the pots as constructed could be used several days without refilling so that the copper sulphate expense was not excessive.

In some localities, the ground was sufficiently moist so that the pots could be set directly upon the ground surface. In sandy soil, a hole several inches deep was scooped out with a trowel and filled with an impure solution of copper sulphate. In a set up on granite, the pots were set on pieces of cloth soaked in copper sulphate.

The other end of the cables, to which the electrodes were connected in use were connected to two single pole double throw switches(S_4,S_5) in such a manner that the potential difference between any two of the potential electrodes in a Lee Configuration could be applied to two end poles of a double pole, double throw switch(S_6). This switch was cross wired so that the potential could be thrown across the two middle poles in either direction. This was necessary in order to have the ground potential applied to the null instrument always in the same direction (opposed to the potentiometer e.m.f.) whatever the direction of applied current, or pair of electrodes used. The two center poles were then connected to two end poles of a second double pole, double throw switch(S_7) so that when the switch blades were thrown to this end of the switch, the porous pots were thrown into the circuit.

When the switch was thrown in the other direction, the potential of a standard cell or "calibration circuit" (see below) was applied to the circuit and used for adjusting the variable resistance (RB) in the potentiometer circuit.

The potentiometer circuit (Plate II) consisted of a Leeds and Northrup student potentiometer,(P) two dry cells(B_2) hooked in series to pass a current through the slide wire, a 4 dial 999.9 ohm decade resistance box (RB) in series with the batteries to adjust the current through the potentiometer to .01 amps, and a single-pole double throw switch(S_8) to select either of the two potentiometer ranges. When the "1" range was used, .01 amperes flowed through the slide wire, giving a total RI drop range of 1.6 volts through the 15 10-ohm resistance coils and the 10-ohm slide wire in series with them. When the switch was in the ".01" position, the current entered the potentiometer through a different terminal and was shunted so that only .0001 amperes flowed through the resistances and slide wire reducing the total range to 16 millivolts. Another single pole double throw switch(S_9) was inserted into the circuit to make sure that this circuit was completely open when not in use.

This instrument proved satisfactory except that the control knob which ran the moving contacts along the slide wire worked unevenly and it was hard to reach the exact balance point without jumping past it when the sensitivity of the null instrument (M_2) was high.

Plate II. Diagram showing details of potential circuit.

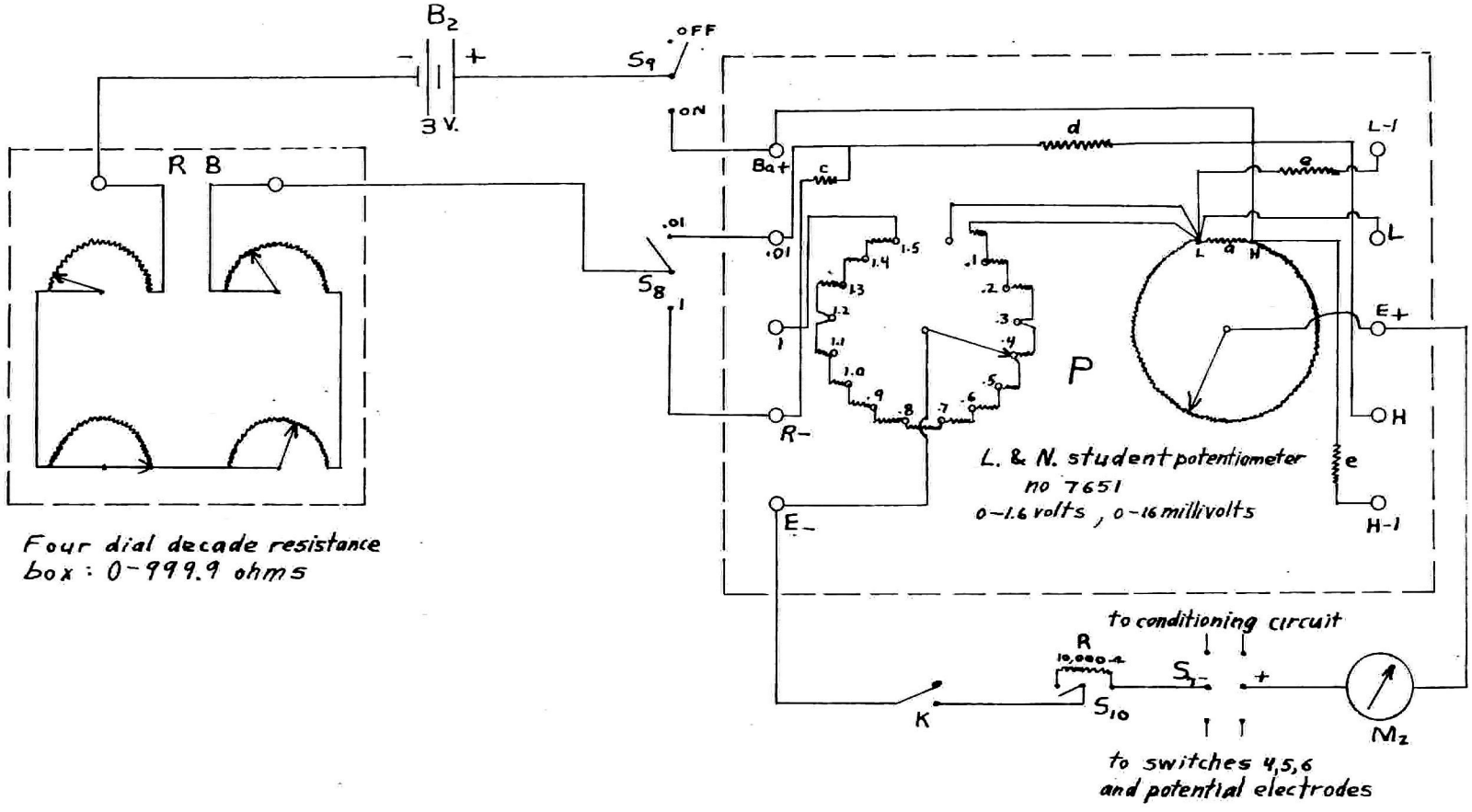

If more field work were done it would be desirable to gear down the control knob so that the contact could be moved along the slide wire in smaller increments.

A telegraph key (K) was used to make and break the current through the circuit and cause a deflection of the null instrument when the opposed potentials were out of balance.

A 10,000 ohm resistor (R) was wired across the two end poles of a single pole, double throw switch (S_{10}) which was placed in series in the circuit by hooking in the center and one end pole. This resistor was left in the circuit to protect the potentiometer and null instrument until approximate balance was obtained. It was then shorted out by reversing the throw of the switch so that a more delicate balance could be obtained.

The potentiometer current was adjusted by moving the resistance box dials in .1 ohm steps until the null indicator did not deflect for a setting on the potentiometer dials equal to that of the known opposed voltage thrown into the circuit in place of the porous pot potential. As field use is too hard on a standard cell, a conditioning circuit similar to that used by Lee[(a)] was set up. This consists of passing a current whose value is measured by a meter in the circuit through two precision resistors of the proper value. The potential drop across one of the resistors is then placed across the terminals of the double pole switch. This voltage is then given

(a) Lee, F.W.--Information Circular, 6899, ug. 1936--U. S. Bur. of Mines

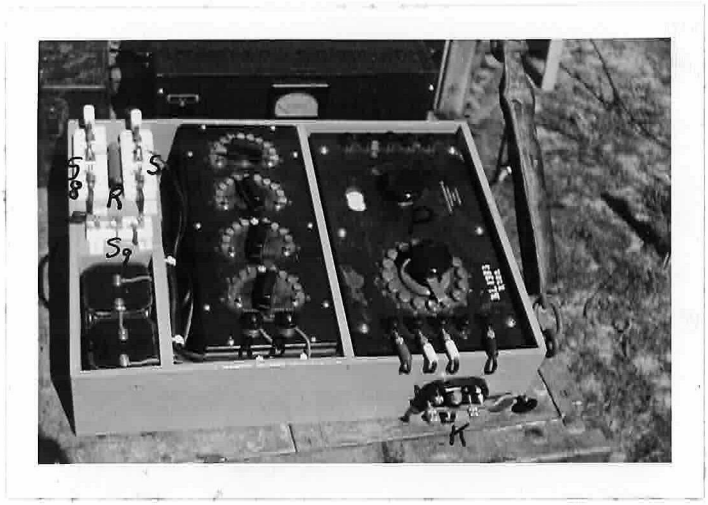

Figure 13. Potentiometer unit: Potentiometer (P), resistance box (RB), dry cells (B_2), switches 8, 9, and 10, protective resistor (R), and key (K).

Figure 14. High gain amplifier with meter in plate circuit of third stage used by Eichelberger as null indicator. (M_2, Plates I and II)

by the product of the resistance in ohms and the current in amperes. The value of the resistance, which is sufficiently constant with good resistors and soldered connections, can be determined initially by comparison with a standard cell. If good resistors are used, and a fresh dry cell, the current in the circuit would not change in the time required to adjust the potentiometer circuit, and changes in current over a period of a day or so caused by fluctuations in the dry cell e.m.f. can be allowed for by taking the product of the resistance and new current values as a new setting for the potentiometer.

In the present case, a 1.5 volt dry cell (B_3) passed current through a 10 milliampere meter (M_3) in series with a 300 ohm Shalcross and a 100 ohm I.R.C. precision resistor. The current was .0039 amperes, and the voltage across the 300 ohm resistor was found to be 1.1406 volts by balancing it against the potentiometer voltage previously set with a Weston standard cell.

This gave a resistance value of 292.4 ohms. As it happened, the current value remained at .0039 amperes through the four days of field use, and the potentiometer setting for calibration was kept at 1.1406 volts.

The choice of an instrument to indicate the degree of balance of the opposed potentials is of great importance, for on it depend the speed, ease, and accuracy of the measurements. If the sensitivity is too low, the system will appear to be in balance for a considerable range of

potentiometer settings and the measurement will not be accurate. If the sensitivity is too high, the system will appear to be out of balance for potentiometer settings sufficiently close to the exact value, and there will be trouble in finding this value.

The instrument should be slightly underdamped. When insufficiently damped, the oscillations of the indicator cause a delay in reaching the balance point, and when overdamped the hesitation of the needle in reaching the full value of deflection will be a source of delay and inaccuracy.

If the instrument does not indicate which of the two out of balance voltages is larger, time is required to determine whether the potentiometer setting should be increased or decreased to reach the balance point.

The instrument commonly used is a portable moving coil galvonometer with deflection in both directions from a central zero. The instruments used by Hawkins(a) and Edge and Laby(b) had a sensitivity of one fourth microampere per scale division of 1 millimeter width, and an internal resistance of about 150 ohms. In this case other instruments were used as described below, but were not very satisfactory, and in any future field work with the apparatus it would be advisable to select a galvonometer of proper sensitivity and required external damping resistance to fit the electrical characteristics of the measuring circuit including the potentiometer and the path through the potential electrodes. An

(a) A.I.M.E. "Geophysical Prospecting" 1934, Page 115.
(b) I.G.E.S. Page 236.

instrument with high external damping resistance is preferable to avoid overdamping when the contact resistance at the potential electrodes is high. In areas of low contact resistance a resistance could be thrown in series with the meter to avoid underdamping.

To avoid the expense of a galvonometer which would be of the order of $25.00 it was decided to use the amplifier-galvonometer unit (Plate IIIc) already assembled in the station wagon for seismic recording. In this unit, the seismometer output was passed through an input transformer to a three stage amplifier and the amplifier output passed through a second transformer whose secondary was in series with the moving coil of the galvonometer which had optical recording. The light from an automobile headlight bulb was reflected from a rotating mirror mounted on the galvonometer coil and thrown onto a slit behind which the film for photographic recording was located. The magnitude of the seismometer voltage is then indicated by the size of the displacement of the light beam along the slit. The total voltage gain of the system is about 1000. For use as a null instrument in the porous pot apparatus, the voltage of unbalance in the potentiometer circuit was applied through the input transformer to the amplifier. The photographic equipment was removed, and the motion of the light spot on the slit was observed visually. The optical system was so unsteady that it was a laborious task to adjust the light spot to fall on the slit, and as the adjustment had to be made every time the truck was jarred the attempt

Plate III. Diagram showing circuit of seismograph amplifier – galvanometer unit used as null instrument. (M_2, Plates I and II)

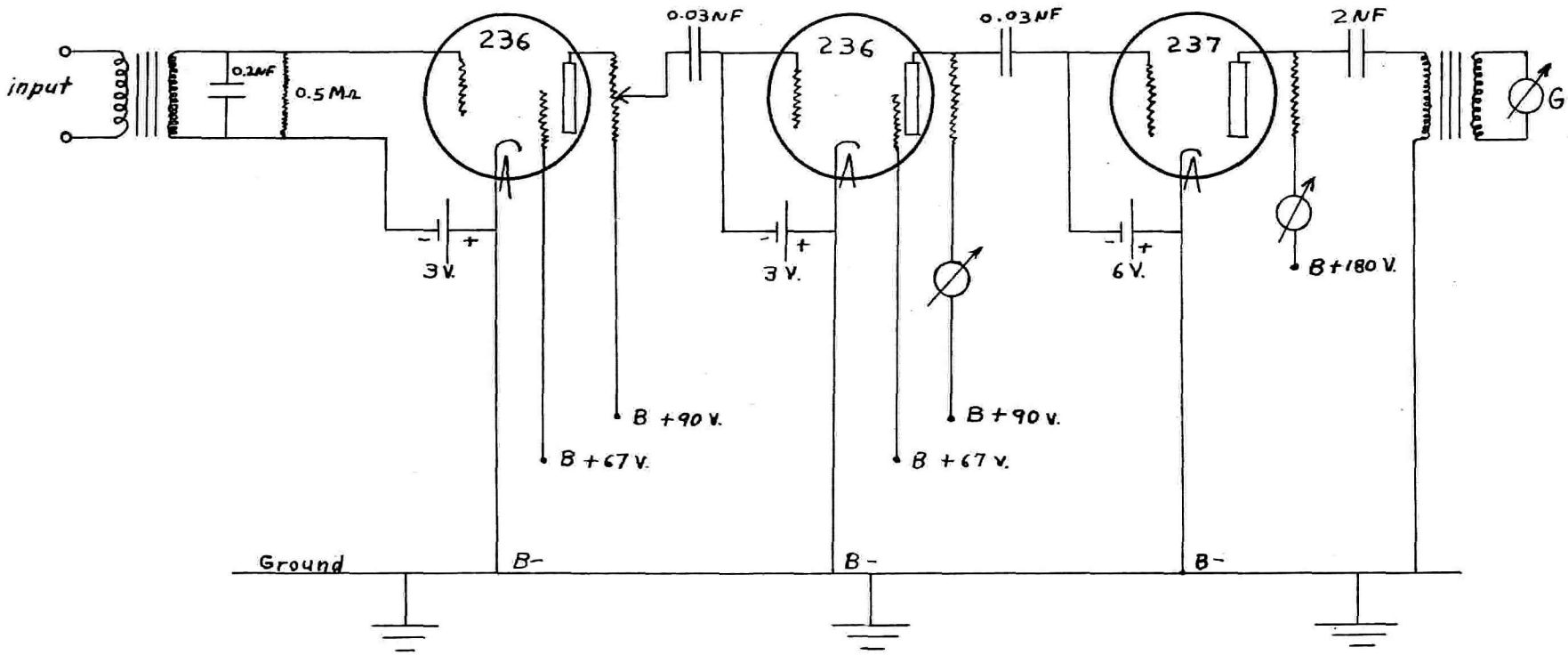

to use the galvonometer was abandoned. However, it was noticed that a 1.5 milliampere direct current meter, connected to a selector switch so that it could be thrown in series with the plate current of either the second or third stages of the amplifier, was deflected when the potentiometer circuit was broken and closed with the key. This made a satisfactory null instrument for reaching a balance when checking the potentiometer voltage against the standard cell or conditioning circuit, where the circuit resistance was low and the balance point known. However, in the field work, it worked satisfactorily only in a few cases. Usually it was too insensitive on the second stage of amplification, and too sensitive on the third stage. It was a laborious task to adjust the sensitivity properly with the rheostat in series with the meter, and often proper sensitivity could not be obtained.

A direct current 1 milliampere full scale meter on the plate current of a three stage amplifier built by Martin Eichelberger (PlateIV) worked much more satisfactorily, but also had the drawback of not indicating by the direction of deflection whether the potentiometer setting was too large or too small.

A Weston Model 301 DC milliameter with full scale range of 1 milliampere, used in the field work near Victorville, California, indicated the direction and degree of unbalance well enough in most cases, but was not sensitive enough in case of high contact resistance

Plate IV.

Circuit diagram of Eichelberger's high gain amplifier used with input transformer as null indicator (M_2, Plates I and II).

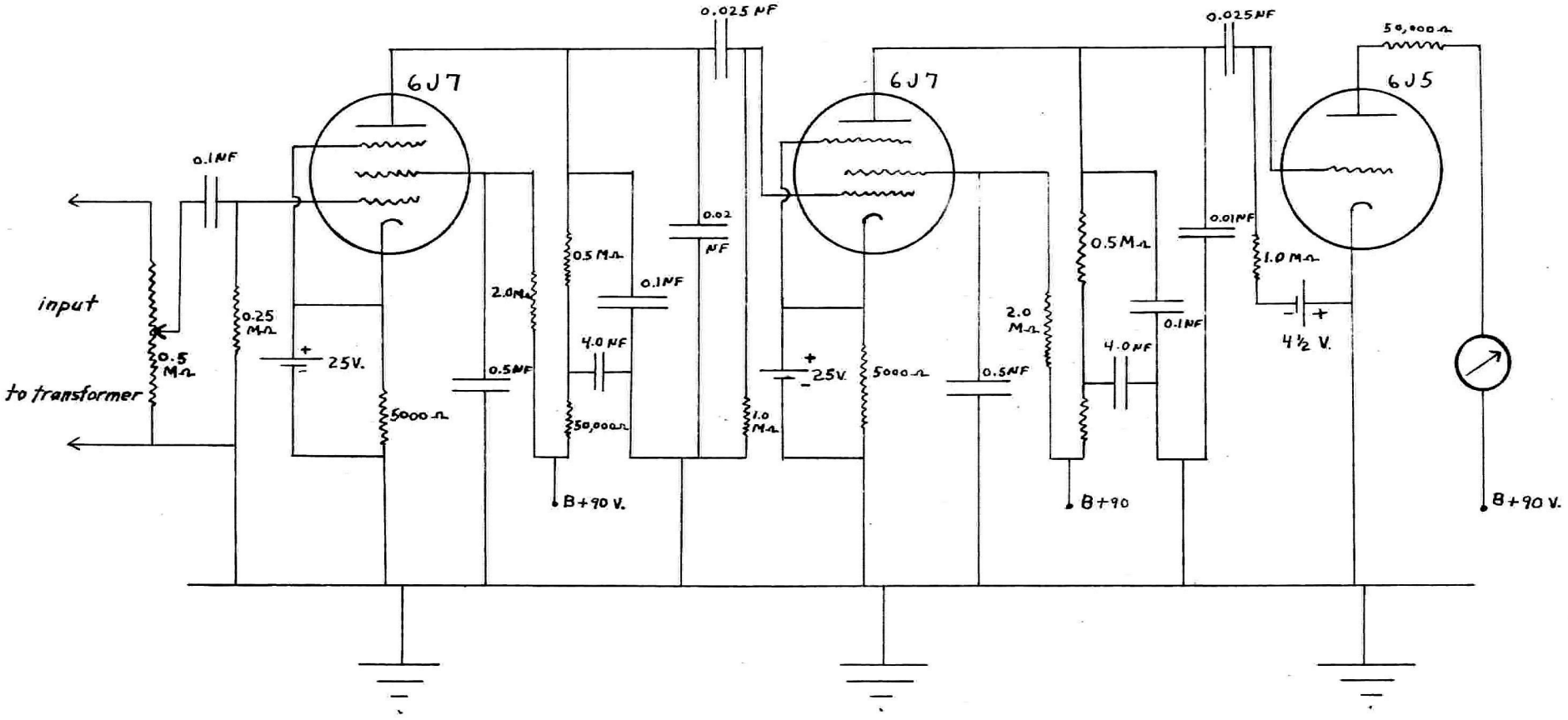

even when the porous pots were buried in ground wet with copper sulphate solution. It also had the disadvantage of deflecting in one direction only so that when wired for positive deflection by the component of current from the potentiometer voltage, the current in the circuit when the potentiometer setting was below the balance point forced the indicating needle against the stops in the negative direction.

VI

Field Work

Introduction

We have seen above that the resistivity of a ground homogeneous to an unlimited depth is given by the expression $\rho = 2\pi a E/I$ (22a) where a is the separation between any two adjacent electrodes in the Wenner configuration, and E is the potential difference between the porous pots when a current I is made to pass between the current stakes. In such a homogeneous body the computed value of resistivity would be the same for any choice of electrode separation, and for spreads of any one separation located anywhere on the ground surface. Actually the ground is never completely homogeneous, and the computed value is not the actual resistivity. As it is useful in determining the actual resistivities, the value is computed from the formula, but is called the apparent resistivity and designated by the symbol ρ_a.

Two main types of field test are made. One method is to take a series of measurements with increasing electrode separations about a single fixed spread center. This will be called a depth profile and the data is usually plotted in the form of a graph with apparent resistivity as ordinate and electrode separation as abscissa. The curve obtained in practice is usually not the straight horizontal line which a truly homogeneous ground would give, but is either smooth or irregular. If the curve

is smooth, and if similar curves taken at the same location with the line of electrodes in different directions are also smooth and of the same type, a theoretical treatment is possible as the symmetry of the problem indicates a regular distribution of resistivities in space. A full description of methods of interpreting such smooth curves is given in Chapter VII, and illustrated with data obtained by the writer in the field. If the curve is jagged, or the curves for different azimuths of electrode lines do not indicate symmetry, an empirical interpretation is necessary. Type curves may be compared with the known geology at a point, and irregularities found to correspond with definite geologic units. If such correlation is found to exist at several points, and a definite relationship to exist between the magnitude of the electrode separation and such physical dimensions of the problem as known depths to formations, it is then possible to estimate such dimensions from the electrode separations at intermediate points of unknown geology, provided the curves obtained are correlatable with the type curves. Even with smooth curves subject to theoretical treatment it is very important to get empirical check on the result if one is to feel much confidence in the interpretation.

In the other field method, the spread is moved from point to point in an area while the electrode separation is kept constant. The computed resistivity as ordinate is then plotted against the location of the spread center

as abscissa. Here, again, the curve obtained is seldom the horizontal straight line which should be found for a single homogeneous ground, but may either be jagged or approximate a smooth curve. The first case requires empirical interpretation, and the other, although subject to theoretical treatment has much more value if subject to frequent check with known geology. The methods of theoretical interpretation of curves obtained in such a traverse are not specifically treated in this paper, but the general method of attack is the same as for the depth profiles in that the field curves are compared with master curves in which the apparent resistivity was derived in terms of a postulated distribution of actual resistivities by the use of the surface potential function.

Depth profiles are commonly used in simple cases of fairly shallow depth such as to determine the depth of overburden covering bed rock, knowledge useful to the civil engineer in planning highway, bridge and dam construction, or to indicate the location of highly conductive ore bodies. Deeper profiles obtained with large electrode spacing have been used to determine the position of aquifers at depths of more than 1000 feet to help in locating water wells, and to locate the presence of possible oil structures at depths of a few thousand feet.

Horizontal traverse profiles are useful in revealing high angle contacts such as fault contacts or those

between vertical beds where the surface traces are obscured by a veneer of surface material, and in indicating the presence of shallow ore bodies. They have the advantage over depth profiles of having greater resolving power as the changes in resistivity take place nearer to the electrodes. They are also of use in regions of smooth apparent resistivity-electrode separation curves in conjunction with the more time consuming depth profiles. For example the depth to a horizontal contact may be found at several points with depth profiles. The depth to the contact may then be estimated at intermediate points by taking a traverse with a critical value of electrode separation and seeing whether the value of apparent resistivity for that separation increases or decreases.

The field work carried out by the writer (See Map I) consists of three parts. The first was a depth profile run at Hastings Ranch near Sierra Madre, to see whether the values obtained would be the same as those obtained with commercial apparatus. The second was a depth profile made near Delano to see how the resistivities and curve interpretations would compare with the information obtained by lowering electrodes into a seismograph shot hole. The third was a series of depth profiles made near Victorville to see whether such profiling was a practicable way of determining the depth of alluvium over the bed rock. The rest of this chapter is devoted to a discussion of these three tests.

Map I. Index map of part of the state of California showing general location of places at which field work was carried out at centers of double circles.

Field Work at Hastings Ranch

To learn whether the apparatus would work satisfactorily in the field, the first test was the running of a depth profile at a location where Mr. Lohman, a consulting geophysicist of South Pasadena, had previously run such a profile with Gish-Rooney apparatus. The work went slowly because of a lack of a sufficient number of field assistants, and some difficulty in getting the potentiometer circuit to balance properly. The days of February 11, 12, and 19 and March 4 and 5, 1939 were required for the work. After the profile had been completed and an apparent resistivity-electrode separation curve plotted, Mr. Lohman gave the writer a copy of the curve which he had obtained two years before. These curves will be discussed later.

The profile was laid out in a nearly north-south direction about a center point 1500 feet north and 500 feet east of the fence corner at the northeast corner of the intersection of Sierra Madre Villa Road and Foothill Boulevard, near Sierra Madre. Directions were taken from a Brunton compass, and distances measured with a 200 foot steel chain. The points to be occupied by porous pots and current stakes were marked out with short pieces of lath. Wenner spacings of from 5 to 260 feet were used, and in some of the spacings a third potential electrode was used with the Lee configuration as a check. For every value of electrode spacing, a, values of the potential

Figure 15. Institute Model A station wagon and apparatus set up for field work at Hasting's Ranch near Sierra Madre, California.

Figure 16.
Line of profile at Hasting's Ranch. San Gabriel Mountains in the background.

difference E between the pots was taken for two values of applied current I in each direction of current between the stakes. The four ratios of E/I = R are then averaged to obtain the apparent resistivity, $\rho_a = 2\pi aR$. Reversing the direction of current and averaging eliminates the effect of constant potentials from other sources which may be present in the ground. Using two magnitudes of applied current affords an indication of how well Ohm's law is holding, and by increasing the number of observations used for each value of resistivity cuts down the effect of non systematic errors in the individual measurements.

Readings were also taken of the potentiometer setting E_{psc} at which balance with the standard cell was attained. From this the value of current through the potentiometer slide wire can be obtained, and if it is different from .01 amperes, corrections in the value of E can be made accordingly. It was found that by adjusting the 4 dial resistance box in series with the slide wire every half hour or so, the values of E were sufficiently accurate without correction. Readings of the resistance box setting R_{RB} at which the potentiometer setting agreed with the standard cell at balance were taken as a check on the voltage stability of the dry cells supplying the potentiometer current.

Values of the applied voltage E_a necessary to obtain the applied current I were also taken, and the ratio computed to give an indication of the size of the stake contact resistance. The large and irregular effect of this contact resistance on the value of E_a/I (Figure 18)

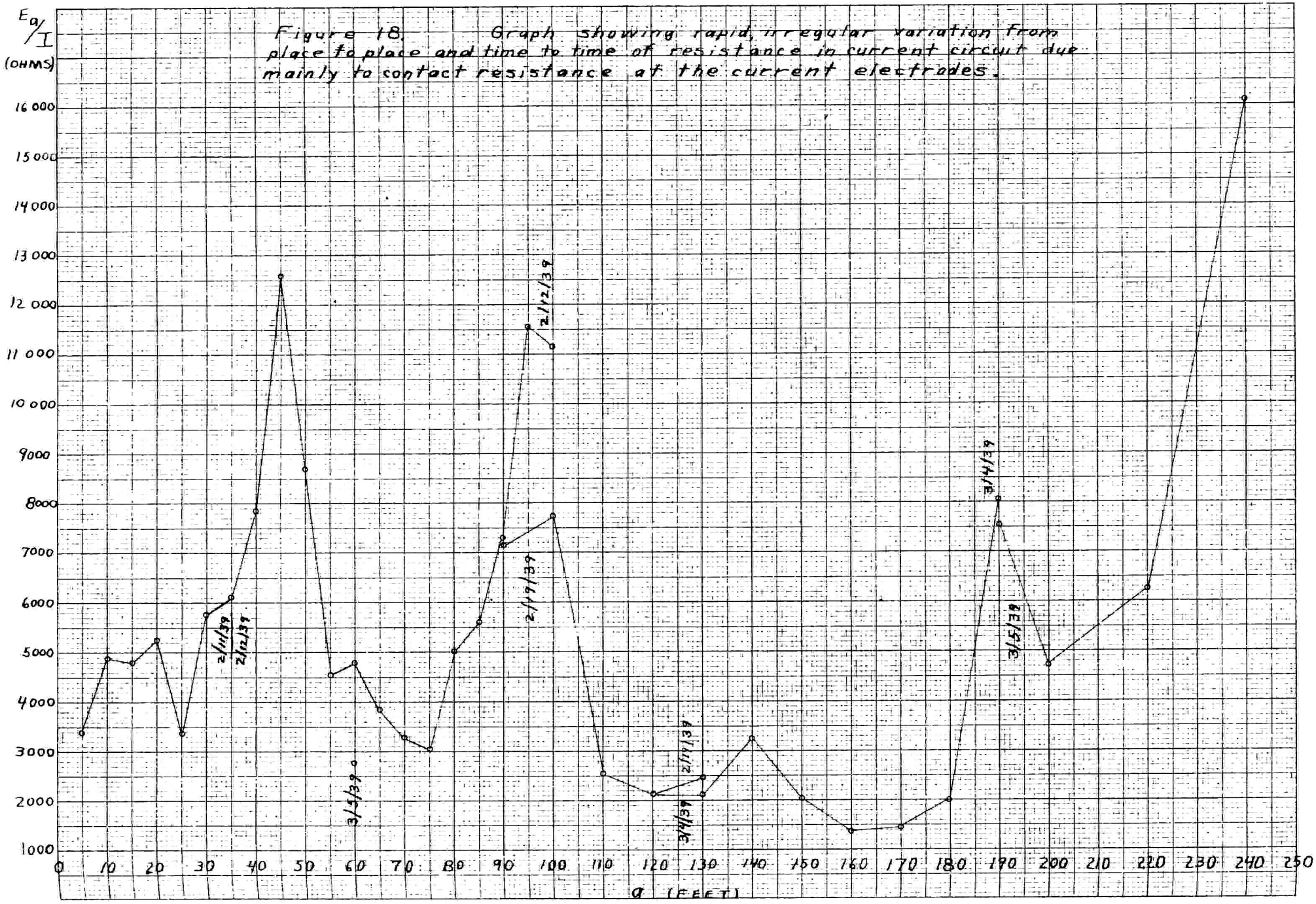
Figure 18. Graph showing rapid, irregular variation from place to place and time to time of resistance in current circuit due mainly to contact resistance at the current electrodes.
E_a/I (OHMS)
16 000
15 000
14 000
13 000
12 000
11 000
10 000
9000
8000
7000
6000
5000
4000
3000
2000
1000
0
10
20
30
40
50
60
70
80
90
100
110
120
130
140
150
160
170
180
190
200
210
220
230
240
250
a (FEET)
2/11/39
2/12/39
2/12/39
2/19/39
3/4/39
3/4/39
3/4/39
3/5/39

has prevented the measuring of variation of ground resistance with two electrodes.

A few measurements of the potential difference existing between the porous pots with no current applied were made when it was noticed that the values of E differed greatly in the two directions. This potential difference ran as high as 50 millivolts with the pots about 250 feet apart.

The identities of the porous pot were kept by patting a different number of pieces of adhesive tape around the terminal of each. Polarization potentials between the pots were checked from time to time by interchanging the pots, and found to be of the order of one or two millivolts, not large enough to make any appreciable error in the values of resistivity. The data obtained in this work are listed in Table II at the end of the chapter.

Mr. Lohman's curve and the writer's are compared in PLATE V. The resistivity values of the latter are lower, and much less regular, and their general trend is a straight line about tangent to Mr. Lohman's curve for electrode spacings of about 200 feet. The higher Gish-Rooney values might seem to contradict the test of Eve and Keys at Fisher Hill[a], New York, where the porous pot values were higher, but it is not improbable that the heavy rains just before the porous pot survey at Hastings Ranch sufficiently watered the ground to reduce the resistivity well below the value at the time two years earlier when Mr. Lohman's test was made.

a) APPLIED GEOPHYSICS, 2ND. ED., 1933, P. 115

Plate V. Comparison of field curves from Hasting's ranch, near Sierra Madre.

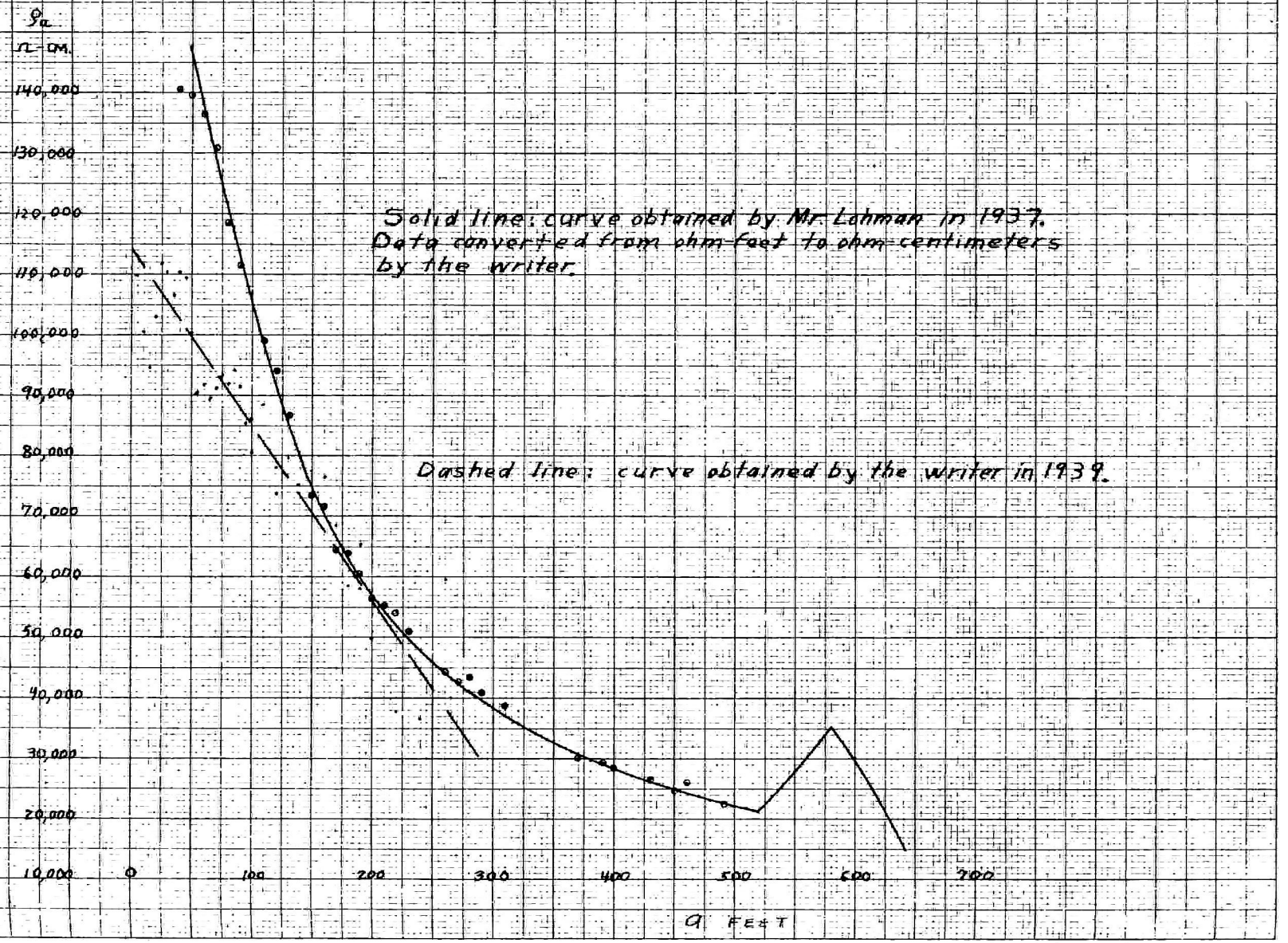

The much smoother curve obtained by Mr. Lohman may be explained by three differences in the field work. Mr. Lohman's work was all carried out in one day, while the writer's required five days over a three week period. It is possible that the ground resistivity varied somewhat from day to day. Also there was difficulty in reaching the correct balance point and this delay in getting the potentiometer balanced affects the value of resistivity determined, because due to polarization around the current electrodes and perhaps other causes, the values of E and I fluctuate. The fluctuations are more noticeable in E than in I, and fluctuations in the measured resistivity result, which would be eliminated by rapid commutation of the current, and reaching the balance point rapidly. Perhaps the largest cause of irregularity is the difficulty in finding the correct balance point when there is insufficient sensitivity. In some places the value taken for E was estimated as the center of a range of potentiometer settings of as much as 10 millivolts over which there was no deflection of the null instrument.

A discontinuity is to be noticed in Mr. Lohman's curve at an electrode separation of 520 feet. This is due to the fact that one of the current electrodes passed over the water main at that separation, but does not mean that the water main was at anywhere near that depth. The effect of such a main at so great a depth on the apparent resistivity of the large mass of ground

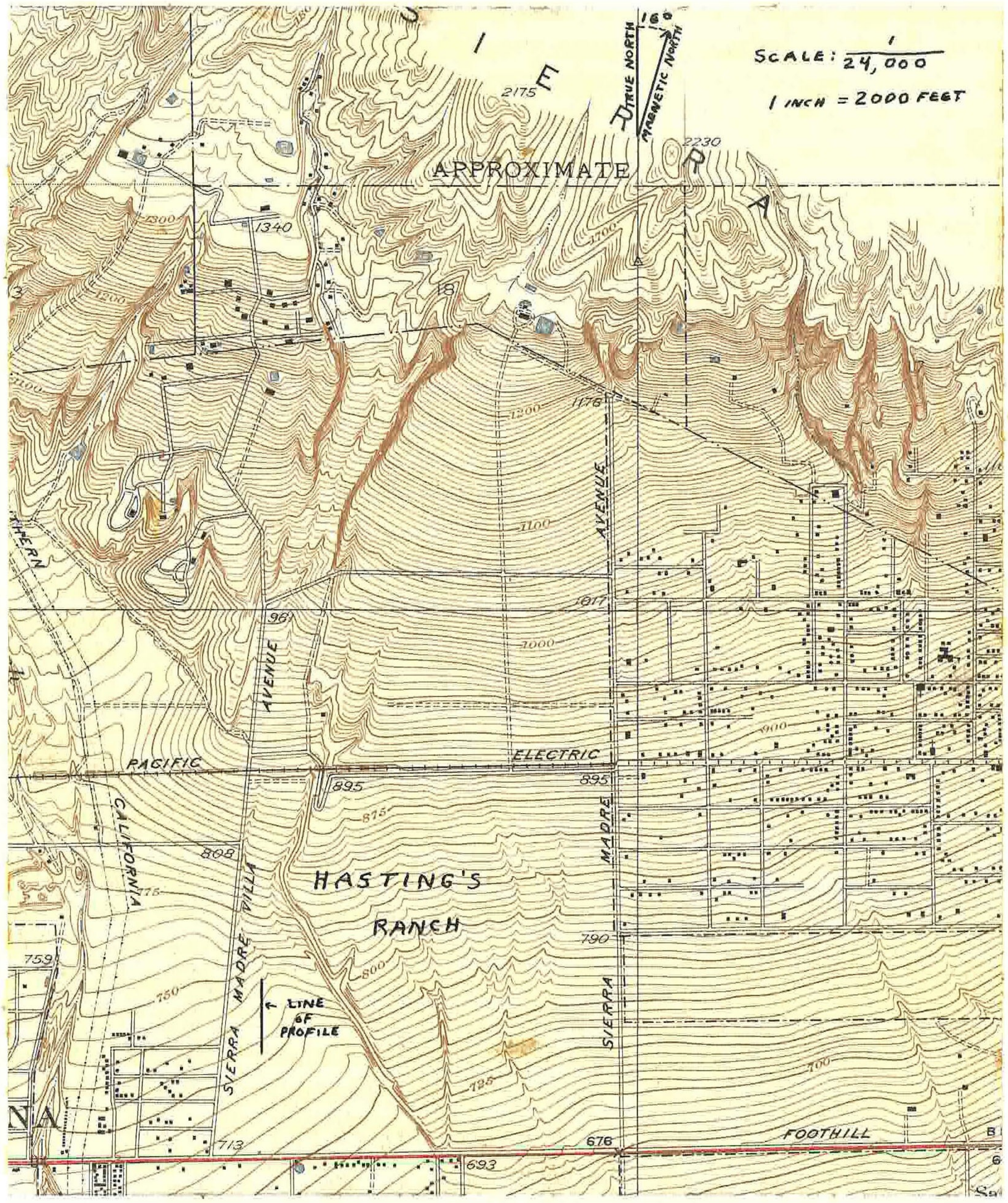

Map II. Part of the United States Geological Survey topographic map of the Sierra Madre Quadrangle, California, edition of 1928. The position of the profile at Hasting's Ranch on an alluvial fan at the foot of the San Gabriel Mountains is shown.

penetrated with a 520 foot spacing or 1560 feet between the current electrodes would be negligible.

Two layer interpretations of the two curves by Roman's superposition method (Chapter VII) do not show close agreement of either curve with a master curve, but a rough approximation gave values of depth to a second lower resistivity layer as about 120 feet for Mr. Lohman's curve, and 90 feet for the writer's. This is mentioned, not in support of the thesis that the difference corresponds with the rising of the water table during heavy rains that lowered also the resistivity of the upper layers, but as an example of the type of speculative interpretation to be avoided. Not only is there no empirical check available, but the location of the profile on an alluvial fan at the base of the San Gabriel Mountains (Map III) suggests that there may be a considerable number of lenses of sand and gravel of varying resistivity down to the depth of 100 feet, so that even if the greatest change of resistivity occurs at the water table, use of master curves based on the assumption of two and only two layers would be prohibited.

Field Work Near Delano

In April 1939, the writer was priviledged to accompany Mr. Michelberger and Dr. Peterson to Bakersfield, San Joaquin Valley headquarters of the United Geophysical Company. The portable battery, potentiometer, and amplifier units were taken along as well as two sets of current and potential electrodes, one to be lowered into

a seismograph shot hole, and the other to be used in a surface depth profile. The United Geophysical Company allowed the use of a shot hole several miles southeast of Delano, California and furnished the use of a truck for field use. A complete description of the whole survey is given in Martin Michelberger's Masters Thesis (Institute Division of Geological Sciences, 1939). For purposes of this paper it is sufficient to say that the four electrodes were placed at a constant spacing of about 3 feet along a hard rubber tube which was lowered into the shot hole on a cable in such a way that the depth of the center of the spread below the ground surface was known. This type of profile is identical with a surface traverse with Wenner configuration of a three foot separation with the exception that the electrodes become completely surrounded by ground (except for the negligible volume of the cylindrical hole) so that the apparent resistivity is given by the formula $\rho_a = 4\pi a E/I$, the expression for an infinite rather than semi-infinite homogeneous medium. The apparent resistivity in this case is approximately the actual resistivity if the ground is homogeneous in layers thick compared to the spread length, and at any rate reflects much more sharply the variation of true resistivity with depth.

A surface depth profile was also made with Wenner configuration and electrode separations of from 5 to 200 feet. A miniature traverse profile was made with 10 foot

electrode separation, and spread centers at 30 foot intervals from 270 feet north of the center point to 270 feet south of the center point of the north south line of electrodes of the depth profile. The purpose of this traverse to see whether horizontal variations in the surface resistivity might be causing breaks in the apparent resistivity values of the depth profile. The surface resistivity as measured with the 10 foot spacing was found to be quite uniform along most of the length of the profile and no correlation was found between surface variations and apparent resistivity in the depth profile. The data are tabulated in Table III at the end of the chapter, and shown graphically in the curves of Figure 19. Curve 1 is the apparent resistivity-depth curve obtained with electrodes in the hole. Curve 2 is the apparent resistivity-electrode separation curve for the surface depth profile. Curve 3 is the apparent resistivity-spread location curve for the traverse profile, and the set of curves 4, is derived from Curve 3 and shows the surface resistivity value for each electrode corresponding to each electrode separation in the depth profile. Curve 1 shows us the depth to the level of water in the hole, found by lowering the electrodes from the surface until there was a sudden sharp increase in the applied current with the applied battery voltage kept constant, to be fifty feet. It also shows a rapid variation of resistivity with depth below the water level, suggesting the presence of numerous layers of ground with different resistivities. It shows also, an average resistivity of

Figure 19. Curves from data obtained near Delano, California.

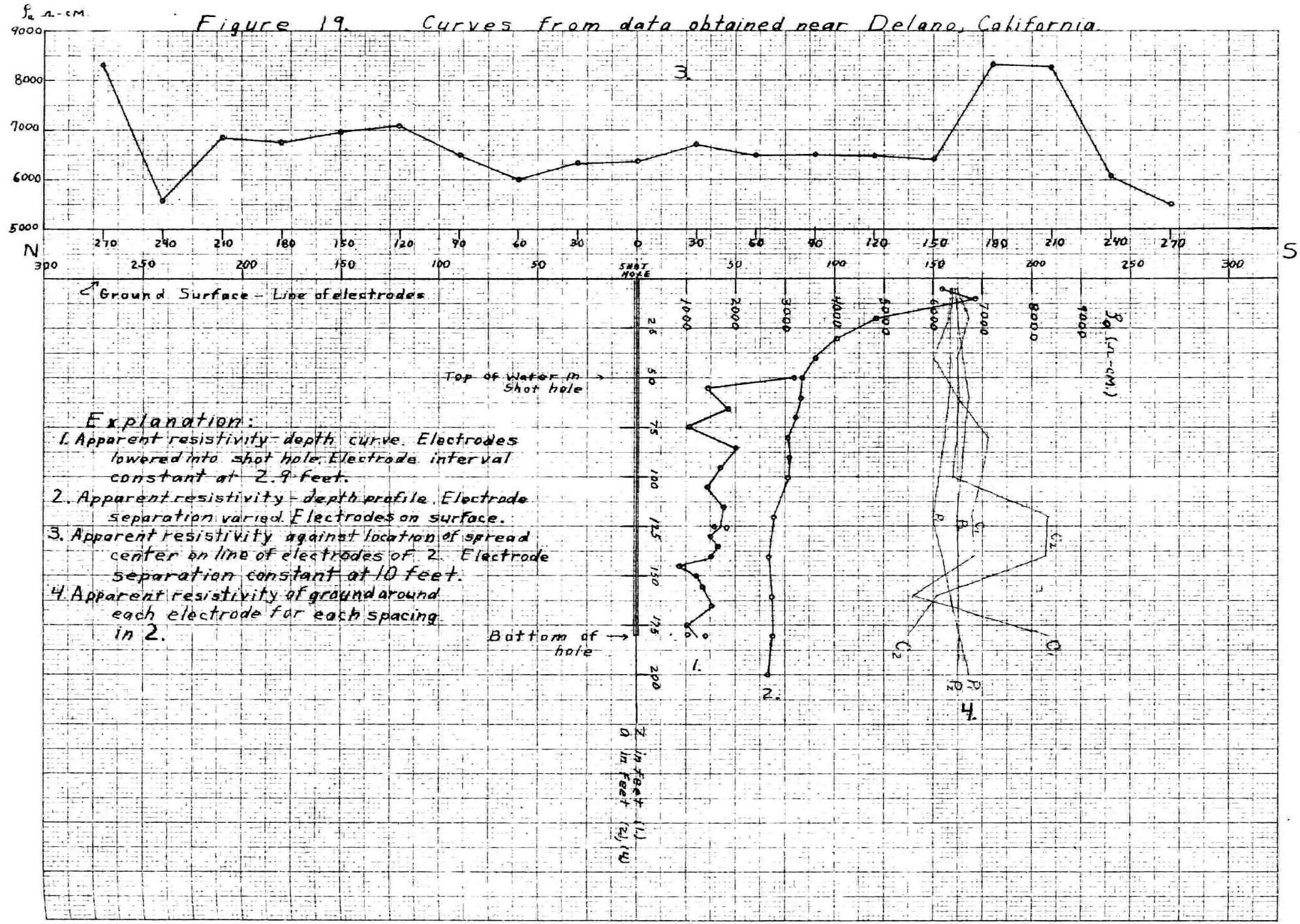

Explanation:

1. Apparent resistivity–depth curve. Electrodes lowered into shot hole. Electrode interval constant at 2.9 feet.
2. Apparent resistivity–depth profile. Electrode separation varied. Electrodes on surface.
3. Apparent resistivity against location of spread center on line of electrodes of 2. Electrode separation constant at 10 feet.
4. Apparent resistivity of ground around each electrode for each spacing in 2.

10 to 15 ohm-meters for ground below the water level. Comparison with curve 2 shows the latter to be much smoother illustrating how small the effect of a change of resistivity at depth is on the apparent resistivity of the whole ground down to and including that depth. It may also be seen that the value of apparent resistivity at the longer electrode separations, corresponding to greater depths of penetration are about twice as great as for the hole survey. This is due in part to the fact that the water in the hole added during drilling may raise the water level there above the regional water table so that the hole electrodes were surrounded by abnormally wet ground, in part to the fact that the hole is lined with a low resistivity layer of drilling mud, and finally to the fact that the electrodes in the hole no longer are greatly influenced by the presence of the higher resistivity surface layer while the apparent resistivity of the surface profile is.

The shape of the surface depth curve would suggest a three layer interpretation with a second layer at shallow depth of resistivity greater than the surface layer overlying the more conductive deeper ground. Insufficient data at the critical electrode separation of the turning point are available for making a three layer interpretation, and it is likely that the resistivity value at the shortest spacing is too low, as the salt water and copper sulphate solutions used to cut down contact resistance may have lowered appreciably the

resistivity of the volume of ground measured with the five foot spacing. Two layer interpretations made in Chapter VII for purpose of illustrating various methods show a depth to the interface of 10 to 15 feet, but in the absence of confirmatory data the presence of a lithologic boundary at that depth is problematical.

Field Work Near Victorville, California

The final field tests were made early in June 1939 at the suggestion of Dr. Maxson. The geologic problem was to determine whether the buried portions of pediment surfaces towards the edge away from the higher portions of the bed rock on which they are cut are convex or concave upwards. The elevation of the surface of the alluvium obscuring the bedrock surface is known from surface mapping. If the depth to bedrock below the surface of alluvium can be determined, the elevation on top of the bedrock is found by subtracting the thickness of alluvium from the elevation of the alluvium surface, and contours of the bedrock surface from this information would show the shape of the pediment surface. Dr. Maxson chose an area for this investigation 3 or 4 miles north of Victorville, southeast of Oro Grande and east of the Mojave River (Map III). He and Mr. L. A. Lewis accompanied the writer on a trip to the area in which a program of field work was outlined. This field work was carried out in the four days June 4 through June 7, 1939, as a preliminary investigation to see whether satisfactory results could be expected from the resistivity method. The work

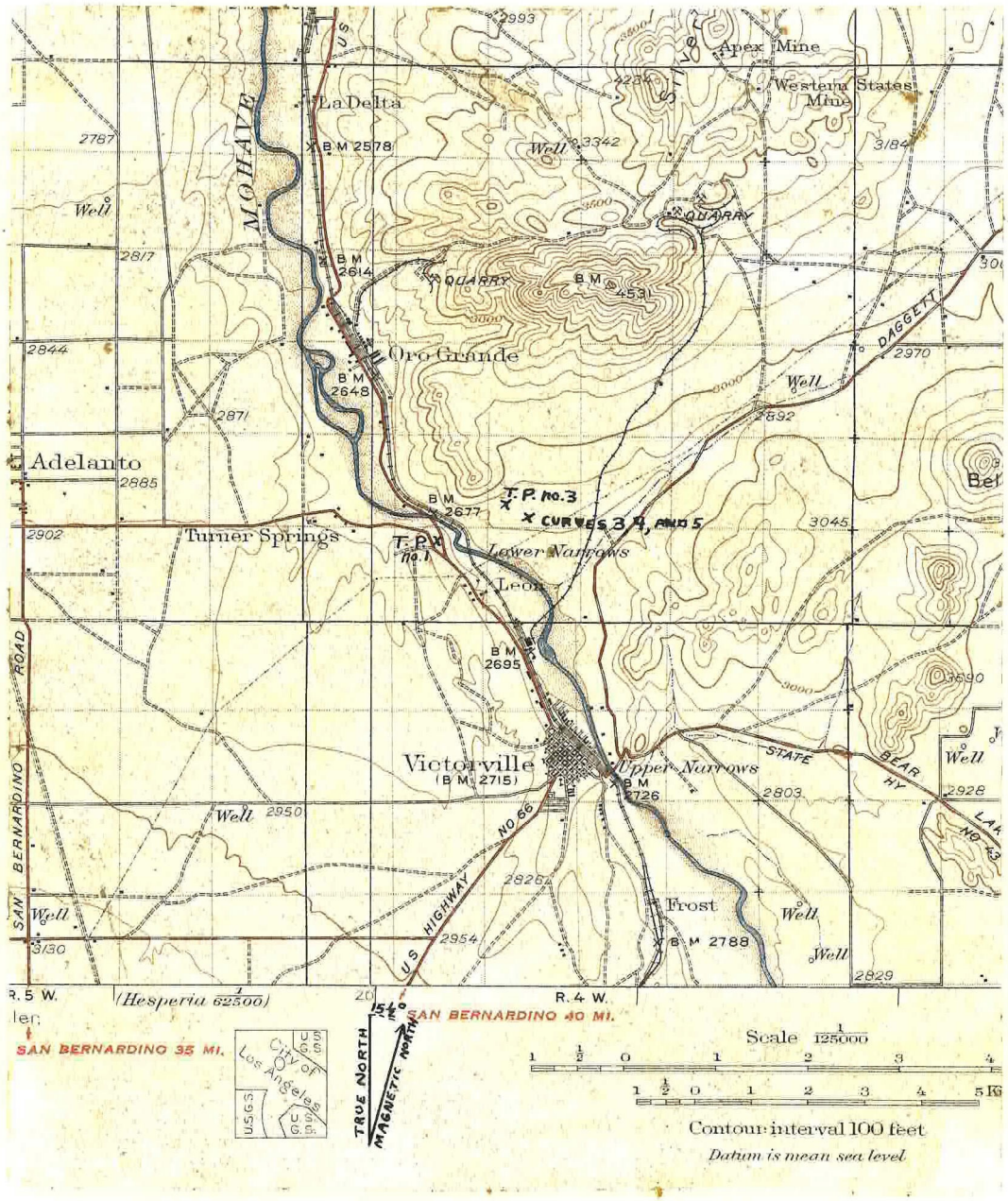

Map III. Part of the United States Geological Survey topographic map of the Barstow Quadrangle, California, edition of 1934. Crosses indicate the points at which resistivity measurements were made.

consisted of five depth profiles, the first at a point where the depth to the granite bedrock was known, to give a check on values reached by theoretical interpretation. The second profile was made on an exposure free of alluvial covering to determine directly the resistivity of the granite basement. The other three tests were made at typical points in the area to see whether smooth curves susceptible of theoretical treatment would be obtained. The data from these profiles are given in Table IV at the end of the chapter, and the apparent resistivity-electrode separation curves are plotted to a log log scale in Figures 32, 34, 35, and 36 below. Test Point no. 1 (see Map III) is located some distance from the other points and across the Mojave River from them. The profile was laid out in a roughly north-south direction parallel to an adjacent road cut in which the section below the electrodes was exposed. This section showed the bed rock contact to be 16 feet below the ground surface on which the electrodes were placed. Unfortunately, no similar exposure was available near the other points. The curve obtained at Test Point no. 1 shows the problem to be a three layer one electrically, with a lower resistivity layer intermediate between the surface layer and the bed rock. This renders interpretation of field curves more complicated and less certain than in the two layer case. The known depth to bed rock of 16 feet checks well with the 15 foot electrode separation at the turning point in agreement with Rooney's

empirical generalization, and with the depth found by superposition (Chapter VII) of 16 feet. However, it is likely that with similar curves at other points, where the minimum of the curve occurs at larger separations, the greater depth to bedrock may change the depth factor or ratio of bedrock depth to electrode separation from unity to some smaller value. In this case, if no further empirical check is available, it would seem safer to trust the theoretical solution if this differed from the electrode separation of the curve minimum.

Test Point no. 2, located about 100 feet from Test Point no. 1, was not profiled, even though it would give a desirable check on the first curve, because of the limited time available. With such slow progress (a whole day was required for the profile at Test Point no. 1) it seemed wiser to see whether curves obtained at points across the river, where it was most important to determine bed rock depth, would be of the same type or sufficiently smooth for theoretical treatment.

Test Point no. 3 was next occupied, and here the resistivity of the unweathered granite basement was found to be of the order of 500,000 ohm-centimeters, something like fifty times that of the overburden. It is interesting to note that the value determined for the bed rock resistivity in Chapter VII is between 25,000 and 50,000 ohm-centimeters, or only 1/10 to 1/20 as great. This suggests that where the bedrock is

Figure 17. The apparatus set up at Test Point no. 3 on granite near Victorville, California. Boulder dam power line in middle distance.

not exposed it may be decayed to some extent by weathering. A ratio of something like 5 to 1 in the resistivities of bedrock and surface gravels should be sufficient to give a pronounced bend in the field curves, even if the depth to the discontinuity should be at considerable depth.

Curve 3 was taken about 200 feet southeast of the nearest granite outcrop. It is a three layer curve like that at #1. Unfortunately measurements were made at too few diagnostic electrode separations, and the value of 68 feet found for the bedrock depth may be more in error than the values at the other points.

Curve 4 was taken at a point about 150 feet south of the center of the spread for Curve 3 and about 300 feet south east of the nearest granite outcrop. It is a 4 layer curve, and indicates a bed rock depth of about 60 feet.

Curve 5 was taken with a center point about 65 feet south of the center of that of Curve 4. This 3 layer curve indicates the bedrock to lie at a depth of about 50 feet.

The data from these tests are given in Table IV at the end of the chapter, and the results of interpretation of the curves are shown in Plate VI. The individual interpretations are discussed in Chapter VII below.

It is the opinion of the writer that this preliminary work indicates the probable success of the method in giving a qualitative answer to the question of the shape

Plate VI. Interpretation of field curves from near Victorville, California. Numbers in columns are resistivities in ohm-centimeters. Broken lines between columns are two of the possible positions of the overburden – "granite" contact within the zone of probable error in determining the depth of the contact.

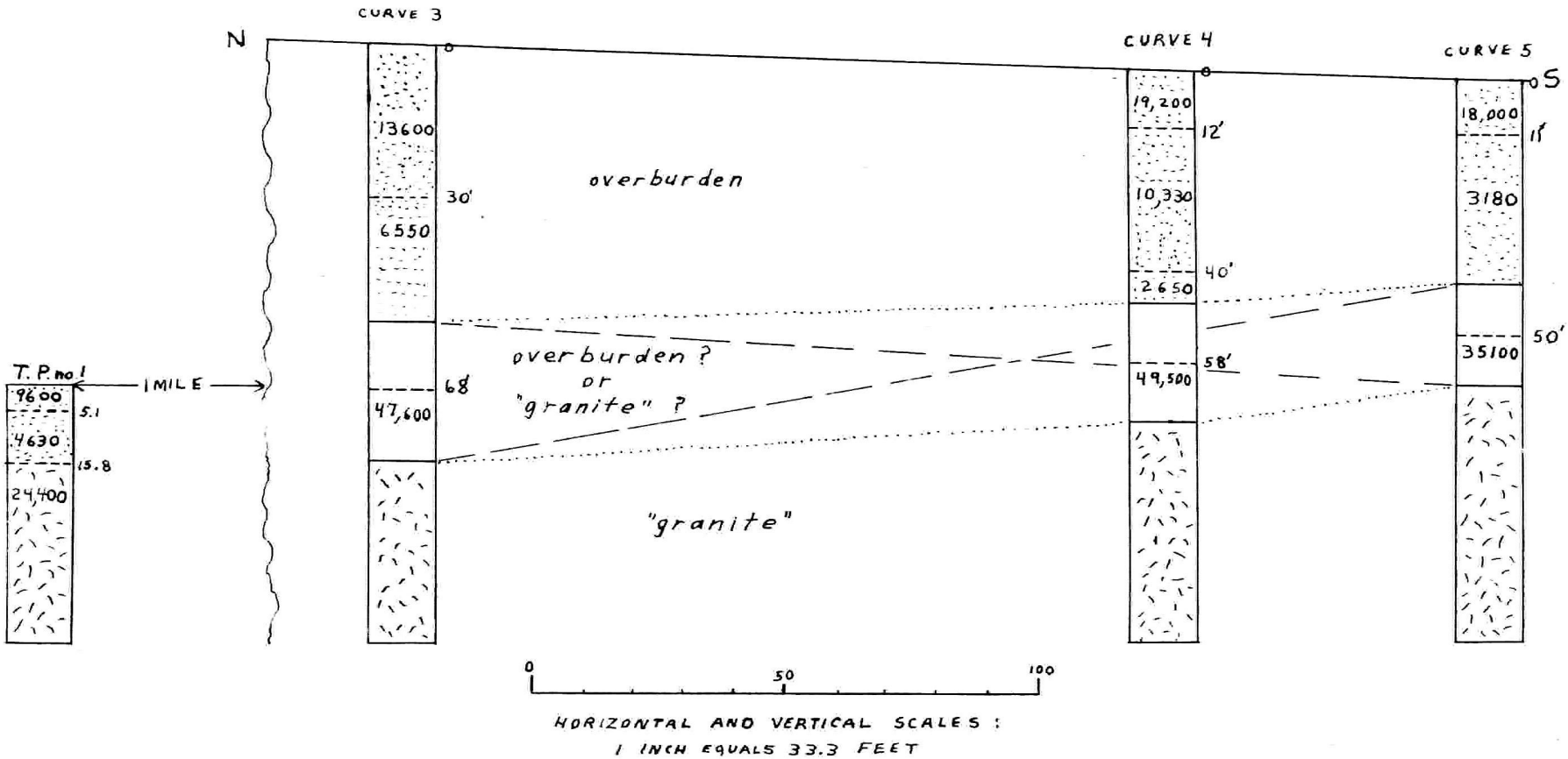

of the bed rock surface. Measurements made with sufficiently good apparatus, and with sufficient care should give the depth to bedrock within 10%. From this it should be possible to determine whether the surface is considerably concave upward, considerably concave downwards or about plane, or whether the surface is step like or irregular. Any future work should be carried out with a better potentiometer and null instrument as suggested in Chapter V. Field curves should be plotted on logarithmic paper in the field so that a sufficient number of accurate values will be had at diagnostic electrode spacings. All the preliminary curves were taken with the electrodes in a roughly east-west line about parallel to the topographic strike. In future work it would be desirable to take spreads in several azimuths at each of a few points to see how much symmetry there is in the resistivity distribution. Points should be accurately profiled at intervals of about $\frac{1}{8}$ mile on a grid with sides parallel to the expected dip and strike of the bedrock. These would be far enough apart so that if there is any pronounced divergence between the slopes of the alluvium and bedrock surfaces it should show up in variations in depth to bed rock large compared to the probable error in determining the depth. To check on the regularity at intermediate points profiles could be run fairly rapidly using only three or four values of electrode separation.

TABLE II

Data from Hastings Ranch near Sierra Madre, California

Part 1. Field observations

Explanation of symbols:

L	Distance between current electrodes in feet
a	Distance between potential electrodes in feet
E_a	Voltage applied between current electrodes
I	Current between current electrodes in amperes
E	Potential measured between potential electrodes in volts
Dir.	Direction from positive to negative electrodes
R_{RB}	Setting of rheostat in potentiometer circuit in ohms
E_{SC}	Measured potential of standard cell in volts

L	a	E_a	I	E	Dir	R_{RB}	E_{SC}
15	5	22.5	0.0070	0.802	N-S	150.0	1.0187
		45	0.0125	1.425			
		45	0.0125	1.43 ?	S-N		
		22.5	0.0070	0.815			1.0215
30	10	90	0.0185	0.976	N-S	149.3	1.0187
		135	0.0280	1.460			
		135	0.0275	1.434	S-N		
		90	0.0180	0.947?			1.0193
45	15	135	0.0285	0.940?	N-S	149.0	1.0187
		225	0.0475	1.562?			
		225	0.0470	1.540?	S-N		
		225	0.0465	1.524			
		135	0.0275	0.916			1.0191
60	20	202.5	0.0386	1.04 ?	N-S	148.8	1.0187
		292.5	0.0565	1.515?			
		292.5	0.0567	1.521	S-N		
		292.5	0.0545	1.464			
		202.5	0.0373	1.011			1.0190
75	25	135	0.0405	0.947	N-S	148.7	1.0187
		180	0.0537	1.264			
		180	0.0535	1.242	S-N		
		180	0.0527	1.232			
		135	0.0395	0.921			1.0190
90	30	270	0.0467	0.907	N-S	148.5	1.0187
		360	0.0623	1.196			
		360	0.0623	1.195	S-N		
		270	0.0465	0.887			1.0189
105	35	0	0	0.0003	N-S	148.4	1.0187
		157.5	0.0263	0.420			
		360	0.0593	0.939			
		360	0.0580	0.910	S-N		
		157.5	0.0257	0.408			1.0191

Above measurements made on February 11, 1939

TABLE II

Part 1. Continued

Measurements made on February 12, 1939

L	a	E_a	I	E	Dir	R_{RB}	Esc
120	40	202.5	0.0265	0.387	N-S	146.6	1.0187
		360	0.0470	0.678			
		360	0.0445	0.642	S-N		
		202.5	0.0250	0.356			1.0187
135	45	180	0.0143	0.188	N-S	146.6	1.0187
		360	0.0283	0.366			
		360	0.0287	0.357	S-N		
		180	0.0143	0.175			1.0190
150	50	180	0.0207	0.232	N-S	146.5	1.0187
		360	0.0405	0.441			
		360	0.0425	0.421	S-N		
		180	0.0207	0.211			
		180	0.0205	0.216			1.0190
165	55	180	0.0405	0.364	N-S	146.4	1.0187
		360	0.0797	0.696			
		360	0.0790	0.694			
		360	0.0775	0.653	S-N		
		180	0.0395	0.330			1.0187
180	60	180	0.0387	0.326	N-S	146.4	1.0187
		360	0.0703	0.629			
		360	0.0745	0.560	S-N		
		180	0.0391	0.283			1.0192
195	65	180	0.0473	0.366	N-S	146.2	1.0187
		360	0.0913	0.687			
		360	0.0918	0.655	S-N		
		180	0.0470	0.316			1.0187
210	70	135	0.0422	0.286	N-S	146.5	1.0187
		315	0.0950	0.655			
		315	0.0930	0.643	S-N		
		135	0.0408	0.272			1.0194
225	75	135	0.0472	0.317	N-S	146.2	1.0187
		270	0.0856	0.559			
		270	0.0861	0.578	S-N		
		135	0.0439	0.273			1.0187
240	80	180	0.0360	0.214	N-S	146.1	1.0187
		360	0.0680	0.431			
		360	0.0722	0.434	S-N		
		180	0.0378	0.218			1.0191

TABLE II

Part 1. Continued

L	a	E_a	I	E	Dir	R_{RB}	E_{SC}	
255	85	180	0.0327	0.206	N-S	145.9	1.0187	
		360	0.0610	0.379				
		360	0.0635	0.354	S-N			
		180	0.0332	0.170			1.0189	
270	90	180	0.0250	0.150	N-S	145.8	1.0187	
		360	0.0485	0.264				
		360	0.0490	0.254	S-N			
		180	0.0245	0.116			1.0187	
285	95	270	0.0235	0.108	N-S	145.6	1.0187	
		360	0.0305	0.148				
		360	0.0320	0.139	S-N			
		270	0.0228	0.112			1.0191	
300	100	180	0.0180	0.092	N-S	145.3	1.0187	
		360	0.0315	0.146				
		360	0.0310	0.146	S-N			
		180	0.0155	0.055			1.0190	
		Measurements made on February 19, 1939						
270	90	247.5	0.0365	0.181	N-S	145.9	1.0187	
		360	0.0530	0.292				
		360	0.0483	0.249	S-N			
		247.5	0.0327	0.183			1.0196	
	45	247.5	0.0330	0.089	N-S	145.6	1.0187	S#
		247.5	0.0310	0.089	S-N			
		360	0.0465	0.138				
		360	0.0523	0.146	N-S			
		360	0.0525	0.123				N
		360	0.0490	0.114	S-N		1.0195	
300	100	225	0.0300	0.133	N-S	145.3	1.0187	
		360	0.0480	0.217				
		360	0.0447	0.180	S-N			
		225	0.0283	0.116			1.0192	
	50	360	0.0485	0.115	N-S	145.1	1.0187	S
		360	0.0483	0.110	S-N			
		360	0.0443	0.088				N
		360	0.0485	0.097	N-S		1.0187	
330	110	90	0.0353	0.155	N-S	144.9	1.0187	
		225	0.0835	0.337				
		225	0.0925	0.339	S-N			
		90	0.0353	0.158				

N and S in last column indicate whether north or south half of spread is tested when Lee partition method is used.

TABLE II

Part 1. Continued

L	a	Ea	I	E	Dir	R_{RB}	E_{SC}	
330	55	225	0.0833	0.175	N-S	144.9		S
		225	0.0863	0.170	S-N		1.0198	
		225	0.0790	0.126	N-S	144.6	1.0187	
		225	0.0865	0.148	S-N		1.0190	
360	120	90	0.0425	0.145?	N-S	144.4	1.0187	
		90	0.0423	0.124?	S-N			
		180	0.0833	0.274				
		180	0.0845	0.276	N-S		1.0189	
	60	180	0.0835	0.157	N-S	144.3	1.0187	S
		180	0.0840	0.150	S-N			
		180	0.0818	0.148?				N
		180	0.0800	0.131	N-S		1.0189	
390	130	112.5	0.0462	0.157	N-S	144.2	1.0187	
		225	0.0885	0.328				
		225	0.0895	0.353	S-N			
		112.5	0.0465	0.124				
	65	225	0.0888	0.194	N-S			S
		225	0.0890	0.135				N
		225	0.0898	0.134	S-N		1.0188	
	Measurements made on March 4, 1939							
360	120	90	0.0425	0.139	N-S	146.7	1.0187	
		180	0.0830	0.280				
		180	0.0805	0.274	S-N			
		90	0.0410	0.138			1.0195	
390	130	157.5	0.0776	0.290	N-S	146.5	1.0187	
		157.5	0.0750	0.180?	S-N			
		360	0.1630	0.500?				
		360	0.1630	0.600?	N-S		1.0197	
420	140	157.5	0.0470	0.184	N-S	145.9	1.0187	
		157.5	0.0487	0.086	S-N		1.0182	
		157.5	0.0475	0.176	N-S	146.0	1.0187	
		157.5	0.0500	0.086	S-N		1.0188	
450	150	180	0.0885	0.287	N-S	145.9	1.0187	
		180	0.0885	0.200?	S-N		1.0187	
		180	0.0895	0.286	N-S	145.7	1.0187	
		180	0.0905	0.189	S-N		1.0192	
480	160	135	0.0970	0.264	N-S	145.2	1.0187	
		135	0.0975	0.227	S-N		1.0178	
510	170	135	0.0925	0.227	N-S	145.3	1.0187	
		135	0.0930	0.167	S-N			
		90	0.0640	0.119				
		90	0.0640	0.144	N-S		1.0189	

TABLE II

Part 1. Concluded

L	a	E_a	I	E	Dir	R_{RB}	E_{SC}	
540/	180	90	0.0445	0.083	N-S	145.2	1.0187	
		180	0.0878	0.170				
		180	0.0880	0.156	S-N			
		90	0.0450	0.060?			1.0187	
570	190	180	0.0223	0.058	N-S	144.7	1.0187	
		360	0.0450	0.100?				
		180	0.0223	0.017	S-N			
		360	0.0440	0.043			1.0183	
	Measurements made on March 5, 1939							
570	190	0		0.035	N-S			
		360	0.0467	0.125		144.9	1.0187	
		360	0.0465	0.057	S-N			
		360	0.0500	0.109	N-S			
	95	360	0.0465	0.053				S
		360	0.0495	0.004?	N-S		1.0192	
600	200	0		0.04 ?	N-S			
		292.5	0.0615	0.082	S-N	143.8	1.0187	
		292.5	0.0613	0.081	N-S			
		180	0.0390	0.050?				
	100	180	0.0390	0.030				S
		180	0.0390	0.032			1.0187	N
660	220	360	0.0575	0.053	N-S	143.6	1.0187	
		360	0.0573	0.052	S-N		1.0187	
720	240	360	0.0215	0.02 ?				
		360	0.0225	0.016?	N-S			
		360	0.0230	0.081#		314.8	1.5980	
		360	0.0225	0.064#	S-N		1.5965	
780	260	360	0.0482	0.0677#	S-N	315.6	1.5980	
		360	0.0502	0.111#	N-S			
		270	0.0375	0.085#				
		270	0.0355	0.058#	S-N		1.5975	
180	60	270	0.0965	1.200#	N-S	316.0	1.5980	
		270	0.0965	0.768		144.0	1.0187	
		270	0.0973	0.745	S-N			
	30	270	0.0967	0.372				S
		270	0.0975	0.393	N-S			
		270	0.0965	0.370	S-N			N
		270	0.0978	0.375	N-S			

Potentiometer reading must be multiplied by 1.0187/ E_{SC} to get correct value of E because slide wire current was decreased in order to get bigger values easier to measure.

TABLE II

Part 2. Apparent resistivities.

Symbols:

L. Distance between current electrodes in feet.

a. Distance between consecutive potential electrodes in feet.

R_{av}. Average value of R (equals E/I) from values in Part 1 for each configuration, expressed in ohms.

ρ_a. Apparent resistivity in ohm-centimeters. Computed from the formulae $\rho_a = k(2/3)\pi LR_{av}$ for Wenner configuration (L = 3a) and $\rho_a = k(4/3)\pi LR_{av}$ for Lee configuration (L = 6a). k equals 30.48 to convert feet to centimeters.

Con. Configuration-
W. Wenner
L. Lee
S. South part of spread
N. North part of spread

L	a	R_{av}	ρ_a ohm-cm.	Con		
15	5	114.8	109,900	W		
30	10	52.4	100,400	W		
45	15	33.0	94,700	W		
60	20	26.9	103,100	W		
75	25	23.4	112,000	W		
90	30	19.2	110,200	W		
105	35	15.9	106,500	W		2/11/39
120	40	14.4	110,200	W		2/12/39
135	45	12.7	109,400	W		
150	50	10.5	100,400	W		
165	55	8.6	90,500	W		
180	60	8.0	91,900	W		
195	65	7.2	89,600	W		
210	70	6.8	91,200	W		
225	75	6.5	93,300	W		
240	80	6.0	91,900	W		
255	85	5.8	94,400	W		
270	90	5.3	91,300	W		
285	95	4.7	85,500	W		
300	100	4.5	86,200	W		2/12/39
270	90	5.3	91,300	W		2/19/39
	45	2.8	96,400	L	S	
	45	2.3	79,200	L	N	
300	100	4.2	80,400	W		
	50	2.4	91,900	L	S	
	50	2.0	76,600	L	N	
330	110	4.2	88,400	W		
	55	2.0	84,300	L	S	
	55	1.6	67,400	L	N	
360	120	3.2	73,500	W		
	60	1.8	82,700	L	S	
	60	1.7	78,100	L	N	
390	130	3.4	84,600	W		
	65	2.2?	109,500?	L	S	
	65	1.5	82,900	L	N	2/19/39

TABLE II

Part 2. Concluded

L	a	R_{av}	ρ_a ohm-cm	Con		
360	120	3.4	78,100	W		3/4/39
390	130	3.2?	79,600?	W		
420	140	2.8	75,100	W		
450	150	2.7	77,600	W		
480	160	2.5	76,600	W		
510	170	2.1	68,400	W		
540	180	1.7?	58,600?	W		
570	190	1.6	58,200	W		
570	190	1.8?	65,500?	W		3/5/39
	95	0.6?	43,700?	L	S	
600	200	1.3	49,800	W		
	100	0.8?	61,300?	L	S	
	100	0.8?	61,300?	L	N	
660	220	0.9	37,900	W		
720	240	0.8?	36,800?	W		
		or 2.0??	92,000??			
780	260	1.2	59,800	W		
180	60	7.8	89,600	W		
	30	3.9	89,600	L	S	
	30	3.8	87,300	L	N	

TABLE III

Data obtained near Delano, California

Part 1. Surface depth profile

Symbols:

L	Distance between current electrodes in feet.
a	Distance between potential electrodes in feet.
I	Current through current electrodes in amperes.
E	Potential difference between potential electrodes in volts.
Dir	Direction from positive to negative electrodes.
R_{av}	Average value of ratio E/I for each value of L. (in Ω).
ρ_a	Apparent resistivity in ohm-centimeters = 191.5 aR_{av}.

L	a	I	E	Dir	R_{av}	ρ_a (Ω-cm)
15	5	0.188	1.217	N-S		
		0.135	1.086	S-N	#	
		0.203	1.308	N-S		
		0.188	1.206	S-N		
					6.45	6,180
30	10	0.148	0.525	N-S		
		0.115	0.422	S-N		
		0.248	0.874	N-S		
		0.188	0.670	S-N		
		0	0.003	S-N	##	
					3.58	6,860
60	20	0.132	0.165	N-S		
		0.133	0.172	S-N		
		0.233	0.287	N-S		
		0.243	0.303	S-N		
		0	0.003	S-N	##	
					1.26	4,830
90	30	0.128	0.087	N-S		
		0.128	0.094	S-N		
		0.197	0.133	N-S		
		0.197	0.140	S-N		
		0	0.004	S-N	##	
					0.70	4,025
120	40	0.123	0.062	N-S		
		0.118	0.053	S-N		
		0.195	0.095	N-S		
		0.190	0.086	S-N		
		0	0.003	N-S	##	
					0.47	3,605
150	50	0.118	0.050	N-S		
		0.112	0.034	S-N		
		0.423	0.143	N-S		
		0.412	0.138	S-N		
		0	0.007	N-S	##	
					0.35	3,353

not included in R_{av}. ## natural and polarization potential

TABLE III

Part 1. Continued

L	a	I	E	Dir	R_{av}	S_a (a-cm.)
180	60	0.142	0.046	N-S		
		0.138	0.036	S-N		
		0.365	0.111	N-S		
		0.373	0.104	S-N		
		0	0.004	N-S		
					0.29	3,333
210	70	0.122	0.030	N-S		
		0.123	0.030	S-N		
		0.364	0.090	N-S		
		0.366	0.089	S-N		
		0	0.0006	N-S		
					0.24	3217
240	80	0.197	0.052	N-S		
		0.197	0.029	S-N		
		0.387	0.090	N-S		
		0.384	0.067	S-N		
		0	0.011	N-S		
					0.20	3064
270	90	0.292	0.042	N-S		
		0.296	0.063	S-N		
		0.573	0.112	N-S		
		0.558	0.089	S-N		
					0.18	3104
300	100	0.298	0.048	N-S		
		0.303	0.048	S-N		
		0.516	0.082	S-N		
		0.498	0.077	N-S		
		0	0.0014	S-N		
					0.16	3064
360	120	0.222	0.026	N-S		
		0.222	0.028	S-N		
		0.552	0.068	N-S		
		0.547	0.069	S-N		
		0	0.0007	S-N		
					0.12	2758
420	140	0.233	0.024	N-S		
		0.228	0.024	S-N		
		0.507	0.052	N-S		
		0.492	0.051	S-N		
					0.10	2683
480	160	0.228	0.024	N-S		
		0.232	0.018	S-N		
		0.533	0.051	N-S		
		0.588	0.046	S-N		
		0	0.003	N-S		
					0.09	2758

TABLE III

Part 1. Concluded

L	a	I	E	Dir	R_{av}	ρ_a (a-cm.)
540	180	0.348	0.028	N-S		
		0.348	0.025	S-N		
		0.663	0.057	N-S		
		0.653	0.049	S-N		
					0.08	2758
600	200	0.328	0.024	N-S		
		0.318	0.020	S-N		
		0.646	0.046	N-S		
		0.618	0.041	S-N	0.07	2682

Above measurements made April 20, 1939

Part 2. Surface traverse profile, April 21, 1939

Wenner configuration, L constant at 30 feet. Locus is distance of center of set up in feet north or south of center point of measurements in Part 1.

Locus	I	E	Dir	R_{av}	ρ_a (a-cm.)
0	0.248	0.832	N-S		
	0.245	0.825	S-N		
	0.462	1.534	S-N		
	0.435	1.452	N-S		
	0.423	1.422	S-N		
	0	0.0034	S-N		
				3.35	6420
30 S	0.282	0.989	N-S		
	0.288	1.014	S-N		
	0.364	1.278	N-S		
	0.377	1.316	S-N		
	0	0			
				3.51	6730
60 S	0.202	0.683	N-S		
	0.198	0.682	S-N		
	0.347	1.172	N-S		
	0.343	1.161	S-N		
	0	0.003	S-N		
				3.39	6500
90 S	0.187	0.639	N-S		
	0.192	0.652	S-N		
	0.402	1.365	N-S		
	0.417	1.409	S-N		
	0	0.002	S-N		
				3.40	6515

TABLE III

Part 2. Continued

Locus	I	E	Dir	R_{av}	ρ_a (ohm-cm.)
120 S	0.226	0.767	N-S		
	0.221	0.772	S-N		
	0.431	1.482	N-S		
	0.431	1.481	S-N		
	0	0.001	S-N		
				3.39	6500
150 S	0.248	0.830	N-S		
	0.247	0.825	S-N		
	0.416	1.386	N-S		
	0.416	1.385	S-N		
	0	0.0006	N-S		
			—	3.34	6410
180 S	0.198	0.861	S-N		
	0.197	0.851	N-S		
	0.287	1.254	S-N		
	0.288	1.250	N-S		
	0	0.003	S-N		
				4.34	8330
210 S	0.198	0.868	N-S		
	0.202	0.867	S-N		
	0.318	1.314	N-S		
	0.323	1.316	S-N		
	0	0.003	N-S		
				4.32	8280
240 S	0.258	0.817	N-S		
	0.256	0.810	S-N		
	0.408	1.290	N-S		
	0.398	1.270	S-N		
	0	0.002	S-N		
				3.17	6080
270 S	0.223	0.637	N-S		
	0.228	0.656	S-N		
	0.471	1.343	N-S		
	0.498	1.429	S-N		
	0	0.003	S-N	2.87	5510
0	0.303	1.009	N-S		
	0.298	0.996	S-N		
	0.414	1.368	N-S		
	0.415	1.362	S-N		
	0	0.001	N-S	3.31	6350
30 N	0.228	0.756	N-S		
	0.228	0.747	S-N		
	0.332	1.094	N-S		
	0.332	1.088	S-N		
	0	0.004	N-S	3.30	6330

TABLE III

Part 2. Concluded

Locus	I	E	Dir	R_{av}	ρ_a (Ω-cm.)
60 N	0.238	0.746	N-S		
	0.240	0.753	S-N		
	0.417	1.301	N-S		
	0.422	1.316	S-N		
	0	0.0025	S-N	3.13	6010
90 N	0.257	0.869	N-S		
	0.244	0.830	S-N		
	0.442	1.506	N-S		
	0.418	1.431	S-N		
				3.40	6520
120 N	0.292	1.081	N-S		
	0.292	1.084	S-N		
	0.398	1.476	N-S		
	0.398	1.473	S-N		
	0	0.005	S-N	3.71	7115
150 N	0.297	1.094	N-S		
	0.302	1.090	S-N		
	0.397	1.432	N-S		
	0.398	1.430	S-N		
	0	0.004	N-S	3.64	6980
180 N	0.182	0.646	N-S		
	0.182	0.642	S-N		
	0.398	1.416	N-S		
	0.396	1.389	S-N		
	0	0.001	S-N	3.54	6780
210 N	0.242	0.869	N-S		
	0.248	0.848	S-N	# Not included in Rav.	
	0.397	1.427	N-S		
	0.392	1.400	S-N		
	0	0.002	N-S	3.59	6880
240 N	0.282	0.832	N-S		
	0.278	0.806	S-N		
	0.457	1.336	N-S		
	0.452	1.309	S-N		
	0	0.005	N-S	2.92	5590
270 N	0.202	0.886	N-S		
	0.202	0.875	S-N		
	0.362	1.572	N-S		
	0.358	1.552	S-N	4.35	8330

TABLE III

Part 3. Summary of data from vertical traverse profile

Measurements made April 19, 1939 with constant Wenner spacing of 2.9 feet and electrodes lowered down seismograph shot hole at center of spread of resistivity depth profile in Part 1. Z is depth of center of electrodes below ground surface in feet. $\rho_a = 1111\ R_{av}$ ohm-cm.

Z	Rav	ρ_a (ohm-cm.)
181 (bottom)	1.25	1388
155	1.19	1322
105	1.34	1489
115	1.61	1789
125	1.42	1578
135	1.52	1689
145	0.89	988
155	1.18	1312
165	1.38	1533
175	0.92	1022
180 (bottom)	0.95	1057
155	1.20	1333
150	1.10	1222
145	0.79	878
140	1.36	1511
135	1.44	1600
130	1.34	1489
125	1.62	1800
115	1.59	1768
105	1.26	1400
95	1.53	1700
85	1.81	2013
75	0.95	1056
65	1.67	1857
55	1.27	1412
50 (water table)	2.86	3175

Observations made in the order listed.

TABLE IV

Data obtained near Victorville, California

Part 1. Resistivity-depth profile at Test Point 1.

Symbols:
- L — Distance between current electrodes in feet.
- a — Distance between potential electrodes in feet.
- I — Current through current electrodes in amperes.
- E — Voltage measured between potential electrodes.
- R_{av} — Average of the ratio E/I for each value of L in ohms.
- ρ_a — Apparent resistivity (equals 191.5 a R_{av}) ohm-centimeters.

L	a	I	E	Dir	R_{av}	ρ_a (Ω-cm.)	
6	2	0.070	1.562	N-S			
		0.070	1.547	S-N			
		0.050	1.130	N-S			
		0.051	1.132	S-N	22.3	8550	
18	6	0.066	0.443	N-S			
		0.055	0.373	S-N			
		0.139	0.929	N-S			
		0.133	0.910	S-N	6.78	7800	
30	10	0.084	0.272	N-S			
		0.075	0.242	S-N			
		0.129	0.422	S-N			
		0.141	0.463	N-S	3.255	6240	
39	13	0.242	0.560	N-S			
		0.233	0.522	S-N	2.275	5670	
	6.5	0.255	0.258	N-S			N
		0.254	0.229	S-N	0.955	4750	
	6.5	0.262	0.344	N-S			S
		0.257	0.343	S-N	1.320	6570	
45	15	0.282	0.575	N-S			
		0.248	0.457	S-N			
		0.120	0.251	N-S			
		0.127	0.234	S-N	1.95	5600	
51	17	0.252	0.428	S-N			
		0.328	0.574	N-S	1.725	5620	
	8.5	0.283	0.212	S-N			N
		0.325	0.265	N-S	0.782	5090	
	8.5	0.272	0.262	S-N			S
		0.282	0.269	N-S	0.958	6230	
60	20	0.288	0.511	N-S			
		0.300	0.528	S-N			
		0.116	0.211	S-N			
		0.093	0.158	N-S	1.765	6760	

TABLE IV

Part 1. Continued

L	a	I	E	Dir	R_{av}	ρ_a (ω-cm.)
75	25	0.286	0.470	N-S		
		0.261	0.423	S-N		
		0.132	0.220	N-S		
		0.130	0.213	S-N	1.64	7850
90	30	0.350	0.542	N-S		
		0.327	0.517	S-N		
		0.129	0.210	N-S		
		0.135	0.208	S-N	1.575	9040
120	40	0.290	0.402	N-S		
		0.282	0.385	S-N		
		0.135	0.183	S-N		
		0.133	0.200	N-S		
		0.130	0.193	N-S		
		0.129	0.172	S-N	1.40	10720
150	50	0.312	0.405	N-S		
		0.328	0.400	S-N		
		0.124	0.162	S-N		
		0.115	0.153	N-S		
		0.112	0.145	N-S	1.29	12340

Above measurements made on June 4, 1939

Part 2. Measurements at Test Point 3. June 5, 1939

6	2	0.0006	0.9	a#	1500	575000
15	5	0.0028	1.45	a		
		0.0029	1.55	a		
		0.0027	1.25	b#	505	474000
60	20	0.006	0.8	a		
		0.009	1.3	a	1385	531000

Part 3. Measurements for Curve 3. June 7, 1939

6	2	0.042	1.302	a		
		0.039	1.195	b	30.8	11800
15	5	0.1435	1.165	a		
		0.128	1.045	b	8.14	7790
30	10	0.174	0.874	a		
		0.162	0.814	b	5.03	9640
60	20	0.162	0.540	a		
		0.164	0.546	b	3.325	12730

Bearing of spread and direction of current not recorded.
a indicates current through the ground in one direction and b in the opposite direction.

TABLE IV

Part 3. Continued

L	a	I	E	Dir	Rav	ρ_a (ω-cm.)
120	40	0.192	0.265	a		
		0.187	0.260	b	1.385	10620
180	60	0.115	0.109	a		
		0.112	0.106	b	0.947	10890
300	100	0.142	0.109	a		
		0.136	0.105	b	0.770	14760
600	200	0.168	0.090	a		
		0.158	0.105	b		
		0.147	0.100	b		
		0.143	0.075	a	0.601	23000

Part 4. Resistivity depth profile of Curve 4, June 6, 1939

6	2	0.0125	1.438	a		
		0.0135	1.555	b	11.51	4410
15	5	0.052	1.323	a		
		0.054	1.372	b	25.42	24330
30	10	0.014	0.130	a		
		0.014	0.129	b	9.25	17720
45	15	0.066	0.358	a		
		0.067	0.369	b	5.465	15720
60	20	0.117	0.431	a		
		0.117	0.430	b	3.680	14100
75	25	0.042	0.113	a		
		0.040	0.113	b	2.755	13200
105	35	0.092	0.168	a		
		0.088	0.148	b	1.755	11780
150	50	0.133	0.133	a		
		0.136	0.129	b	0.975	9340
225	75	0.142	0.085	b		
		0.149	0.065	a		
		0.126	0.065	a	0.54	7760
300	100	0.132	0.087	a		
		0.132	0.078	b	0.625	11980
375	125	0.046	0.035	a		
		0.049	0.020	b		
		0.049	0.036	a		
		0.027	0.010	b	0.57	13650

TABLE IV

Part 4. Continued

L	a	I	E	Dir	R_{av}	ρ_a (a-cm.)
450	150	0.115	0.075	a		
		0.111	0.057	b	0.58	16680
600	200	0.129	0.078	a		
		0.123	0.052	b		
		0.114	0.072	a		
		0.112	0.044	b	0.51	19550
750	250	0.133	0.067	a		
		0.127	0.055	b	0.465	22250
1050	350	0.073	0.019	b		
		0.074	0.043	a		
		0.135	0.046	a		
		0.134	0.043	b		
		0.134	0.040	b	0.415	27820

Part 5. Resistivity depth profile of Curve 5, June 7, 1939

6	2	0.011	1.483	a		
		0.011	1.410	b	131.5	50350
15	5	0.070	1.469	a		
		0.062	1.310	b	21.05	20400
30	10	0.122	0.882	a		
		0.119	0.861	b	7.23	13840
60	20	0.121	0.217	a		
		0.116	0.229	b	1.88	7210
120	40	0.102	0.071	a		
		0.1015	0.091	b		
		0.101	0.068	a		
		0.1005	0.091	b	0.792	6060
180	60	0.101	0.051	a		
		0.094	0.058	b		
		0.092	0.053	a		
		0.088	0.049	b	0.564	6480
240	80	0.165	0.061	a		
		0.133	0.090	b		
		0.128	0.038	a		
		0.122	0.084	b	0.507	7770
300	100	0.082	0.033	a		
		0.078	0.045	b		
		0.076	0.030	a		
		0.074	0.043	b	0.489	9370

TABLE IV

Part 5. Concluded

L	a	I	E	Dir	R_{av}	ρ_a (a-cm.)
450	150	0.142	0.065	a		
		0.138	0.055	b		
		0.138	0.064	a		
		0.136	0.052	b	0.426	12220
600	200	0.105	0.032	a		
		0.101	0.052	b		
		0.104	0.031	a		
		0.101	0.051	b	0.406	15550

VII

Interpretation of
Apparent Resistivity-Electrode Separation Curves

Introduction It is the purpose of this Chapter to discuss in some detail the various methods that have been proposed for determining the depths to horizontal discontinuities in resistivity, and the magnitudes of resistivity from field measurements of apparent resistivity at different electrode separations using Wenner's configuration, of three equal intervals between the four electrodes. To avoid the confusion which would result from plunging into detailed descriptions at the outset, the first part of the chapter is devoted to a general outline of the methods, and of their relative importance in practice. Most of them are of historical importance only. The balance of the chapter is given to detailed examples of the various methods as applied to data obtained in the field by the writer.

General Outline of Methods The following outline will be used as a guide for the following discussion, and the detailed examples at the end of the chapter will be considered in the order in which they fit into this scheme.

I. Empirical Methods.

II. Theoretical Methods.
  A. Analytical
  B. Graphical
    1. Tagg's method and variations.
      a. Two layer case
        (1) Tagg's original method (Examples I and II-Delano Data)

(2) Tagg's modified method (Example III-Delano Data)

b. Three and more layers

(1) Pirson's approximation method (Example IV-Victorville test point #1)

(2) Tagg's modified method

2. Superposition Methods

a. Two layer case.

(1) Roman's method.

(2) Paletca method. (Example V-Delano data)

b. Three and more layers

(1) Three-layer master curves

(2) Paletca method (Examples VI, VII, VIII, IX-Victorville curves 1, 3, 4, and 5)

I. A number of empirical rules for interpreting the resistivity-separation curves were mentioned in Chapter IV. Of these the most valuable is the one which states that the depth to an interface causing a bend in the field curve is about 1/3 the distance between the current electrodes at which the effect of the change in resistivity appears in the apparent resistivity. This rule is not universally applicable and is much less reliable than theoretical methods. It is, however, a useful check on the order of magnitude of theoretically obtained values, and to choose the most probable value if the other methods give several apparently equally likely values. It's use will be illustrated in connection with the examples of the Paletca method.

IIA. For the sake of completeness it is well to point out that there are no analytical methods of determining the depths to discontinuities, and resistivites from the field data, by use of the resistivity formulae. Even in the simplest case of two layers the expression for apparent resistivity $\rho_a = \rho_1 \left[1 + 4 \sum_{n=1}^{\infty} \left(\frac{\rho_2 - \rho_1}{\rho_2 + \rho_1}\right)^n \left(\frac{1}{\sqrt{1+(2n\frac{h}{a})^2}} - \frac{1}{\sqrt{4+(2n\frac{h}{a})^2}}\right)\right]$ (52)

is so complicated that there is no possibility of solving for h and ρ_2 . For that reason graphical methods must be used.

IIB. There are two main types of method for graphical interpretation of field data. The first of these plots the field data in curves with the apparent resistivity as ordinate and the distance between the potential electrodes "a" as abscissa. It further requires numerical calculations from a set of theoretical master curves described below and the drawing of other sets of graphs. The other method plots the field data on double logarithmic scale, and determines the depths and resistivities directly from the master curves without any calculation or further curve drawing. This latter method is so superior to the other that for practical work it may be considered the only method. It is an interesting fact that although this superposition method (Paletca method) was developed in Russia as early or earlier than the first method, it was not introduced in the United States for a number of years after its inception, probably because of the language barrier. Meanwhile the Tagg method had become entrenched in the literature of this country. It is illustrated here because of its historical interest and for comparison to demonstrate the great superiority of the superposition method. The procedures, and difficulties which are encountered are brought out in the examples and will not be discussed further here.

Preparation of the Theoretical Two-Layer Master Curves

The two-layer methods of interpretation to be described below make use of sets of master curves derived from the expression

$$\frac{\rho_a}{\rho_1} = 1 + 4\sum_{n=1}^{\infty}\left(\frac{\rho_2-\rho_1}{\rho_2+\rho_1}\right)^n\left[\frac{1}{\sqrt{1+(2nx)^2}} - \frac{1}{\sqrt{4+(2nx)^2}}\right] \qquad (52)$$

derived in Chapter IV. This equation gives the value of the ratio of apparent resistivity to surface resistivity in terms of the resistivities of the two layers, the depth "h" to their horizontal plane interface, and the Wenner configuration electrode separation "a". It is to be noted that the resistivities in the right hand member occur only in the reflection factor $k = \frac{\rho_2-\rho_1}{\rho_2+\rho_1}$ and that the depth and electrode separation occur only in the form of their ratio. The right member of equation (52) has been evaluated by various workers, but the only set of tabulated values to which the writer has access are those given by Irwin Roman. These are included in his article Some Interpretations of Earth Resistivity Data[a] and are also appended to his paper How to Compute Tables for Determining Electrical Resistivity of Underlying Beds and their Application to Geophysical Problems.[b] Because many interpretations given below are based on these tables, they are copied here as Table V[c]. In working with the curves made up from these tables (Figure 21, Plates VIII and IX) it was found necessary in some cases to interpolate for values of "k" intermediate to those given in Table V. This

(a) A.I.M.E. "Geophysical Prospecting" 1934 p. 183
(b) U.S.Bureau of Mines, Technical Paper #502 (1931)
(c) The notation used in this paper is substituted for that of Roman who uses "Q" for the reflection factor "k", "d" for the electrode separation "a" and "c" for the interface depth "h".

TABLE V[a]

Body of table gives ratio g_s/g_1 corresponding to values of k listed at top and a/h at the side.

a/h	k				
	0.1	0.2	0.3	0.4	0.5
0.1	1.0001	1.0002	1.0002	1.0003	1.0004
0.2	1.0006	1.0012	1.0018	1.0024	1.0031
0.3	1.0019	1.0038	1.0058	1.0079	1.0101
0.4	1.0042	1.0085	1.0131	1.0177	1.0226
0.5	1.0076	1.0156	1.0238	1.0323	1.0412
0.6	1.0122	1.0249	1.0380	1.0516	1.0658
0.7	1.0178	1.0361	1.0552	1.0751	1.0959
0.8	1.0241	1.0490	1.0750	1.1022	1.1307
0.9	1.0310	1.0632	1.0968	1.1320	1.1691
1.0	1.0383	1.0782	1.1200	1.1639	1.2104
1.1	1.0458	1.0937	1.1441	1.1972	1.2535
1.2	1.0534	1.1095	1.1686	1.2312	1.2977
1.3	1.0610	1.1253	1.1932	1.2654	1.3424
1.4	1.0685	1.1408	1.2176	1.2995	1.3872
1.5	1.0758	1.1560	1.2415	1.3331	1.4316
1.6	1.0828	1.1708	1.2649	1.3660	1.4753
1.7	1.0895	1.1851	1.2876	1.3981	1.5180
1.8	1.0959	1.1987	1.3094	1.4292	1.5597
1.9	1.1020	1.2118	1.3304	1.4593	1.6002
2.0	1.1078	1.2243	1.3505	1.4883	1.6395
2.1	1.1134	1.2362	1.3698	1.5162	1.6776
2.2	1.1186	1.2475	1.3882	1.5429	1.7143
2.3	1.1235	1.2582	1.4058	1.5686	1.7497
2.4	1.1281	1.2683	1.4225	1.5932	1.7838
2.5	1.1325	1.2780	1.4384	1.6168	1.8168
2.6	1.1367	1.2871	1.4536	1.6395	1.8486
2.7	1.1406	1.2957	1.4681	1.6612	1.8792
2.8	1.1442	1.3039	1.4820	1.6820	1.9087
2.9	1.1476	1.3117	1.4952	1.7019	1.9372
3.0	1.1508	1.3190	1.5077	1.7210	1.9646
3.1	1.1538	1.3259	1.5196	1.7392	1.9910
3.2	1.1567	1.3325	1.5309	1.7567	2.0164
3.3	1.1595	1.3388	1.5417	1.7735	2.0409
3.4	1.1621	1.3448	1.5521	1.7896	2.0646
3.5	1.1645	1.3504	1.5620	1.8051	2.0875
3.6	1.1668	1.3558	1.5715	1.8200	2.1096
3.7	1.1690	1.3609	1.5806	1.8343	2.1309
3.8	1.1711	1.3657	1.5892	1.8479	2.1514
3.9	1.1730	1.3703	1.5974	1.8610	2.1712
4.0	1.1748	1.3747	1.6053	1.8737	2.1905

a. Taken from Roman, AIME Geophysical Prospecting 1934 p. 183, with change of notation.

TABLE V continued

a/h	k = 0.6	0.7	0.8	0.9	1.0
0.1	1.0005	1.0006	1.0007	1.0008	1.0009
0.2	1.0038	1.0045	1.0053	1.0061	1.0070
0.3	1.0123	1.0146	1.0171	1.0198	1.0227
0.4	1.0276	1.0329	1.0385	1.0445	1.0512
0.5	1.0504	1.0602	1.0705	1.0816	1.0939
0.6	1.0807	1.0964	1.1131	1.1311	1.1513
0.7	1.1178	1.1409	1.1656	1.1924	1.2225
0.8	1.1607	1.1926	1.2268	1.2640	1.3062
0.9	1.2084	1.2502	1.2952	1.3445	1.4008
1.0	1.2596	1.3123	1.3694	1.4322	1.5045
1.1	1.3134	1.3779	1.4480	1.5257	1.6157
1.2	1.3689	1.4458	1.5298	1.6235	1.7329
1.3	1.4253	1.5151	1.6138	1.7245	1.8550
1.4	1.4819	1.5851	1.6991	1.8278	1.9810
1.5	1.5383	1.6553	1.7851	1.9327	2.1099
1.6	1.5942	1.7251	1.8713	2.0385	2.2410
1.7	1.6492	1.7942	1.9572	2.1448	2.3740
1.8	1.7031	1.8624	2.0424	2.2510	2.5083
1.9	1.7558	1.9295	2.1268	2.3571	2.6438
2.0	1.8072	1.9954	2.2103	2.4627	2.7799
2.1	1.8573	2.0599	2.2926	2.5678	2.9167
2.2	1.9059	2.1230	2.3737	2.6721	3.0540
2.3	1.9531	2.1847	2.4535	2.7756	3.1916
2.4	1.9989	2.2450	2.5321	2.8782	3.3294
2.5	2.0434	2.3039	2.6093	2.9800	3.4675
2.6	2.0865	2.3613	2.6852	3.0808	3.6057
2.7	2.1283	2.4173	2.7598	3.1806	3.7439
2.8	2.1688	2.4719	2.8330	3.2795	3.8823
2.9	2.2081	2.5252	2.9050	3.3774	4.0208
3.0	2.2462	2.5772	2.9757	3.4743	4.1593
3.1	2.2831	2.6280	3.0451	3.5703	4.2978
3.2	2.3189	2.6776	3.1133	3.6653	4.4364
3.3	2.3536	2.7259	3.1804	3.7593	4.5750
3.4	2.3873	2.7730	3.2463	3.8525	4.7135
3.5	2.4200	2.8191	3.3109	3.9447	4.8522
3.6	2.4518	2.8640	3.3746	4.0360	4.9907
3.7	2.4825	2.9079	3.4371	4.1263	5.1924
3.8	2.5124	2.9508	3.4986	4.2159	5.2679
3.9	2.5415	2.9928	3.5590	4.3045	5.4065
4.0	2.5698	3.0338	3.6184	4.3922	5.5452

TABLE V continued

a/h	k				
	0.1	0.2	0.3	0.4	0.5
4.1	1.1765	1.3789	1.6128	1.8859	2.2092
4.2	1.1781	1.3829	1.6200	1.8977	2.2271
4.3	1.1797	1.3867	1.6269	1.9090	2.2444
4.4	1.1813	1.3903	1.6336	1.9199	2.2613
4.5	1.1827	1.3938	1.6400	1.9304	2.2776
4.6	1.1840	1.3972	1.6461	1.9405	2.2933
4.7	1.1853	1.4004	1.6519	1.9502	2.3086
4.8	1.1865	1.4034	1.6575	1.9596	2.3234
4.9	1.1877	1.4062	1.6630	1.9687	2.3377
5.0	1.1888	1.4091	1.6683	1.9775	2.3517

a/h	k				
	-0.1	-0.2	-0.3	-0.4	-0.5
0.1	0.9999	0.9999	0.9998	0.9997	0.9996
0.2	0.9994	0.9989	0.9983	0.9978	0.9973
0.3	0.9982	0.9964	0.9946	0.9929	0.9912
0.4	0.9959	0.9919	0.9880	0.9842	0.9804
0.5	0.9925	0.9853	0.9782	0.9713	0.9646
0.6	0.9881	0.9767	0.9654	0.9545	0.9439
0.7	0.9828	0.9662	0.9500	0.9343	0.9190
0.8	0.9768	0.9543	0.9326	0.9114	0.8909
0.9	0.9702	0.9414	0.9137	0.8867	0.8606
1.0	0.9633	0.9279	0.8938	0.8609	0.8290
1.1	0.9562	0.9141	0.8736	0.8346	0.7969
1.2	0.9490	0.9002	0.8534	0.8084	0.7650
1.3	0.9419	0.8865	0.8335	0.7827	0.7339
1.4	0.9350	0.8732	0.8142	0.7579	0.7039
1.5	0.9284	0.8604	0.7958	0.7342	0.6754
1.6	0.9220	0.8482	0.7783	0.7118	0.6485
1.7	0.9159	0.8366	0.7617	0.6908	0.6233
1.8	0.9101	0.8257	0.7462	0.6711	0.5999
1.9	0.9047	0.8155	0.7317	0.6528	0.5782
2.0	0.8996	0.8059	0.7182	0.6358	0.5582
2.1	0.8949	0.7970	0.7056	0.6201	0.5398
2.2	0.8904	0.7887	0.6940	0.6056	0.5229
2.3	0.8862	0.7810	0.6833	0.5923	0.5075
2.4	0.8823	0.7738	0.6734	0.5801	0.4934
2.5	0.8787	0.7672	0.6642	0.5689	0.4806
2.6	0.8753	0.7610	0.6558	0.5587	0.4689
2.7	0.8721	0.7553	0.6480	0.5494	0.4582
2.8	0.8691	0.7500	0.6409	0.5408	0.4485
2.9	0.8664	0.7451	0.6344	0.5329	0.4397
3.0	0.8639	0.7406	0.6283	0.5256	0.4316

TABLE V continued

a/h	k = 0.6	0.7	0.8	0.9	1.0
4.1	2.5973	3.0738	3.6767	4.4791	5.6838
4.2	2.6240	3.1129	3.7343	4.5651	5.8824
4.3	2.6499	3.1512	3.7908	4.6504	5.9610
4.4	2.6751	3.1886	3.8464	4.7348	6.0997
4.5	2.6996	3.2251	3.9010	4.8183	6.2384
4.6	2.7235	3.2609	3.9548	4.9012	6.3769
4.7	2.7469	3.2959	4.0076	4.9832	6.5155
4.8	2.7696	3.3302	4.0597	5.0646	6.6542
4.9	2.7915	3.3637	4.1110	5.1451	6.7928
5.0	2.8130	3.3965	4.1614	5.2250	6.9315

a/h	k = -0.6	-0.7	-0.8	-0.9	-1.0
0.1	0.9995	0.9995	0.9995	0.9994	0.9993
0.2	0.9968	0.9963	0.9958	0.9953	0.9948
0.3	0.9896	0.9880	0.9864	0.9848	0.9833
0.4	0.9768	0.9732	0.9697	0.9662	0.9629
0.5	0.9580	0.9515	0.9452	0.9390	0.9330
0.6	0.9335	0.9233	0.9134	0.9037	0.8942
0.7	0.9041	0.8896	0.8754	0.8615	0.8479
0.8	0.8710	0.8516	0.8326	0.8141	0.7960
0.9	0.8353	0.8107	0.7867	0.7633	0.7405
1.0	0.7981	0.7682	0.7391	0.7108	0.6833
1.1	0.7605	0.7253	0.6911	0.6580	0.6259
1.2	0.7233	0.6829	0.6439	0.6061	0.5696
1.3	0.6870	0.6418	0.5982	0.5561	0.5154
1.4	0.6522	0.6024	0.5546	0.5085	0.4640
1.5	0.6192	0.5652	0.5135	0.4638	0.4159
1.6	0.5881	0.5304	0.4751	0.4222	0.3714
1.7	0.5592	0.4980	0.4396	0.3839	0.3305
1.8	0.5324	0.4682	0.4071	0.3488	0.2932
1.9	0.5077	0.4408	0.3773	0.3169	0.2594
2.0	0.4850	0.4157	0.3502	0.2880	0.2289
2.1	0.4642	0.3929	0.3257	0.2620	0.2016
2.2	0.4452	0.3723	0.3036	0.2387	0.1773
2.3	0.4280	0.3536	0.2836	0.2178	0.1556
2.4	0.4124	0.3367	0.2657	0.1991	0.1364
2.5	0.3982	0.3215	0.2497	0.1825	0.1194
2.6	0.3854	0.3078	0.2354	0.1677	0.1044
2.7	0.3738	0.2955	0.2226	0.1546	0.0911
2.8	0.3633	0.2844	0.2111	0.1430	0.0795
2.9	0.3538	0.2744	0.2009	0.1327	0.0693
3.0	0.3452	0.2655	0.1918	0.1236	0.0604

TABLE V concluded

a/h	k				
	-0.1	-0.2	-0.3	-0.4	-0.5
3.1	0.8615	0.7364	0.6227	0.5190	0.4243
3.2	0.8593	0.7324	0.6175	0.5130	0.4176
3.3	0.8573	0.7288	0.6128	0.5075	0.4116
3.4	0.8554	0.7255	0.6084	0.5024	0.4061
3.5	0.8536	0.7224	0.6043	0.4977	0.4011
3.6	0.8519	0.7195	0.6005	0.4934	0.3965
3.7	0.8503	0.7168	0.5970	0.4895	0.3923
3.8	0.8488	0.7143	0.5939	0.4859	0.3884
3.9	0.8474	0.7119	0.5910	0.4825	0.3849
4.0	0.8461	0.7097	0.5882	0.4794	0.3817
4.1	0.8449	0.7076	0.5856	0.4765	0.3788
4.2	0.8437	0.7057	0.5832	0.4739	0.3761
4.3	0.8426	0.7039	0.5810	0.4715	0.3736
4.4	0.8416	0.7022	0.5790	0.4693	0.3712
4.5	0.8406	0.7007	0.5771	0.4672	0.3690
4.6	0.8397	0.6992	0.5753	0.4652	0.3671
4.7	0.8389	0.6978	0.5736	0.4634	0.3654
4.8	0.8380	0.6965	0.5720	0.4618	0.3637
4.9	0.8372	0.6953	0.5705	0.4603	0.3621
5.0	0.8366	0.6941	0.5691	0.4587	0.3607

	k				
	-0.6	-0.7	-0.8	-0.9	-1.0
3.1	0.3374	0.2575	0.1838	0.1156	0.0526
3.2	0.3304	0.2503	0.1766	0.1085	0.0457
3.3	0.3241	0.2438	0.1702	0.1023	0.0397
3.4	0.3183	0.2380	0.1645	0.0968	0.0345
3.5	0.3130	0.2328	0.1594	0.0919	0.0299
3.6	0.3083	0.2282	0.1548	0.0876	0.0259
3.7	0.3041	0.2240	0.1507	0.0839	0.0225
3.8	0.3003	0.2202	0.1471	0.0806	0.0195
3.9	0.2968	0.2167	0.1440	0.0777	0.0169
4.0	0.2935	0.2136	0.1412	0.0751	0.0146
4.1	0.2905	0.2108	0.1386	0.0728	0.0126
4.2	0.2879	0.2083	0.1362	0.0708	0.0109
4.3	0.2855	0.2061	0.1341	0.0690	0.0095
4.4	0.2833	0.2041	0.1323	0.0674	0.0082
4.5	0.2813	0.2022	0.1307	0.0660	0.0070
4.6	0.2794	0.2004	0.1292	0.0648	0.0061
4.7	0.2777	0.1988	0.1278	0.0637	0.0053
4.8	0.2761	0.1974	0.1266	0.0627	0.0046
4.9	0.2746	0.1962	0.1255	0.0618	0.0039
5.0	0.2733	0.1950	0.1245	0.0610	0.0034

TABLE VI

a/h	k				
	0.15	0.25	0.35	0.45	0.55
1.5	1.116	1.199	1.288	1.382	1.485
1.6	1.127	1.218	1.316	1.420	1.534
1.7	1.138	1.236	1.343	1.458	1.584
1.8	1.148	1.254	1.369	1.494	1.632
1.9	1.157	1.271	1.394	1.530	1.678
2.0	1.166	1.287	1.419	1.564	1.724
2.2	1.184	1.318	1.466	1.628	1.810
2.4	1.198	1.345	1.508	1.688	1.892
2.6	1.212	1.370	1.547	1.744	1.968
2.8	1.224	1.393	1.582	1.796	2.039
3.0	1.235	1.414	1.614	1.843	2.106
3.3	1.250	1.440	1.658	1.908	2.198
3.6	1.262	1.464	1.696	1.965	2.281
3.9	1.272	1.484	1.729	2.016	2.356
4.2	1.280	1.502	1.759	2.062	2.462
4.5	1.288	1.517	1.785	2.104	2.489
4.8	1.294	1.530	1.809	2.142	2.546
5.0	1.299	1.538	1.823	2.165	2.582

a/h	k			
	0.65	0.75	0.85	0.95
1.5	1.596	1.720	1.859	2.022
1.6	1.660	1.798	1.954	2.140
1.7	1.722	1.876	2.051	2.260
1.8	1.782	1.952	2.146	2.380
1.9	1.843	2.028	2.242	2.500
2.0	1.901	2.102	2.336	2.622
2.2	2.014	2.248	2.523	2.863
2.4	2.122	2.388	2.705	3.104
2.6	2.224	2.523	2.873	3.344
2.8	2.320	2.652	3.056	3.581
3.0	2.412	2.776	3.225	3.816
3.3	2.540	2.953	3.470	4.167
3.6	2.658	3.120	3.706	4.514
3.9	2.768	3.276	3.932	4.855
4.2	2.868	3.424	4.150	5.224
4.5	2.962	3.563	4.360	5.528
4.8	3.050	3.695	4.562	5.860
5.0	3.104	3.778	4.693	6.078

TABLE VI continued

a/h	k				
	-.15	-.25	-.35	-.45	-.55
0.8	0.966	0.943	0.922	0.901	0.881
0.9	0.956	0.928	0.900	0.874	0.848
1.0	0.946	0.911	0.877	0.846	0.814
1.1	0.935	0.894	0.854	0.816	0.779
1.2	0.925	0.877	0.831	0.787	0.744
1.3	0.914	0.860	0.808	0.758	0.710
1.4	0.904	0.844	0.786	0.731	0.678
1.5	0.894	0.828	0.765	0.705	0.647
1.6	0.885	0.813	0.745	0.680	0.618
1.7	0.876	0.799	0.726	0.657	0.591
1.8	0.868	0.786	0.709	0.636	0.566
1.9	0.860	0.774	0.692	0.616	0.543
2.0	0.853	0.762	0.677	0.597	0.522
2.1	0.846	0.751	0.663	0.580	0.502
2.2	0.840	0.741	0.650	0.564	0.484
2.3	0.834	0.732	0.638	0.550	0.468
2.4	0.828	0.724	0.627	0.537	0.453
2.5	0.823	0.716	0.617	0.525	0.439
2.6	0.818	0.708	0.607	0.514	0.427
2.7	0.814	0.702	0.599	0.504	0.416
2.8	0.810	0.695	0.591	0.495	0.406
2.9	0.806	0.690	0.584	0.486	0.397
3.0	0.802	0.684	0.577	0.479	0.388
3.1	0.799	0.680	0.571	0.472	0.381
3.2	0.796	0.675	0.565	0.465	0.374
3.3	0.793	0.671	0.560	0.460	0.368
3.4	0.790	0.667	0.555	0.454	0.362
3.5	0.788	0.663	0.551	0 449	0 357
3.6	0.786	0.660	0.547	0.445	0.352
3.7	0.784	0.657	0.543	0.441	0.348
3.8	0.782	0.654	0.540	0.437	0.344
3.9	0.780	0.651	0.537	0.434	0.341
4.0	0.778	0.649	0.534	0.431	0.338
4.1	0.776	0.647	0.531	0.428	0.335
4.2	0.775	0.644	0.529	0.425	0.332
4.3	0.773	0.642	0.526	0.423	0.330
4.4	0.772	0.641	0.524	0.420	0.327
4.5	0.771	0.639	0.522	0.418	0.325
4.60	0.769	0.637	0.520	0.416	0.323
4.70	0.768	0.636	0.518	0.414	0.322
4.8	0.767	0.634	0.517	0.413	0.320
4.9	0.766	0.633	0.515	0.411	0.318
5.0	0.765	0.632	0.514	0.410	0.317

TABLE VI continued

a/h	k			
	-0.65	-0.75	-0.85	-0.95
0.8	0.861	0.842	0.823	0.805
0.9	0.823	0.799	0.775	0.752
1.0	0.783	0.754	0.725	0.697
1.1	0.743	0.708	0.675	0.642
1.2	0.703	0.663	0.625	0.588
1.3	0.664	0.620	0.577	0.536
1.4	0.627	0.578	0.532	0.486
1.5	0.592	0.539	0.489	0.440
1.6	0.559	0.503	0.449	0.397
1.7	0.529	0.467	0.412	0.357
1.8	0.500	0.438	0.378	0.321
1.9	0.474	0.409	0.347	0.288
2.0	0.450	0.383	0.319	0.258
2.1	0.429	0.359	0.294	0.232
2.2	0.409	0.338	0.271	0.208
2.3	0.391	0.319	0.251	0.187
2.4	0.375	0.301	0.232	0.168
2.5	0.360	0.286	0.216	0.151
2.6	0.347	0.272	0.202	0.136
2.7	0.335	0.259	0.189	0.123
2.8	0.324	0.248	0.177	0.111
2.9	0.314	0.238	0.167	0.101
3.0	0.305	0.229	0.158	0.0920
3.1	0.297	0.221	0.150	0.0841
3.2	0.290	0.213	0.143	0.0771
3.3	0.284	0.207	0.136	0.0710
3.4	0.278	0.201	0.131	0.0656
3.5	0.273	0.196	0.126	0.0609
3.6	0.268	0.192	0.121	0.0568
3.7	0.264	0.187	0.117	0.0532
3.8	0.260	0.184	0.114	0.0500
3.9	0.257	0.180	0.111	0.0473
4.0	0.254	0.177	0.108	0.0448
4.1	0.251	0.175	0.106	0.0427
4.2	0.248	0.172	0.104	0.0408
4.3	0.246	0.170	0.102	0.0392
4.4	0.244	0.168	0.0998	0.0378
4.5	0.242	0.166	0.0984	0.0365
4.6	0.240	0.165	0.0970	0.0354
4.7	0.238	0.163	0.0958	0.0345
4.8	0.237	0.162	0.0946	0.0336
4.9	0.235	0.161	0.0936	0.0328
5.0	0.234	0.160	0.0928	0.0322

TABLE VI continued

a/h	k						
	-.125	-.175	-.225	-.275	-.325	-.375	-.425
1.2	0.937	0.912	0.888	0.865	0.842	0.820	0.798
1.3	0.928	0.900	0.873	0.847	0.821	0.796	0.770
1.4	0.920	0.888	0.858	0.829	0.800	0.772	0.744
1.5	0.911	0.877	0.844	0.812	0.780	0.750	0.720
1.6	0.904	0.866	0.830	0.796	0.762	0.728	0.696
1.7	0.896	0.856	0.818	0.780	0.744	0.708	0.674
1.8	0.889	0.847	0.806	0.766	0.728	0.690	0.654
1.9	0.882	0.838	0.795	0.753	0.712	0.672	0.634
2.0	0.876	0.830	0.786	0.740	0.698	0.656	0.616
2.1	0.870	0.822	0.774	0.728	0.684	0.642	0.600
2.2	0.865	0.814	0.765	0.718	0.672	0.628	0.585
2.3	0.860	0.808	0.756	0.708	0.660	0.615	0.571
2.4	0.855	0.801	0.749	0.698	0.650	0.604	0.558
2.5	0.851	0.795	0.742	0.690	0.640	0.593	0.547
2.6	0.846	0.790	0.734	0.682	0.632	0.583	0.536
2.7	0.843	0.784	0.728	0.675	0.624	0.574	0.526
2.8	0.840	0.780	0.722	0.668	0.616	0.566	0.518
2.9	0.836	0.776	0.718	0.662	0.609	0.558	0.510
3.0	0.833	0.772	0.712	0.656	0.602	0.552	0.502
3.1	0.830	0.768	0.708	0.652	0.597	0.545	0.496
3.2	0.828	0.764	0.704	0.646	0.592	0.539	0.489
3.3	0.825	0.761	0.700	0.642	0.586	0.534	0.484
3.4	0.822	0.758	0.696	0.638	0.582	0.528	0.478
3.5	0.821	0.755	0.692	0.634	0.578	0.526	0.474
3.6	0.819	0.753	0.690	0.630	0.574	0.520	0.469
3.7	0.817	0.750	0.687	0.627	0.570	0.516	0.465
3.8	0.816	0.748	0.684	0.624	0.567	0.513	0.462
3.9	0.814	0.746	0.682	0.621	0.564	0.510	0.458
4.0	0.812	0.744	0.680	0.618	0.561	0.506	0.455
4.1	0.810	0.742	0.678	0.616	0.558	0.504	0.452
4.2	0.809	0.740	0.675	0.614	0.556	0.502	0.450
4.3	0.808	0.738	0.673	0.612	0.554	0.499	0.448
4.4	0.807	0.737	0.672	0.610	0.552	0.496	0.444
4.5	0.806	0.736	0.670	0.608	0.550	0.494	0.442
4.6	0.804	0.734	0.668	0.606	0.548	0.492	0.440
4.7	0.803	0.733	0.667	0.605	0.546	0.490	0.438
4.8	0.802	0.732	0.665	0.603	0.544	0.489	0.437
4.9	0.802	0.730	0.664	0.602	0.542	0.488	0.436
5.0	0.801	0.730	0.663	0.600	0.542	0.486	0.434

TABLE VI continued

a/h	k						
	-.475	-.525	-.575	-.625	-.675	-.725	-.775
1.2	0.776	0.754	0.734	0.713	0.693	0.673	0.654
1.3	0.746	0.722	0.698	0.676	0.653	0.631	0.609
1.4	0.718	0.691	0.665	0.640	0.614	0.590	0.566
1.5	0.690	0.661	0.633	0.606	0.578	0.552	0.526
1.6	0.664	0.633	0.603	0.574	0.544	0.516	0.489
1.7	0.640	0.607	0.575	0.544	0.514	0.482	0.454
1.8	0.618	0.583	0.549	0.516	0.484	0.453	0.422
1.9	0.597	0.560	0.526	0.491	0.458	0.425	0.393
2.0	0.578	0.540	0.504	0.468	0.433	0.400	0.366
2.1	0.560	0.521	0.483	0.446	0.411	0.376	0.342
2.2	0.544	0.504	0.464	0.427	0.390	0.355	0.321
2.3	0.529	0.488	0.448	0.410	0.372	0.336	0.302
2.4	0.515	0.473	0.432	0.394	0.356	0.319	0.284
2.5	0.503	0.460	0.418	0.379	0.341	0.304	0.268
2.6	0.492	0.448	0.406	0.366	0.328	0.292	0.256
2.7	0.481	0.437	0.395	0.355	0.316	0.278	0.241
2.8	0.472	0.427	0.384	0.344	0.304	0.266	0.230
2.9	0.463	0.418	0.376	0.334	0.294	0.256	0.220
3.0	0.456	0.410	0.366	0.325	0.286	0.248	0.210
3.1	0.448	0.402	0.359	0.317	0.278	0.240	0.202
3.2	0.442	0.396	0.352	0.310	0.270	0.232	0.195
3.3	0.436	0.390	0.346	0.304	0.264	0.226	0.188
3.4	0.430	0.384	0.340	0.298	0.258	0.220	0.182
3.5	0.425	0.379	0.335	0.293	0.253	0.214	0.178
3.6	0.420	0.374	0.330	0.288	0.248	0.210	0.174
3.7	0.416	0.370	0.326	0.284	0.244	0.206	0.169
3.8	0.412	0.366	0.322	0.280	0.240	0.202	0.166
3.9	0.410	0.363	0.319	0.277	0.237	0.198	0.162
4.0	0.406	0.360	0.316	0.274	0.234	0.196	0.159
4.1	0.404	0.357	0.312	0.270	0.231	0.193	0.157
4.2	0.400	0.354	0.310	0.268	0.228	0.190	0.154
4.3	0.398	0.352	0.308	0.266	0.226	0.188	0.152
4.4	0.396	0.349	0.305	0.264	0.224	0.186	0.150
4.5	0.394	0.347	0.303	0.262	0.222	0.184	0.148
4.6	0.392	0.345	0.301	0.260	0.220	0.182	0.147
4.7	0.390	0.344	0.300	0.258	0.218	0.181	0.146
4.8	0.388	0.342	0.298	0.256	0.217	0.180	0.144
4.9	0.387	0.340	0.296	0.255	0.215	0.178	0.143
5.0	0.386	0.339	0.295	0.254	0.214	0.178	0.142

TABLE VI concluded

a/h	k			
	-.825	-.875	-.925	-.975
1.2	0.634	0.616	0.597	0.579
1.3	0.588	0.566	0.546	0.526
1.4	0.544	0.520	0.497	0.475
1.5	0.502	0.476	0.452	0.428
1.6	0.462	0.436	0.410	0.384
1.7	0.426	0.398	0.370	0.344
1.8	0.392	0.364	0.335	0.307
1.9	0.362	0.332	0.302	0.274
2.0	0.334	0.304	0.273	0.244
2.1	0.310	0.278	0.247	0.217
2.2	0.288	0.255	0.224	0.192
2.3	0.268	0.234	0.202	0.172
2.4	0.249	0.216	0.184	0.152
2.5	0.233	0.199	0.166	0.135
2.6	0.218	0.185	0.152	0.120
2.7	0.206	0.172	0.139	0.107
2.8	0.194	0.160	0.127	0.096
2.9	0.184	0.150	0.117	0.085
3.0	0.175	0.141	0.108	0.0762
3.1	0.167	0.133	0.100	0.0684
3.2	0.160	0.126	0.092	0.0614
3.3	0.153	0.119	0.086	0.0554
3.4	0.148	0.114	0.0812	0.0500
3.5	0.142	0.109	0.0764	0.0454
3.6	0.138	0.104	0.0722	0.0414
3.7	0.134	0.100	0.0686	0.0368
3.8	0.130	0.098	0.0653	0.0348
3.9	0.128	0.094	0.0625	0.0321
4.0	0.124	0.092	0.0600	0.0297
4.1	0.122	0.090	0.0578	0.0276
4.2	0.120	0.088	0.0558	0.0258
4.3	0.118	0.086	0.0541	0.0244
4.4	0.116	0.0836	0.0526	0.0230
4.5	0.114	0.0822	0.0512	0.0218
4.6	0.113	0.0809	0.0501	0.0208
4.7	0.112	0.0798	0.0491	0.0199
4.8	0.111	0.0786	0.0480	0.0191
4.9	0.110	0.0778	0.0473	0.0184
5.0	0.108	0.0769	0.0466	0.0178

interpolation was linear and the values computed by the writer are listed in Table VI. A few characteristics of these curves may be seen from an examination of equation (52). The value of ρ_a approaches ρ_1 for infinitely small values of the electrode separation "a" as the term a/h then becomes infinitely great and the expression in the brackets approaches zero. Similarly, for infinitely large values of "a" where a is large compared to nh for even very large values of n, the term in the brackets approaches the value $\frac{1}{2}$ and $\frac{\rho_a}{\rho_1}$ approaches

$$1 + 2\sum_{n=1}^{\infty}\left(\frac{\rho_2-\rho_1}{\rho_2+\rho_1}\right)^n = 1+\left[\frac{1}{1-\left(\frac{\rho_2-\rho_1}{\rho_2+\rho_1}\right)}-1\right] = \frac{\rho_2}{\rho_1} \qquad \text{where } \frac{\rho_2-\rho_1}{\rho_2+\rho_1} < +1$$

If $\frac{\rho_a}{\rho_1}$ is plotted against a/h, curves for all values of k will start at (1,0) and approach $\frac{\rho_a}{\rho_1} = \frac{\rho_2}{\rho_1}$ for very large values of a/h. The curves approach the values $\rho_a/\rho_1 = 1$ and $\rho_a/\rho_1 = \rho_2/\rho_1$ horizontally(a) so that for very small finite values of a, ρ_a is still very nearly ρ_1, and for large finite values of a, ρ_a is nearly ρ_2. The Paletca superposition method makes use of master curves in which ρ_a/ρ_1 is plotted against L/h on double logarithmic paper where L equals 3a, and is the distance between the current electrodes. The data for these Paletca curves was computed from the integral form of the expression for the apparent resistivity. Tables of data are not generally available, but the curves are shown in Plate VII at the end of the text through the courtesy of Dr. Potapenko. Differences in the manner of plotting the data for the master curves are illustrated in the examples

(a) Hummel A.I.M.E. "Geophysical Prospecting" 1932 p.404

The use of Tagg's modified method requires curves showing the value of the ratio of two apparent resistivities gotten with a chosen ratio of electrode separations in terms of the ratio of the smaller separation to the interface depth h for various values of k. That is, values of

$$\frac{\rho_{na}}{\rho_a} = \frac{\rho_{na}/\rho_1}{\rho_a/\rho_1} = \frac{1 + 4\sum_{r=1}^{\infty} K^r \left[\frac{1}{\sqrt{1+(2rh/na)^2}} - \frac{1}{\sqrt{4+(2rh/na)^2}}\right]}{1 + 4\sum_{r=1}^{\infty} K^r \left[\frac{1}{\sqrt{1+(2rh/a)^2}} - \frac{1}{\sqrt{4+(2rh/a)^2}}\right]}$$

are computed for a chosen value of n in terms of a/h and for a series of different values of k. Table VII shows the values computed with the aid of Table V for the case n = 2. The values of $\frac{\rho_a}{\rho_1}$ are listed in Table V opposite the value of a/h corresponding to the electrode separation a. The value ρ_{2a}/ρ_1 corresponding to an electrode separation 2a is then found in Table V opposite a value of a/h twice as large. The division of $\frac{\rho_{2a}}{\rho_1}$ by ρ_a/ρ_1 was carried out on a slide rule. The curves plotted from this data are shown in Figure 24, below. It may be noted here that whether the ratio taken as abscissa is expressed as a/h or the reciprocal h/a makes no difference in the evaluation of the curves, or in their use, other than in the matter of convenience of the numerical units in which the abscissa is expressed. The same is true of the use of the resistivity ratio ρ_a/ρ_1 or the conductivity ratio $\frac{\sigma_a}{\sigma_1}$ as ordinate. Tagg preferred the use of the conductivities where the lower layer has the greater resistivity as this limits to unity the range of ordinate values, but the writer has used the resistivity form because that is the form used in Roman's tables. It is true that use of reciprocal values of coordinates will

TABLE VII

The body of the table lists values of σ_{2a}/σ_a corresponding to the values of k in the top of the table and of a/h on the side.

a/h	k = -0.1	-0.2	-0.3	-0.4	-0.5
0.1	0.999	0.999	0.998	0.998	0.997
0.2	0.998	0.994	0.990	0.986	0.983
0.3	0.952	0.961	0.971	0.980	0.989
0.4	0.909	0.962	0.944	0.926	0.909
0.5	0.970	0.942	0.913	0.886	0.860
0.6	0.961	0.921	0.884	0.847	0.811
0.7	0.951	0.904	0.857	0.811	0.766
0.8	0.943	0.888	0.834	0.781	0.728
0.9	0.938	0.877	0.816	0.756	0.697
1.0	0.934	0.869	0.804	0.739	0.672
1.1	0.932	0.863	0.795	0.725	0.656
1.2	0.929	0.859	0.789	0.718	0.645
1.3	0.929	0.858	0.787	0.714	0.639
1.4	0.929	0.859	0.787	0.713	0.637
1.5	0.931	0.861	0.789	0.716	0.639
1.6	0.932	0.864	0.794	0.720	0.644
1.7	0.934	0.867	0.799	0.727	0.651
1.8	0.936	0.873	0.806	0.735	0.661
1.9	0.938	0.877	0.812	0.744	0.672
2.0	0.940	0.881	0.819	0.755	0.684
2.1	0.943	0.885	0.827	0.764	0.697
2.2	0.945	0.890	0.834	0.775	0.711
2.3	0.948	0.896	0.842	0.785	0.724
2.4	0.949	0.900	0.850	0.797	0.737
2.5	0.952	0.905	0.857	0.806	0.751

a/h	k = -0.6	-0.7	-0.8	-0.9	-1.0
0.1	0.996	0.996	0.996	0.996	0.996
0.2	0.980	0.977	0.974	0.971	0.9675
0.3	0.943	0.934	0.926	0.917	0.909
0.4	0.891	0.875	0.858	0.843	0.826
0.5	0.833	0.807	0.782	0.757	0.733
0.6	0.774	0.739	0.705	0.671	0.638
0.7	0.722	0.677	0.634	0.590	0.548
0.8	0.674	0.622	0.571	0.519	0.467
0.9	0.638	0.577	0.517	0.457	0.396
1.0	0.608	0.541	0.474	0.405	0.335
1.1	0.586	0.513	0.439	0.363	0.284
1.2	0.570	0.493	0.413	0.329	0.240
1.3	0.561	0.480	0.394	0.302	0.203
1.4	0.557	0.472	0.381	0.282	0.171
1.5	0.557	0.470	0.374	0.266	0.145

TABLE VII concluded

a/h	k				
	-0.6	-0.7	-0.8	-0.9	-1.0
1.6	0.562	0.472	0.372	0.257	0.123
1.7	0.569	0.478	0.374	0.252	0.104
1.8	0.579	0.488	0.381	0.251	0.0884
1.9	0.592	0.500	0.390	0.254	0.0752
2.0	0.606	0.514	0.403	0.260	0.0638
2.1	0.620	0.530	0.418	0.270	0.0541
2.2	0.637	0.548	0.436	0.282	0.0463
2.3	0.653	0.566	0.456	0.298	0.0392
2.4	0.670	0.587	0.476	0.315	0.0337
2.5	0.687	0.606	0.498	0.334	0.0284

change the shape of the curves if a conventional numbering of coordinate units is maintained, but in the final result, it is merely a matter of whether one wishes to think of the depth as twice the electrode separation, or of the electrode separation as ½ the depth.

1. Tagg's Method; a. Interpretation of Two-Layer Field Curves

(1) Tagg's original method. The following description of the procedure is quoted from Tagg's paper Earth-Resistivity Surveying.(a)

1. Determine the surface resistivity, ρ_1, by a series of careful measurements at small electrode intervals.
2. Determine the apparent resistivity for a number of values of electrode interval.
3. Plot a curve of apparent resistivity against electrode separation.
4. From this curve read off the values of apparent resistivity ρ_a for various values of electrode separation "a", and for each value of "a" determine the value of ρ_a/ρ_1 if ρ_a is less than ρ_1, or the value of σ_a/σ_1 if ρ_a is greater than ρ_1.
5. From the master curves read off for each value of "a" a series of corresponding values of h/a and k, and from these calculate a series of corresponding values of "h" and "k".
6. Plot curves, for each value of electrode interval, of "h" against "k". These curves should all intersect in a point giving the true values of "h" and "k".

Example I. To illustrate this method we will use the data from the profile taken near Delano. (Table III Part I end of Chapter VI)

1. Let us assume, for purposes of illustration, that the apparent resistivity value obtained for the five foot separation is the average of a series of careful measurements with several short separations. $\rho_1 = 6180$ ohm-cm.
2. The values of apparent resistivity obtained for a number of values of electrode separation are shown in the following table.

(a) The Mining Magazine, Vol. LIII #3 (Sept. 1935) p 150

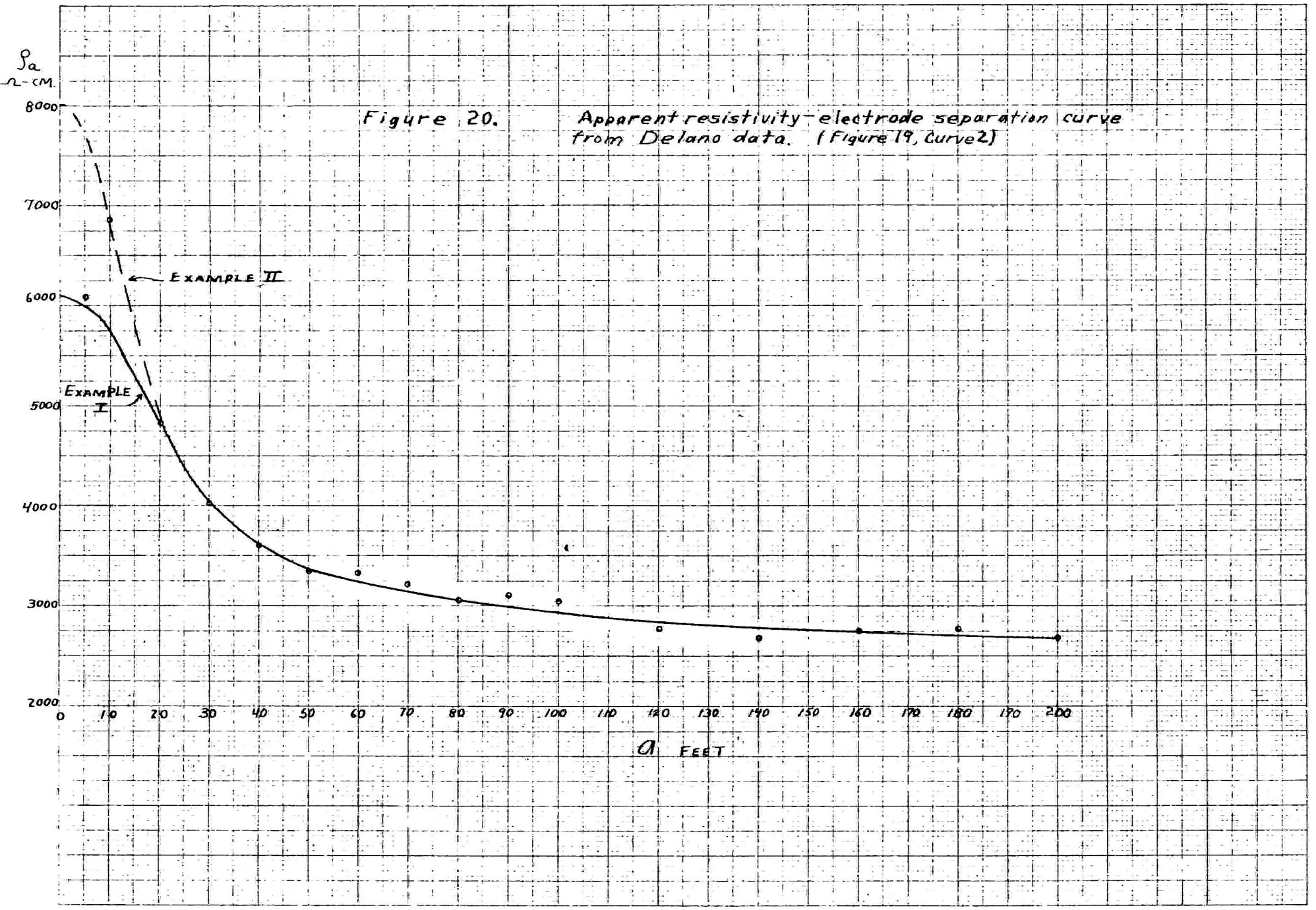

Figure 20. Apparent resistivity-electrode separation curve from Delano data. (Figure 19, Curve 2)

a (Feet)	ρ_a (Ω-cm.)	a (Feet)	ρ_a (Ω-cm.)
20	4830	90	3100
30	4020	100	3060
40	3600	120	2760
50	3350	140	2680
60	3330	160	2760
70	3220	180	2760
80	3060	200	2680

3. The curve of apparent resistivity against electrode separation is shown in Figure 20.

4. The following values of ρ_a and corresponding values of "a" were read off the curve of Figure 20. As these values are less than ρ_1, the values of ρ_a/ρ_1 are computed (using the value ρ_1 = 6180 Ω-cm. from 1.) rather than the values of σ/σ_1. As the curve deviates considerably from some of the observed values, points were chosen where the curve coincides with the experimental data. The value for the 100 foot separation taken from the curve is lower than the experimental value and included to see how consistent the values of h and k obtained for this point of the curve are with the values obtained at points where the curve is closer to the observed values.

a (Ft.)	ρ_a (Ω-M)	ρ_a/ρ_1	a (Ft.)	ρ_a (Ω-M)	ρ_a/ρ_1
20	48.3	.781	80	30.6	.495
30	40.2	.650	100	29.3	.474
40	36.0	.582	160	27.6	.446
50	33.5	.542	200	26.8	.433

5. The corresponding values of a/h and k were then read from the master curves (Figure 21). These may be checked by laying a straight edge across the figure parallel to the a/h axis for the values of ρ_a/ρ_1 listed above. By dividing the values of a/h into the corresponding values of "a", a series of corresponding values of h and k are obtained. These values are listed in the following table.

Figure 21. Two layer master curves plotted from data of Table V.

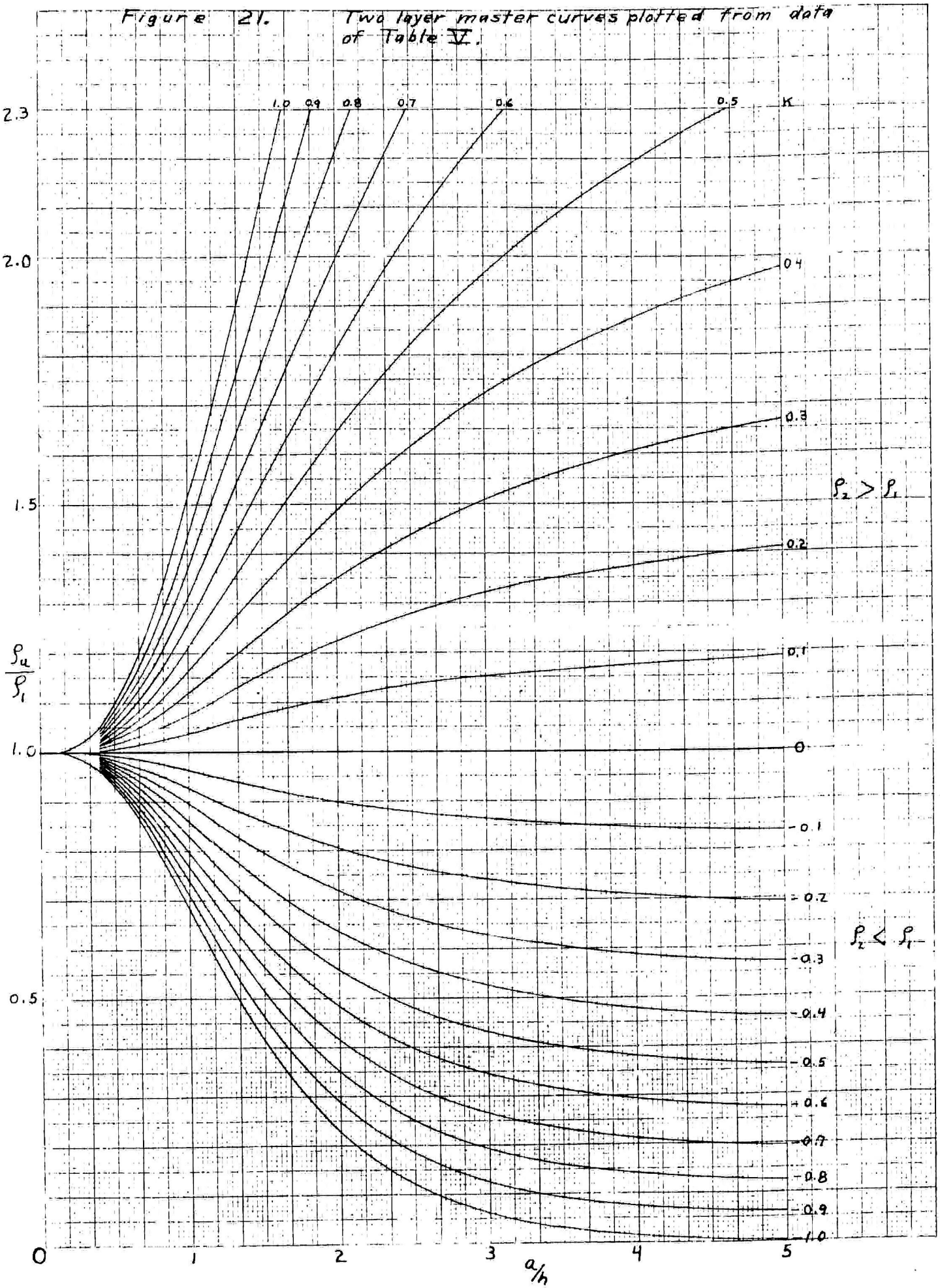

a FEET	ρ_a/ρ_1	K=1.0		K=0.9		K=0.8		K=0.7		K=0.6		K=0.5		K=0.4		K=0.3		K=0.2	
		a/h	FEET h	a/h	FEET h	a/h	FEET h	a/h	FEET h	a/h	FEET h	a/h	FEET h	a/h	FEET h	a/h	FEET h	a/h	FEET h
20	.781	0.83	24.1	0.87	23.0	0.91	22.0	0.97	20.6	1.04	19.2	1.15	17.4	1.30	15.4	1.57	12.7	2.30	8.70
30	.650	1.05	28.6	1.11	27.0	1.18	25.4	1.27	23.6	1.40	21.4	1.58	19.0	1.91	15.7	2.65	11.3		
40	.582	1.16	34.5	1.25	32.0	1.33	30.1	1.45	27.6	1.63	24.6	1.87	21.4	2.38	16.8	4.39	9.11		
50	.542	1.25	40.0	1.33	37.6	1.43	35.0	1.56	32.0	1.76	28.4	2.09	23.9	2.78	18.0				
80	.495	1.34	59.7	1.43	56.0	1.55	51.6	1.70	47.1	1.94	41.2	2.34	34.2	3.53	22.7				
100	.474	1.38	72.4	1.47	68.0	1.60	62.5	1.77	56.5	2.05	48.8	2.55	39.2	4.23	23.6				
160	.446	1.43	112	1.54	104	1.68	95.3	1.87	85.6	2.19	73.1	2.83	56.6						
200	.433	1.46	137	1.57	127	1.71	117	1.92	104	2.25	88.9	2.96	67.6						

6. Curves of h against k were plotted for each value of "a" in Figure 22. Those for separations of 20, 30, and 40 feet intersect at h = 14.5', k = -.375. The curves for larger separations cannot be extended below h = 15', k = -.4 from the data in Figure 21, because for large values of "a", the smaller values of h correspond to values of a/h greater than five. By interpolating k it is possible to extend some of the curves to values of a/h closer to the upper limit of five to which Roman's tables extend. The dotted portions of the curves in Figure 22, were extended by use of Plate VIII in which master curves are shown for values of k at .025 intervals. Its use is no different from that of Figure 21 although a double logarithmic scale is used. The fact that no extension of the h-k curve for the 100' spacing obtained indicates only that h is less than 20 feet for values of k equal to and greater than -.375, so that as far as our data goes, it may be consistent with the curves for the other spacings. Let us assume that the correct value of h and k is h = 15 feet, k = -.375. ρ_2 is then equal to $\rho_1(1+K)/(1-K) = 6180 \times 625/1375$ or about 2800 ohm centimeters.

Example II.

1. As an illustration of the effect of an error in the determination of ρ_1 on the value of h and k obtained, let us assume that the apparent resistivity for the ten foot spacing (6860 ohm-centimeters) is correct, and that the surface resistivity is still larger, say 8000 ohm-centimeters. We will discard the low apparent resistivity

Figure 22. Example I, Tagg's original method: h-K curve.

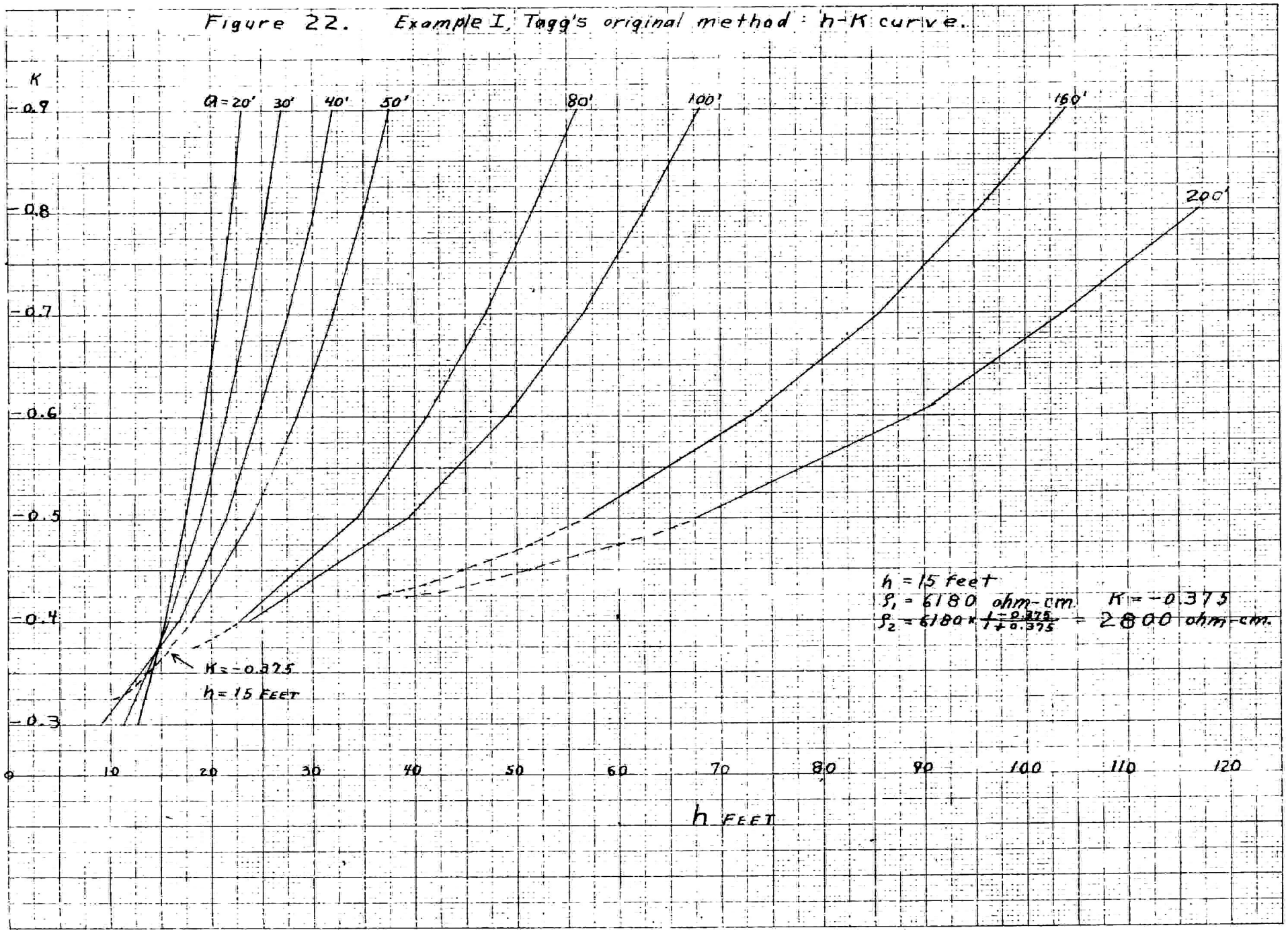

of the five foot spacing which is now inconsistent with a two-layer interpretation.

2. The apparent resistivity for the various spacings was shown in the table at the top of page 82.

3. The apparent resistivity-electrode separation is shown in Figure 20. It coincides with that of Example I except for small electrode separations where it is shown by the broken line.

4. The same values of apparent resistivity and electrode separation are used, but the use of a different value of ρ_1 gives the following different values of ρ_a/ρ_1.

a (Ft.)	ρ_a (Ω-cm.)	ρ_a/ρ_1	a (Ft.)	ρ_a (Ω-cm.)	ρ_a/ρ_1
20	4830	.603	80	3060	.382
30	4020	.502	100	2930	.366
40	3600	.449	160	2760	.345
50	3350	.418	200	2680	.335

5. The following values of a/h and k were read from Figure 21, and sets of corresponding values of h and k computed.

a FEET	ρ_a/ρ_1	K=-1.0		K=-0.9		K=-0.8		K=-0.7		K=-0.6		K=-0.5		K=-0.4		K=-0.3	
		a/h	FEET h	a/h	FEET h	a/h	FEET h	a/h	FEET h	a/h	FEET h	a/h	FEET h	a/h	FEET h	a/h	FEET h
20	.603	1.14	17.6	1.20	16.7	1.29	15.5	1.33	14.0	1.55	12.9	1.78	11.2	2.21	9.05	3.53	5.67
30	.502	1.33	22.6	1.40	21.4	1.53	19.6	1.67	18.0	1.91	15.7	2.33	12.9	3.37	8.90		
40	.449	1.43	28.0	1.53	26.2	1.67	24.0	1.86	21.5	2.17	18.4	2.78	14.4				
50	.418	1.49	33.6	1.61	31.0	1.75	28.6	1.99	25.1	2.37	21.1	3.20	15.6				
80	.382	1.57	51.0	1.70	47.1	1.88	42.6	2.16	37.0	2.63	30.4	4.02	19.9				
100	.366	1.62	61.7	1.75	57.2	1.94	51.6	2.24	44.7	2.78	36.0	4.70	21.3				
160	.345	1.67	95.8	1.80	88.9	2.03	78.9	2.36	67.8	3.00	53.3						
200	.335	1.69	118	1.83	109	2.06	97.1	2.42	82.6	3.11	64.3						

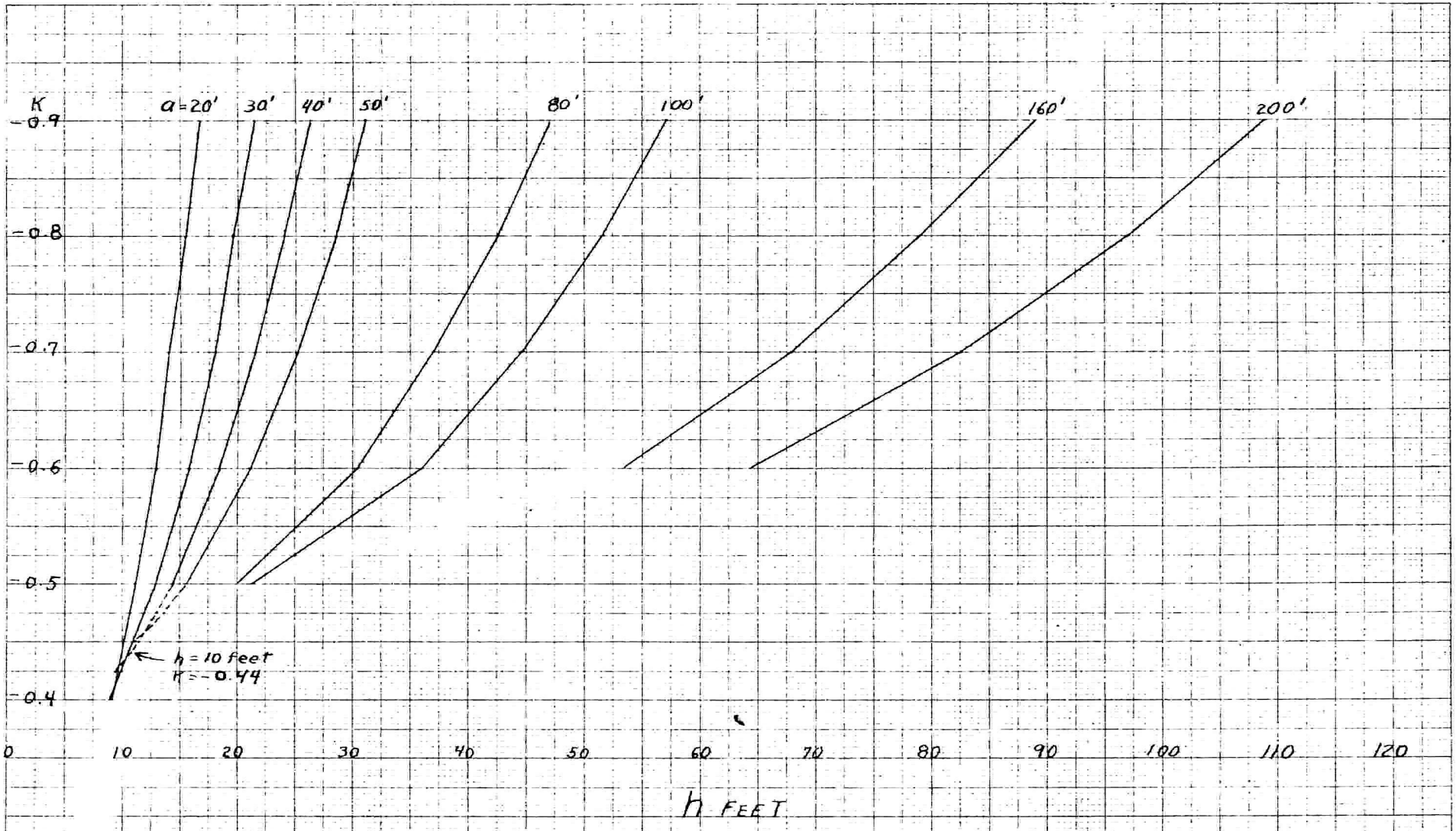

Figure 23. Example II, Tagg's original method: h-K curves.
$h = 10$ feet $\quad \rho_1 = 8000$ ohm-cm $\quad K = -0.44$
$\rho_2 = 8000 \times \frac{1-0.44}{1+0.44} = 3110$ ohm-cm.

6. The values of h and k are plotted in Figure 23. The curves for the forty and fifty foot spacings were extended (broken lines) using Plate VIII as in Example I. The data from Plate VIII is shown in the following table.

a (Ft.)		k = -0.5		k = -0.475		k = -0.45		k = -0.425	
		a/h	h	a/h	h	a/h	h	a/h	h
40	.449	2.78	14.4	3.09	13.0	3.51	11.4	4.28	9.4
50	.418	3.18	15.7	3.65	13.7	4.50	11.1		

The center of the points of intersection is in this case at about h = 10 feet, k = -.44. The assumption of a higher surface resistivity led in this case to a value of interface depth about a third less than that obtained in Example I.

(2) Tagg's modified method. To avoid the necessity of knowing the surface resistivity in finding h and k, Tagg suggested the following method(a) which is illustrated step by step with the same data used in Examples I and II.

Example III.

1. Determine the apparent resistivities for a number of different electrode intervals. These values are tabulated on page ? .

2. Plot an apparent resistivity-electrode separation curve. This has been done in Figure 20.

3. Read from the curve the apparent resistivities corresponding to a number of different electrode intervals. Also read the apparent resistivities corresponding to a second set of electrode intervals bearing a set ratio to the first. For example, let us take for the first set of intervals 20, 30, 40, and 50 feet. Our second set is then 40, 60, 80, and 100 feet if we select the ratio 2. (We have chosen the ratio two, because the master curves in Figure 24 were derived for such a ratio. There is no reason for not using pairs of resistivities for a series of ratios of electrode spacings such as 20 and 40 feet, n = 2; 20 and 30 feet, n = 1.5 etc. As will be shown below the preparation of a set of master curves for each ratio is not necessary. The only limit to the choice of ratios is that they be large enough so that the difference between the intervals represents a significant portion of the apparent resistivity curve and that they are not so large that the larger interval is more than five times the depth.

(a) The Mining Magazine, Vol. LIII, #3 (September 1935) p.148

Figure 24. Two layer master curve for Tagg's modified method.

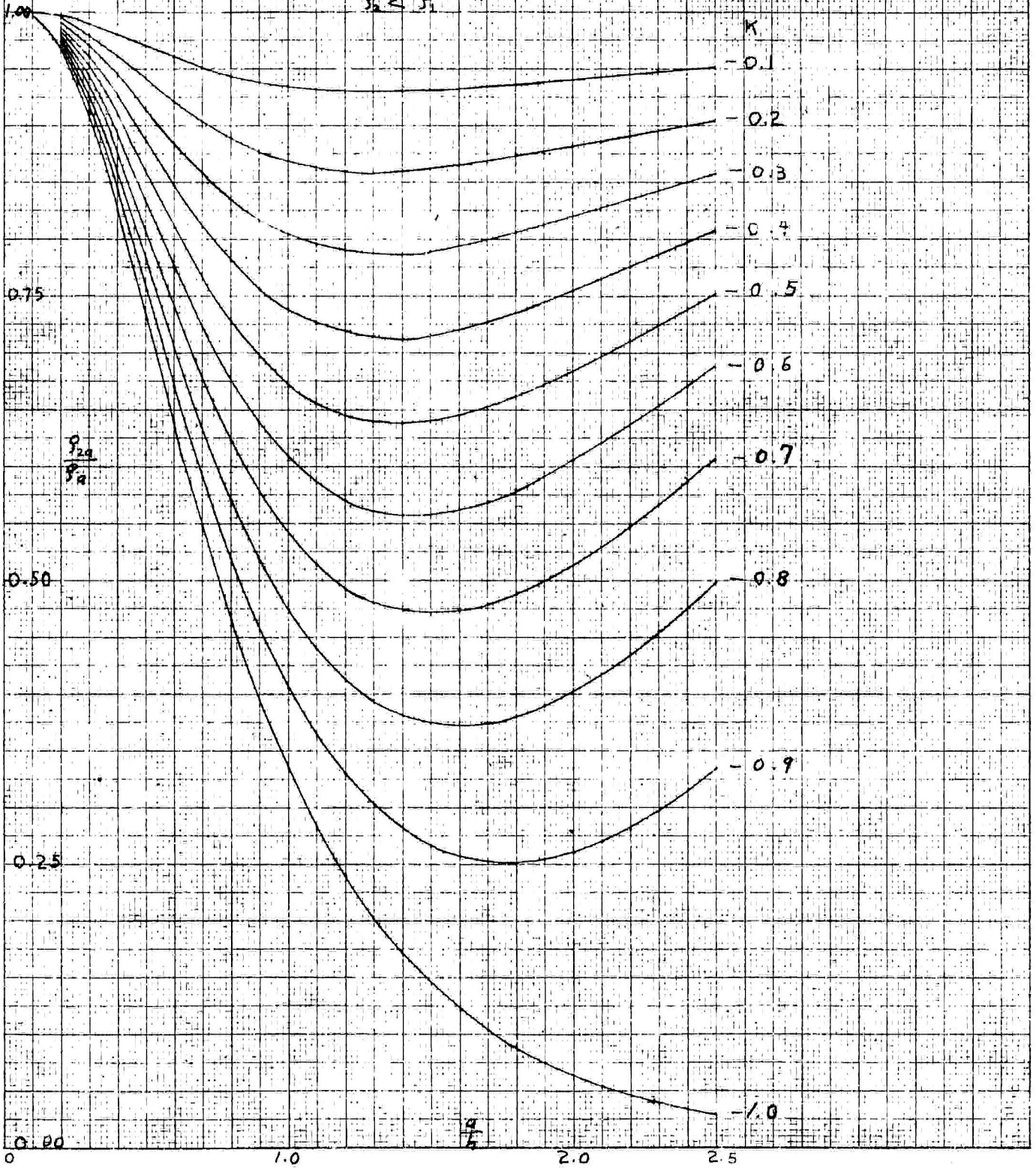

The second restriction is imposed because of the limited range of Roman's tables. For purposes of illustrating the method as first given by Tagg, we will assume master curves of the type in Figure 24 are necessary, and to avoid the labor of computing several sets of such curves, use only the ratio 2.) We will designate the first set of resistivities ρ_a, the second set ρ_{2a}. The ratio of the resistivities for each value of a is shown in the following table.

a(Ft.)	ρ_a (Ω-cm.)	2a (Ft.)	ρ_{2a} (Ω-cm.)	ρ_{2a}/ρ_a
20	4830	40	3600	.746
30	4020	60	3250	.808
40	3600	80	3060	.849
50	3350	100	2930	.875

4. From Figure 24 we read the following corresponding values of a/h and k in the same manner as from Figure 21 in Example I. From these values of a/h and the corresponding values of "a", the corresponding values of h are computed

a FEET	ρ_{2a}/ρ_a	K=-1.0		K=-0.9		K=-0.8		K=-0.7		K=-0.6		K=-0.5		K=-0.4		K=-0.3		K=-0.2	
		a/h	FEET h	a/h	FEET h	a/h	FEET h	a/h	FEET h	a/h	FEET h	a/h	FEET h	a/h	FEET h	a/h	FEET h	a/h	FEET h
20	.746	0.486	41.2	0.516	38.8	0.548	36.5	0.592	33.8	0.656	30.5	0.757	26.4	0.960	20.8				
												2.46	8.1	1.91	10.5				
30	.808	0.420	71.4	0.442	67.9	0.466	64.4	0.500	60.0	0.543	55.3	0.606	49.6	0.710	42.2	0.964	31.1		
																1.83	16.4		
40	.849	0.374	107	0.396	101	0.414	96.7	0.440	91.1	0.474	84.3	0.520	77.0	0.596	67.2	0.736	54.4		
																2.38	16.8		
50	.875	0.340	147	0.358	140	0.378	132	0.402	124	0.424	118	0.468	107	0.526	95.2	0.632	79.2	0.916	54.6
																		1.84	27.2

5. The curves of h against k for each value of "a" are shown in Figure 25 as solid lines. The data are insufficient to show any of the points of intersection. The broken lines in Figure 25 extend the curves so as to intersect. The values of h and k for the extended portions of the curves were obtained from Plate VIII by the following method. A piece of tracing paper was placed over Plate VII and three dots marked on it. One was over the origin of the graph, a second along the log(a/h) axis at a distance from the origin equal to the ratio of electrode intervals (in this case 2), and the third with the same abscissa, and an ordinate equal to the ratio ρ_{2a}/ρ_a. The tracing paper was then slid over the master curves until the first and third of these dots both fell on the same curve. For the value of k corresponding to this curve, a value of a/h could then be read from the abscissa opposite the first dot.

Figure 25. Example III, Tagg's modified method: h-K curves.

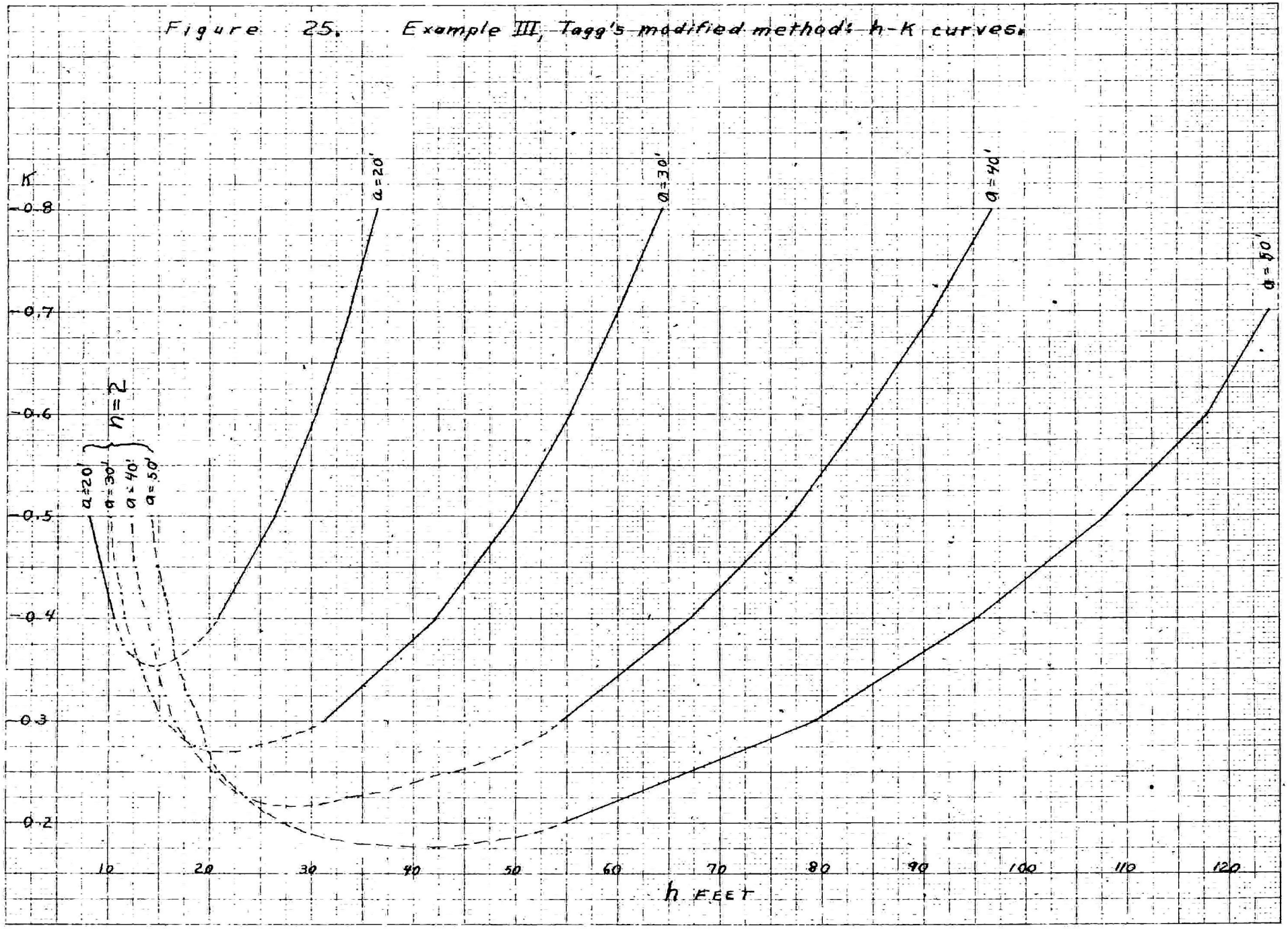

As the curves are plotted on a log log scale, what we have done is to find a value of a/h on a curve with a given value of k, for which the antilog of $\log(\rho_{2a}/\rho_1) - \log(\rho_a/\rho_1)$ (or ρ_{2a}/ρ_a) has the desired value. This is in effect what was done in step 4, above, except that the use of a logarithmic scale obviated the intermediate step of making a table and set of graphs such as those in Figure 24. Care must be taken to keep the axes of the master curves and of the tracing paper parallel by keeping the first and second of the three dots parallel to the abscissa of the master curves. This graphical method has another advantage in the use of tables which are only extended to values of a/h as great as 5. As the curves approach horizontal assymptotes for large values of a/h, and are smooth, it is possible to approximate fairly closely by eye the extension of the curves to larger values of a/h, and this makes possible the extension of the h-k curves to the critical smaller values of h. Figure 26 shows several curves for various values of a and n obtained graphically. These curves converge at a value of h of about 15 feet, indicating that the lower resistivity used in Example I was the better. The data for these curves is given in the following table.

a Feet	n	ρ_{ma}/ρ_a	K = −0.5		K −0.45		K −0.425		K −0.4		K −0.375		K −0.35		K −0.325		K −0.3		K −0.275		K −0.25		K −0.225		K −0.2	
			a/h	FT. h	a/h	FT. h	a/h	FT. h	a/h	FT. h	a/h	FT. h	a/h	FT. h	a/h	FT. h	a/h	FT. h	a/h	FT. h	a/h	FT. h	a/h	FT. h	a/h	FT. h
20	2	.746	2.5	8.0	2.25	8.9	2.1	9.5	1.95	10.3	1.75	11.4														
			0.75	26.7	0.82	24.4	0.88	22.5	0.97	20.6	1.08	18.5														
30	2	.808	2.75	10.2	2.80	10.7	2.65	11.3	2.58	11.6	2.42	12.4	2.25	13.3	2.10	14.3	1.92	15.6	1.62	18.5						
			0.60	50.0	0.66	45.4	0.68	44.1	0.70	42.8	0.76	39.5	0.80	37.5	0.88	34.1	1.00	30.0	1.25	24.0						
40	2	.849	3.25	12.3	3.15	12.7	3.05	13.1	2.90	13.8	2.80	14.3	2.70	14.8	2.55	15.7	2.42	16.5	2.20	18.2	1.95	20.5	1.70	23.6		
			0.52	77.5	0.58	69.6	0.59	67.8	0.57	67.8	0.64	62.5	0.67	59.7	0.70	57.2	0.72	55.2	0.80	50.0	0.92	43.5	1.20	33.4		
50	2	.875	3.5	14.3	3.35	14.9	3.2	15.6	3.1	16.1	3.05	16.4	2.95	17.0	2.8	17.9	2.65	18.9	2.55	19.6	2.4	20.8	2.12	23.6	1.8	27.8
			0.48	104					0.53	99.4			0.60	83.4	0.61	82.1	0.65	77.0	0.70	71.4	0.78	64.1	0.89	56.2	1.04	48.1
20	1.5	.834	2.75	7.3	2.45	8.9	2.25	8.9	2.10	9.5	1.75	11.4														
			0.91	22.0	1.00	20.0	1.09	18.4	1.19	16.8	1.3	15.4														
20	2.5	.694	2.30	8.7	2.05	9.8	1.92	10.4	1.77	11.3	1.6	12.5														
			0.66	30.4	0.72	27.8	0.77	26.0	0.84	23.8	0.96	20.8														
20	4	.634	2.05	9.8	1.85	10.8	1.7	11.8	1.55	12.9	1.48	13.5	1.27	15.8												
			0.44	45.5	0.49	40.8	0.52	38.5	0.56	35.8	0.61	32.8	0.70	28.6												
30	1.33	.895	3.10	9.7	2.85	10.5	2.75	10.9	2.55	11.8	2.4	12.5	2.1	14.3	1.75	17.1										
			0.90	33.4	0.96	31.2	1.02	29.4	1.05	28.6	1.2	25.0	1.35	22.2	1.60	18.8										
30	1.67	.833	2.95	10.2	2.75	10.9	2.6	11.5	2.48	12.1	2.30	13.0	2.10	14.3	1.90	15.8	1.45	20.7								
			0.75	40.0	0.80	37.5	0.85	35.3	0.87	34.5	0.96	31.3	1.05	28.6	1.16	25.8										

Figure 26. Example III, Tagg's modified method: h-K curves.

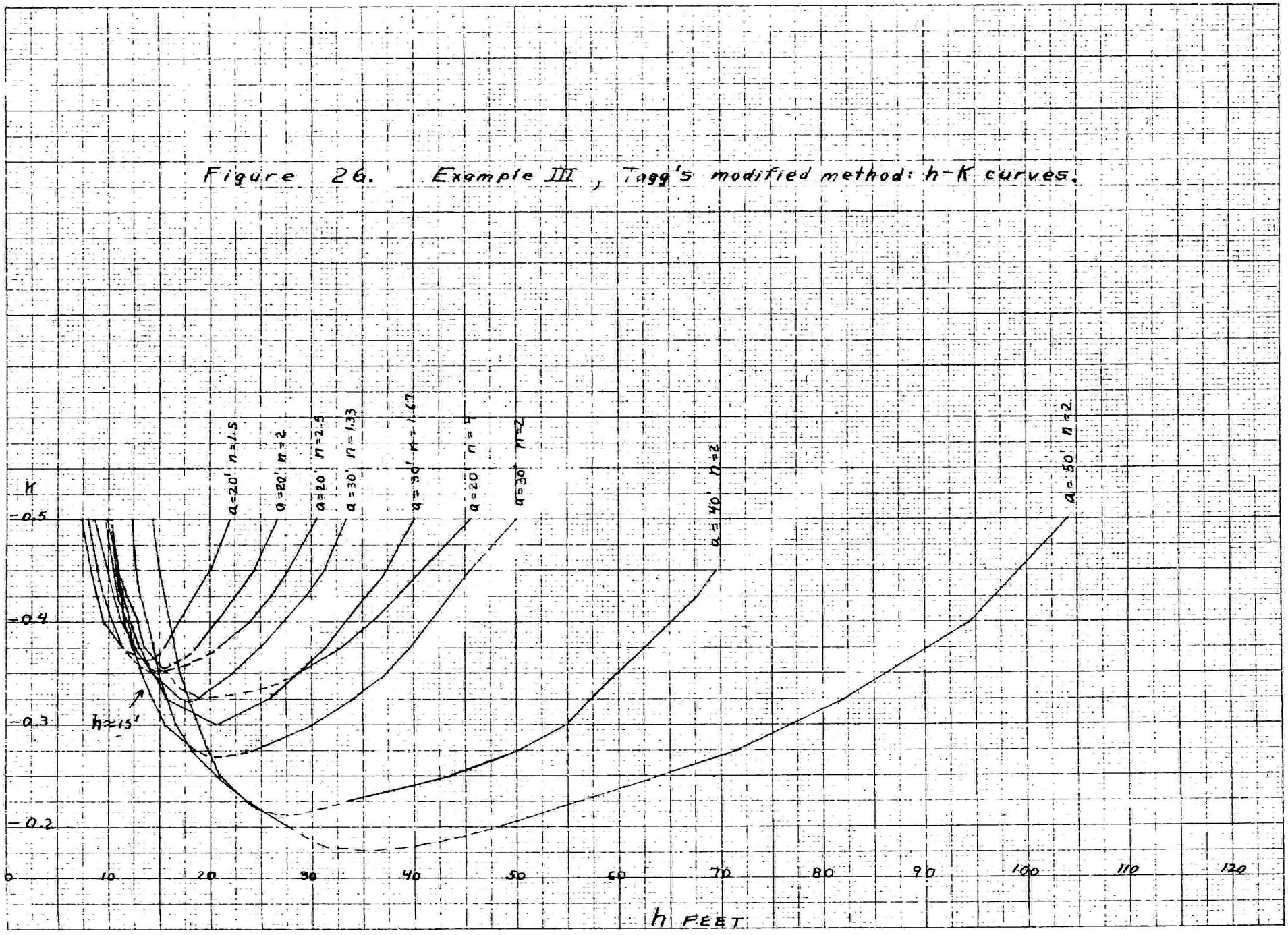

1b. Interpretation of field curves involving more than two layers

(1) Pirson's successive approximation method

The extension of two layer methods to the case of three layers is based on the assumption which experience has shown to be correct that the two upper layers may be treated as a single layer of their combined thickness, and of an effective resistivity intermediate to their individual resistivities. The third layer is then the lower layer of a second two layer problem. To use Tagg's original method it is necessary to know the value of this effective resistivity of the combined upper layers. As this value depends on the depth to the third layer which is not known from the solution of the curve for the upper two layers, a value is guessed by an empirical approximation and a tentative value of the effective resistivity is computed. Using this value as an effective first layer resistivity the depth to the third layer is calculated by Tagg's original method and if this value differs much from the assumed value, it is used to calculate an improved value of the effective resistivity and the method is repeated.

Example IV

To illustrate this method, the data (Table IV) obtained at Test Point #1 near Victorville are used because the depths to the interfaces are shallow and the depth to the second interface is known from observation of an adjacent road cut to be about 16 feet. The apparent resistivity-electrode separation curve is shown in Figure 27. We will estimate the value of ρ_1 to be 12,000 ohm-centimeters. (This value is that given by the superposition method Example VI below. The lower value of ρ_1 of about 8600 ohm-centimeters suggested by the values of apparent resistivity for small spacings does not give a good intersection of h, k curves and may be considerably in error because of the effect on the resistivity of the ground for a small distance around the electrodes which were watered to cut down contact resistance.

Figure 27. Example IV, Pirson's successive approximation method. Apparent resistivity data from Test Point no. 1 near Victorville, and two two-layer approximation curves.

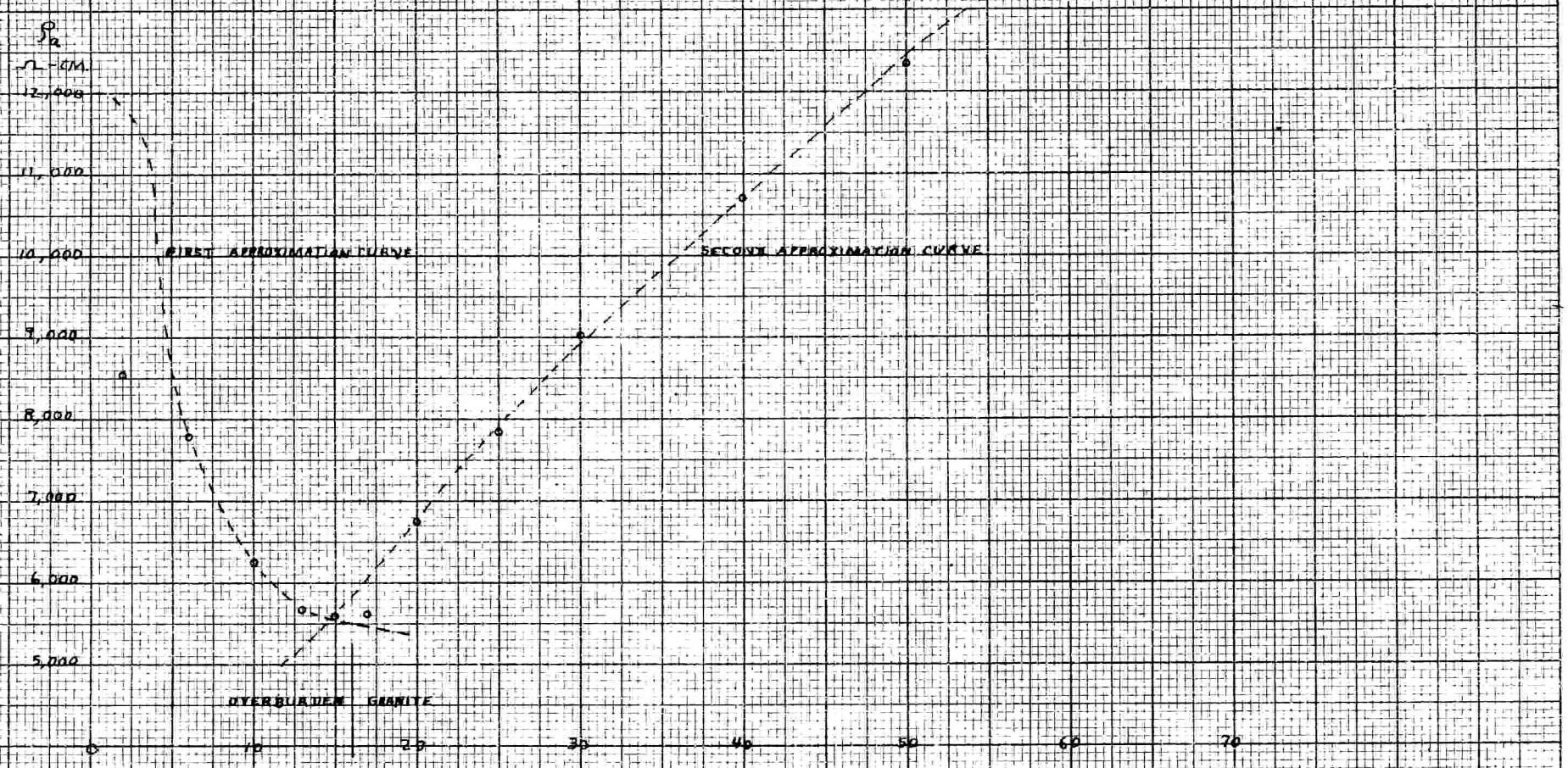

a FEET	ρ_a Ω-cm	ρ_a/ρ_1	K=-1.0		K=-0.9		K=-0.8		K=-0.7		K=-0.6		K=-0.5		K=-0.425		K=-0.4		K=-0.375		K=-0.35		K=-0.325		K=-0.3	
			q/h	FT. h	q/h	FT. h	q/h	FT. h	q/h	FT. h	q/h	FT. h	q/h	FT. h	q/h	FT. h	q/h	FT. h	q/h	FT. h	q/h	FT. h	q/h	FT. h	q/h	FT. h
6	7800	.651	1.05	5.71	1.11	5.41	1.18	5.08	1.28	4.69	1.40	4.29	1.59	3.78	1.80	3.33	1.91	3.14	2.03	2.96	2.20	2.73	2.39	2.51	2.66	2.26
8	7000	.580	1.18	6.78	1.25	6.40	1.34	5.97	1.46	5.48	1.63	4.91	1.90	4.21	2.24	3.57	2.41	3.32	2.64	3.03	2.94	2.72	3.42	2.35	4.40	1.82
10	6240	.521	1.28	7.87	1.37	7.30	1.48	6.76	1.63	6.14	1.85	5.41	2.20	4.89	2.75	3.64	3.07	3.26	3.60	2.78	4.58	2.18				
13	5670	.473	1.38	9.43	1.48	8.80	1.60	8.13	1.78	7.32	2.05	6.35	2.55	5.11	3.50	3.72	4.20	3.10								
15	5600	.467	1.40	10.7	1.50	10.0	1.62	9.26	1.80	8.33	2.09	7.18	2.61	5.75	3.66	4.10	4.54	3.30								

The above table gives the data obtained from Plate VIII for the h, k curves in Figure 28. The intersection of the curves gives values for h, and k, of 3 feet and -0.4. The next problem is to find the depth h_2 to the second interface. To do this, the two upper layers are considered replaced by an equivalent single layer of thickness h_2 and resistivity ρ'. The first step is to find this effective resistivity so that the ratios ρ_a/ρ' may be computed and values for the h, k curves obtained from the two-layer master curves. Hummel[a] has shown that for electrode separations large with respect to the second interface depth h_2, the effective resistivity of the two upper layers is given by Kirchoff's law for resistances in parallel. The value is therefore calculated from the formula

$$\frac{h_2}{\rho'} = \frac{h_1}{\rho_1} + \frac{h_2 - h_1}{\rho_2} \qquad \text{or} \qquad \rho' = \frac{h_2}{\frac{h_1}{\rho_1} + \frac{h_2 - h_1}{\rho_2}}$$

Of the quantities necessary for determining ρ', h_1, ρ_1, and ρ_2 are known from the interpretation of the first approximation curve. It is still necessary to get a value of h_2. The Lancaster-Jones approximation of two-thirds the depth to the inflection point in the second part of the field curve is used to get a preliminary value of h_2. In this case we have the values $h_1 = 3'$, $\rho_1 = 12000$ Ω-cm, $\rho_2 = 12000 \times .6/1.4 \approx 5000$ Ω-cm., and $h_2 = 2/3 \times 35' \approx 23'$.

We calculate the value $\rho' = \frac{23}{\frac{3}{12000} + \frac{20}{5000}} \approx 5400$ Ω-cm. and use this as an equivalent surface resistivity. The following table gives the data for the h, k curves of Figure 29.

(a) AIME Geophysical Prospecting 1932 p 418

Figure 28.

Example IV, Pirson's successive approximation method: h-K curves for upper two layers at Test Point no. 1, Victorville. $h_1 = 3$ ft., $\rho_1 = 12000$ Ω-cm., $K_1 = -0.4$, $\rho_2 = \rho_1 \times \frac{1+K_1}{1-K_1} \approx 5000$ Ω-cm.

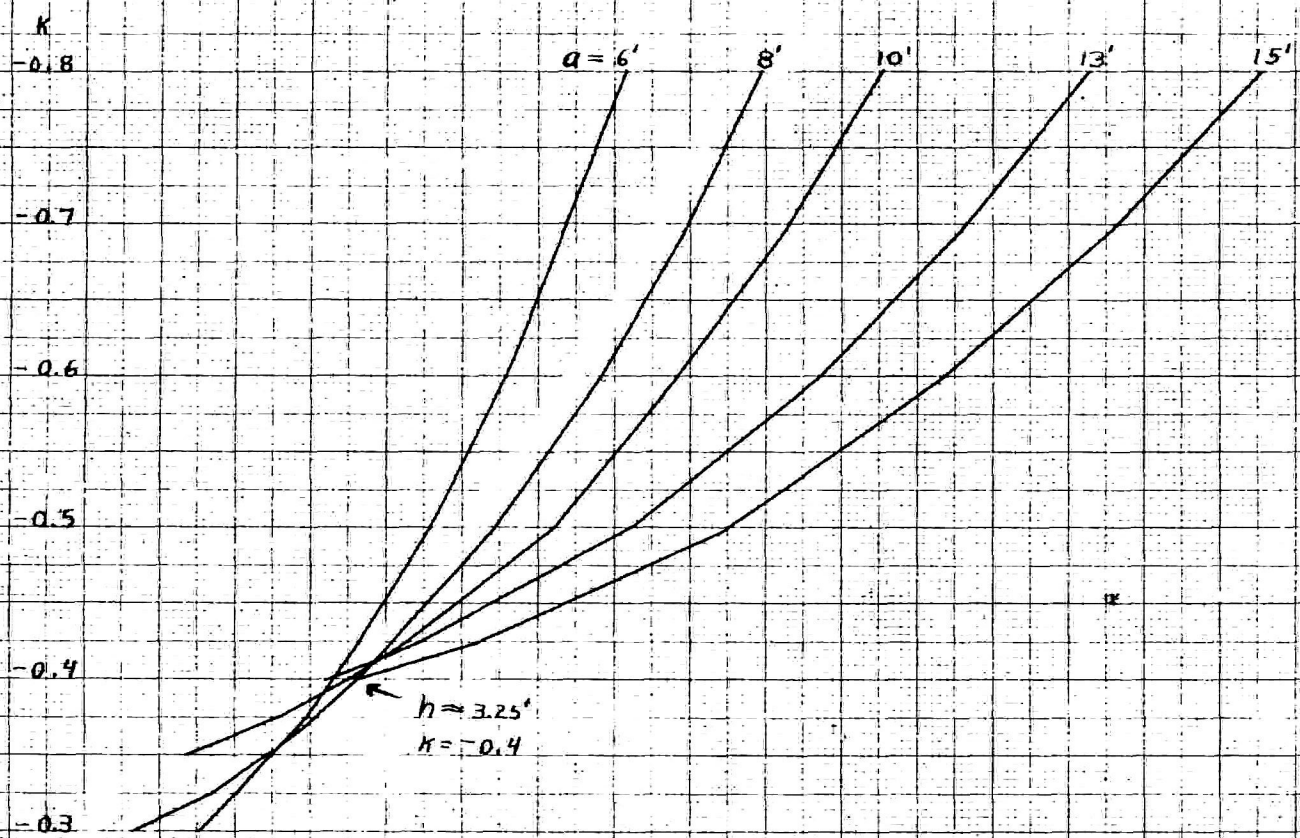

Figure 29. Example IV, Pirson's successive approximation method: h-K curves for lower two layers at Victorville Test Point no. 1.
First approximation: $\rho' = 5400$ ohm-cm.
$h_2 = 20$ ft., $K_1 = 0.7$, $\rho_3 = \rho' \times \frac{1+K_1}{1-K_1} \simeq 30{,}000$ ohm-cm.

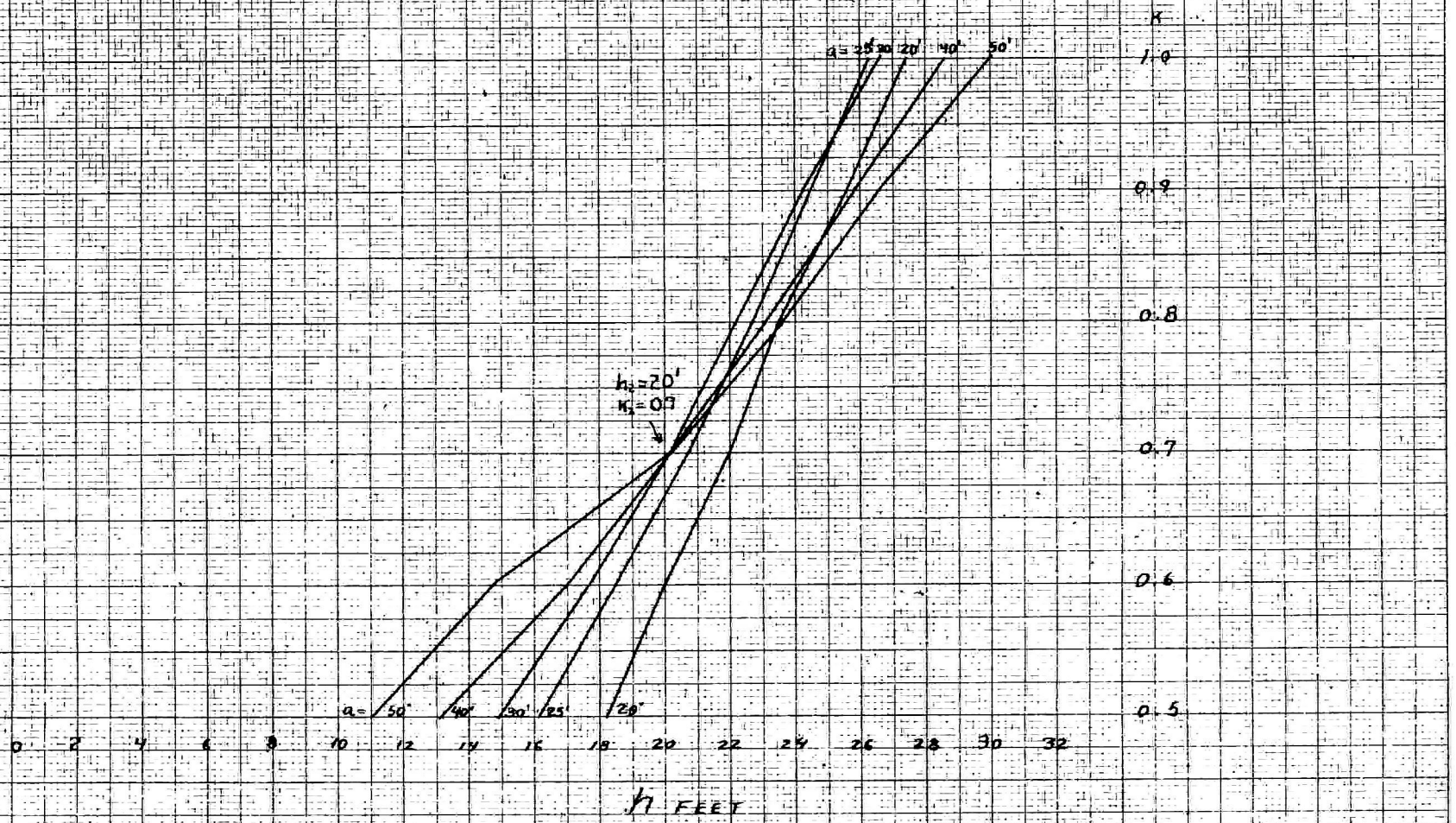

a feet	ρ_a ohm-cm.	ρ_a/ρ'	κ 1.0		κ 0.9		κ 0.8		κ 0.7		κ 0.6		κ 0.5		κ 0.4		κ 0.3		κ 0.2	
			a/h	FT. h	a/h	FT. h	a/h	FT. h	a/h	FT. h	a/h	FT. h	a/h	FT. h	a/h	FT. h	a/h	FT. h	a/h	FT. h
20	6750	1.25	0.73	27.4	0.78	25.6	0.85	23.5	0.91	22.0	1.00	20.0	1.10	18.2	1.25	16.0	1.55	12.9	2.20	9.1
25	7900	1.46	0.95	26.3	1.02	24.5	1.10	22.7	1.21	20.7	1.35	18.5	1.55	16.1	1.90	13.2	2.61	9.6		
30	8900	1.65	1.13	26.6	1.24	24.2	1.35	22.2	1.49	20.2	1.70	17.7	2.02	14.9	2.62	11.5	4.6	6.4		
40	10700	1.98	1.40	28.6	1.55	25.8	1.74	23.0	1.98	20.2	2.35	17.0	3.06	13.1	5.0	8.0				
50	12450	2.31	1.67	30.0	1.88	26.6	2.12	23.6	2.48	20.2	3.17	15.8	4.55	11.0						

From Figure 29 the value of h_2 may be taken as 20 feet, the value at the intersection of the curves for the thirty, forty, and fifty foot spacings. It is to be noted that the values for the spacings nearer the minimum in apparent resistivity curve-the 20 and 25 foot spacings-are not consistent with the others. This is an illustration of the fact that the two layer approximation curves deviate most from the theoretical three layer curves at electrode separations in the region where they intersect. We may now apply Hummel's formula again to get a new and better value of ρ' using the better value of h_2.

$$\rho' = \frac{20}{3/12000 + 17/5000} \approx 5500 \text{ ohm-cm.}$$

We may now reapply Tagg's original method to the second approximation curve using the improved value of the effective resistivity of the upper layers. The data for the curves in Figure 30 are given in the following table.

Figure 30. Example IV, Pirson's successive approximation method: h-K curves for lower two layers at Victorville, Test Point no. 1.

Second approximation: $\rho' = 5500$ Ω-cm.

$h_2 = 21$ ft., $K_2 = 0.7$, $\rho_3 = \rho' \times \frac{1+K_2}{1-K_2} \approx 31000$ Ω-cm.

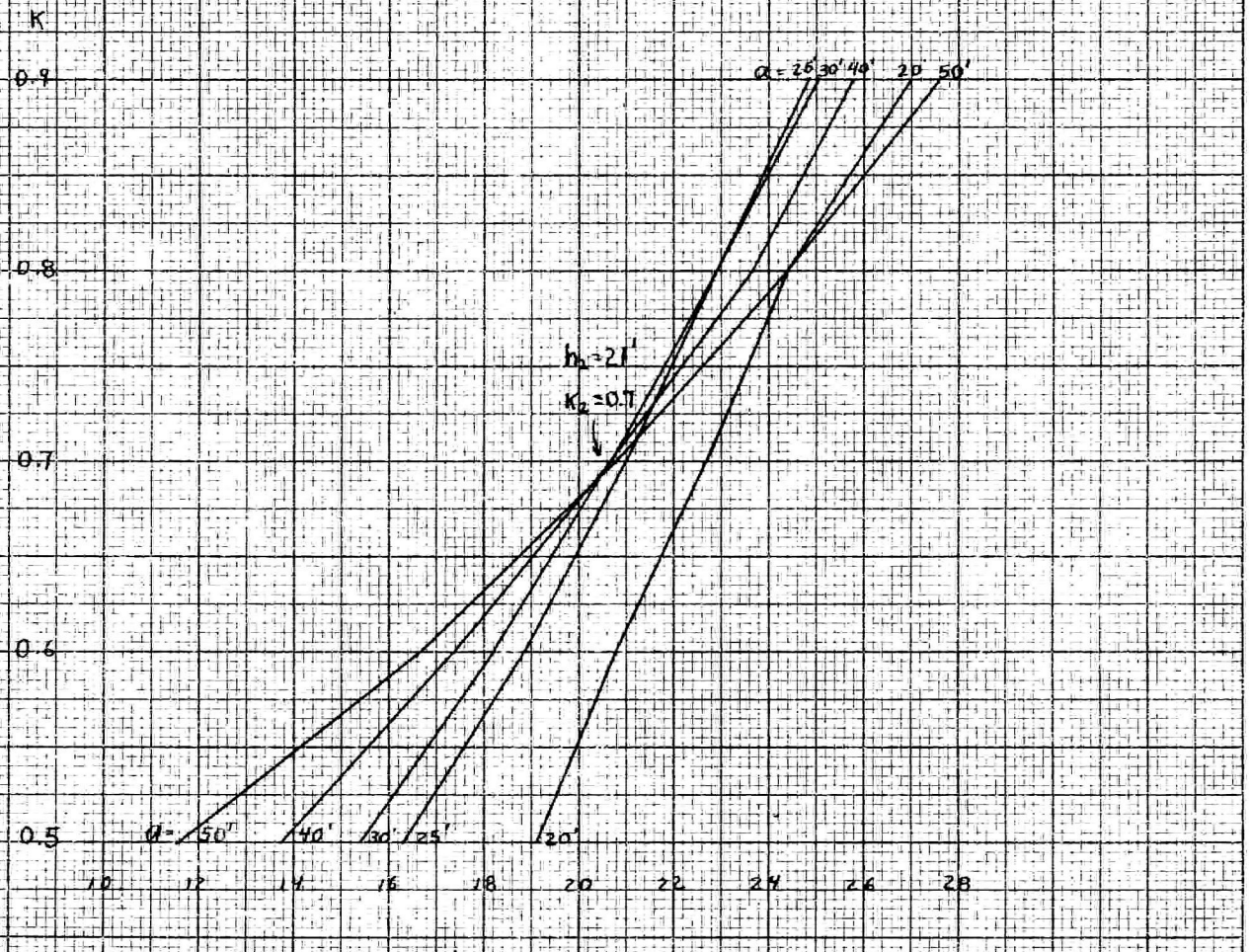

a FEET	ρ_a a-cm	$\frac{\rho_a}{\rho_1}$	K 1.0		K 0.9		K 0.8		K 0.7		K 0.6		K 0.5		K 0.4		K 0.3		K 0.2	
			a/h	FT. h	a/h	FT. h	a/h	FT. h	a/h	FT. h	a/h	FT. h	a/h	FT. h	a/h	FT. h	a/h	FT. h	a/h	FT. h
20	6750	1.23	0.71	28.2	0.74	27.0	0.82	24.4	0.88	22.7	0.96	20.8	1.05	19.1	1.19	16.8	1.48	13.5	2.04	9.8
25	7900	1.44	0.94	26.6	1.01	24.8	1.09	22.9	1.19	21.0	1.32	18.9	1.53	16.3	1.87	13.4	2.50	10.0		
30	8900	1.62	1.10	27.3	1.20	25.0	1.31	22.9	1.45	20.7	1.65	18.2	1.95	15.4	2.48	12.1	4.20	7.1		
40	10700	1.95	1.37	29.2	1.55	25.8	1.69	23.7	1.93	20.7	2.30	17.4	2.92	13.7	4.60	8.7				
50	12450	2.26	1.62	30.8	1.81	27.6	2.05	24.4	2.40	20.8	3.0	16.7	4.3	11.6						

From Figure 30 the intersection of the h,k curves for the 25, 30, 40, and 50 foot spacings gives the value of about 21 feet for h_2. This value is so near that used in calculating the improved value of effective resistivity that there is no reason to repeat the method in this case. If the improved value of h had been smaller, perhaps of the order of fifteen feet, a still closer approximation might have been expected by repeating the method.

If a fourth layer had been present and represented by a third bend in the field curve to which a third approximation curve might be fitted, the method could be applied using an effective resistivity calculated from the formula

$$\frac{h_3}{\rho'_3} = \frac{h_1}{\rho_1} + \frac{h_2 - h_1}{\rho_2} + \frac{h_3 - h_2}{\rho_3}$$

where h_3 is the depth to the top of the fourth layer and estimated as before by the Lancaster-Jones approximation. In the case of n layers the formula

$$\frac{h_{m-1}}{\rho'_{m-2}} = \frac{h_1}{\rho_1} + \frac{h_2 - h_1}{\rho_2} + \text{----} + \text{----} + \frac{h_{m-1} - h_{m-2}}{\rho_{m-1}}$$

is used to determine the effective resistivity of the top n-1 layers. It is apparent that the method is more and more laborious as more and more layers are involved, and that errors in determining the resistivities and thicknesses of the upper layers will produce errors in the values computed for the lower layers.

(2) Tagg's modified method This method, described under interpretation of two layer field curves, may be applied unchanged to any segment of an n-layer field curve, and eliminates the necessity of predetermining the effective resistivity of the upper layers. It has the inherent disadvantage of requiring each bend of the field curve approximated by a two layer curve to be sufficiently long that values of "a" can be found on it which are sufficiently far from maxima and minima of apparent resistivity and which are yet far enough apart to give values of ρ_{ma}/ρ_a appreciably different from unity.

2. Superposition methods a. Interpretation of two layer field curves

The superposition methods differ only as to the mechanical details used in applying the common principle on which they are all based. This is the fact that if the logarithm of apparent resistivity is plotted against the logarithm of the distance between the electrodes the shape and size of the curve is independent of the units in which the field data are expressed, and of the absolute size of the values since the distance and direction between any two points on the curve is determined only by the ratios of the two values of ordinate and of abscissa. Further these curves will be identical with those two layer master curves (when plotted on the same double logarithmic scale) which are derived for the same ratio of resistivities (or k value) regardless of the absolute value of the resistivities. When a field curve is plotted on transparent paper and slid over a set of master curves until it coincides with a particular curve, the value of k which represents the ratio of resistivities in the ground is given directly by the master curve with which the fit was made. In making the fit, the axes of the field and master

curves must be kept parallel so that in shifting the field curve the only change made is in the relative positions of the two ordinates. From the intercepts of the axes of the master curves on the axes of the field curve, when a match has been made, are obtained the depth to the interface between the two layers, and the size of the resistivities in the ground. The zero abscissa of the master set is the line along which the log of the ratio of apparent resistivity to the surface resistivity is zero, or the ratio itself is unity. This will intersect the zero ordinate of the field curve at a value of apparent resistivity which is equal to the resistivity of the surface layer. Similarly the zero ordinate of the master set will intersect the zero abscissa of the field curve at a value of electrode separation equal to the depth of the interface.

(1) Roman's method Irwin Roman was the first in this country to publish the suggestion of using a superposition method.(a) He determined the logarithms of the data for the field and master curves from a set of log tables and plotted them on ordinary graph paper. It was then necessary to compute antilogarithms to find the surface resistivity and interface depth.

(2) Paletca method This method was developed in Russia several years before Roman described his method, and although it has been discussed in Russian has not yet found its way into English.(b) It differs in two respects from Roman's method. The most important change is that the curves are plotted on logarithmic paper in which the coordinates are expressed in the field units and ratios involved, but are spaced according to the logarithms of these values. This eliminates the use of log tables. The other change is in using for electrode separation the distance between the

(a) Some Interpretations of Earth Resistivity Data A.I.M.E. Geophysical Prospecting, 1934, p. 183.

(b) The discussion of the Paletca method given here is based on lectures given by Dr. Potapenko in a course on electrical methods of prospecting.

Figure 31. Example IV, Superposition method. Broken lines show position of master curves closest to field curve at best fit: K = -0.36. From position of origin of master curves h = 14 feet, ρ_1 = 6300 ohm-centimeters.

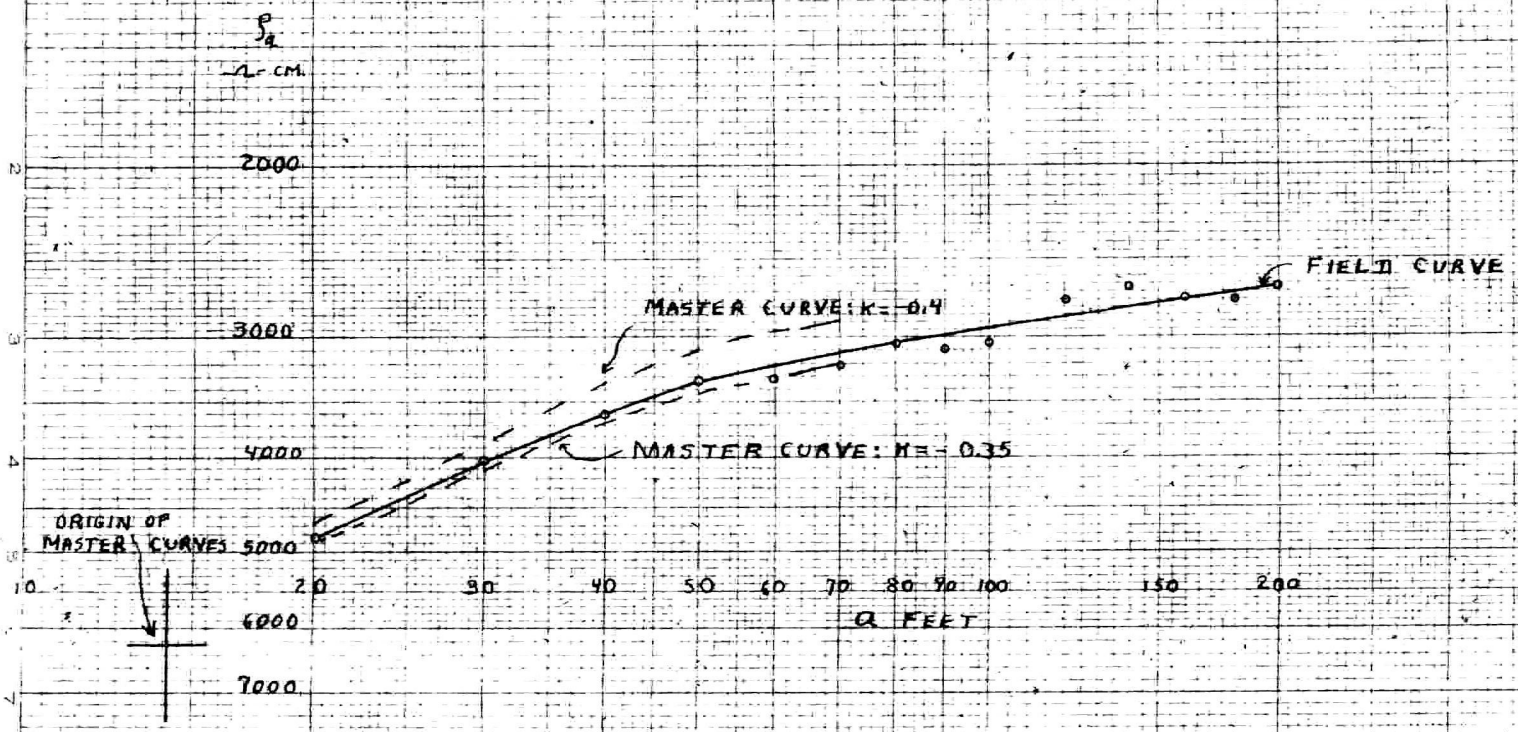

current electrodes rather than that between the potential electrodes. This has been found convenient where field conditions necessitate the shifting of potential electrodes from the exact locations required by the Wenner configuration.

Example V. Figure 31 illustrates the great simplicity of the superposition method. The data used in Examples I, II, and III is plotted on logarithmic graph paper and the fit with the master curves of Plate VIII is shown. The values $h_1 = 14$ feet and $\rho_1 = 6300$ ohm-centimeters are in close agreement with those obtained in Examples I and III and hours of computing were saved. Plate VIII is a hybrid between Roman and Paletca because it uses a logarithmic graph paper but uses the potential electrode separation instead of the current electrode separation. It is also unique in that to fit the master curves on the sheet of logarithm paper it was necessary to plot decreasing values of log (ρ_a/ρ_1) in the direction of increasing ordinate. It shows however the great advantage of the superposition principle.

2b. Interpretation of field curves of more than two layers.

In general field curves will not be simple two-layer curves but will be considerably more complicated. The superposition method can be used for these field curves as well as for the two layer case. Theoretical master curves have been prepared for the three layer case and are discussed below. However these are clumsy to use and impractical. No data for theoretical curves for cases of more than three layers is available, and interpretation of more complicated curves are carried out by repeated use of the two-layer master curves. As this extended use of the superposition method is by far the best method to use in routine interpretations of depth profile field data, it is described in some detail in connection with the three layer field curves obtained at Victorville.

(1) Use of three-layer theoretical curves. Theoretically it is more accurate to compare three-layer field curves with master curves computed especially for that case. If the field curves are approximated by two two-layer curves, these will

TABLE VIII[a]

The table lists the value of ρ_2/ρ_1 or ρ_2 since $\rho_1 = 1$.

Part 1. $h_1 = 6$, $h_2 = 8$

$\rho_1 : \rho_2 : \rho_3$	$8a/h_2$ = 2	4	6	8	10
1:.01:.1	0.979	0.869	0.693	0.518	0.366
:1/3	0.979	0.869	0.698	0.527	0.376
:1	0.979	0.870	0.706	0.536	0.388
:3	0.979	0.871	0.708	0.542	0.393
:10	0.979	0.871	0.709	0.544	0.396
1:.1:.01	0.970	0.848	0.674	0.510	0.380
:1/3	0.983	0.898	0.761	0.634	0.529
:1	0.986	0.918	0.808	0.691	0.621
:3	0.987	0.927	0.831	0.750	0.719
:10	0.988	0.933	0.845	0.773	0.745
:100	0.989	0.936	0.854	0.789	0.763
1:1/3:.01	0.970	0.865	0.713	0.550	0.416
:.1	0.980	0.894	0.765	0.623	0.495
: 1	0.989	0.949	0.898	0.855	0.832
: 3	0.997	0.994	0.998	1.030	1.080
:10	0.999	1.000	1.020	1.092	1.223
:100	1.000	1.023	1.060	1.148	1.284
1:3:.01	0.990	0.980	0.970	0.900	0.815
:.1	1.000	0.995	0.980	0.945	0.875
:1/3	1.000	1.020	1.025	1.005	0.965
:1	1.010	1.045	1.100	1.150	1.180
:10	1.025	1.135	1.345	1.590	1.850
:100	1.04	1.170	1.42	1.73	2.09
1:10:.01	1.01	1.05	1.14	1.250	1.280
:.1	1.01	1.06	1.16	1.265	1.300
:1/3	1.02	1.08	1.18	1.300	1.365
:1	1.02	1.11	1.24	1.375	1.480
:3	1.04	1.150	1.30	1.495	1.675
:100	1.04	1.19	1.49	1.885	2.260
1:100:.1	1.02	1.13	1.40	1.700	2.010
:1/3	1.02	1.13	1.41	1.705	2.02
:1	1.02	1.14	1.43	1.715	2.05
:3	1.02	1.14	1.45	1.730	2.08
:10	1.02	1.15	1.47	1.78	2.14

a. Wetzel and McMurry, Geophysics, Vol. 2, #4, 1937
Table II, p.334, Table III, p.335,
Table IV, p.336

TABLE VIII

Part 1. Concluded $h_1 = 6$, $h_2 = 8$

$\rho_1 : \rho_2 : \rho_3$	$8a/h_2$ = 15	20	25	30	40
1:.01:.1	0.136	0.0785	0.0763	0.0810	0.0861
:1/3	0.160	0.1075	0.1150	0.1275	0.1490
:1	0.190	0.144	0.157	0.178	0.227
:3	0.194	0.158	0.177	0.205	0.266
:10	0.203	0.166	0.188	0.218	0.285
1:.1:.01	0.148	0.062	0.032	0.0196	0.0116
:1/3	0.398	0.356	0.345	0.341	0.340
:1	0.605	0.625	0.645	0.665	0.700
:3	0.745	0.865	1.00	1.13	1.350
:10	0.835	1.025	1.23	1.425	1.820
:100	0.880	1.11	1.36	1.620	2.150
1:1/3:.01	0.182	0.077	0.035	0.0196	0.013
:.1	0.278	0.186	0.147	0.129	0.112
:1	0.830	0.850	0.873	0.895	0.930
:3	1.26	1.44	1.60	1.74	1.98
:10	1.61	2.00	2.38	2.71	3.28
:100	1.76	2.28	2.86	3.42	4.52
1:3:.01	0.550	0.323	0.182	0.106	
:.1	0.650	0.430	0.294	0.212	0.128
:1/3	0.840	0.680	0.540	0.460	0.382
:1	1.20	1.175	1.13	1.10	1.08
:10	2.49	3.05	3.55	4.02	4.82
:100	3.01	3.99	4.99	5.98	7.95
1:10:.01	1.21	1.01	0.775	0.558	0.230
:.1	1.26	1.07	0.850	0.650	0.350
:1/3	1.36	1.21	1.04	0.895	0.653
:1	1.625	1.610	1.54	1.45	1.30
:3	2.05	2.32	2.53	2.67	2.86
:100	3.35	4.42	5.52	6.60	8.75
1:100:.1	2.69	3.16	3.49	3.65	3.68
:1/3	2.72	3.20	3.52	3.71	3.82
:1	2.75	3.28	3.65	3.90	4.10
:3	2.83	3.42	3.90	4.23	4.60
:10	3.01	3.81	4.53	5.17	6.02

TABLE VIII

Part 2. $h_1 = 4$, $h_2 = 8$

$\delta_1 : \delta_2 : \delta_3$	$2a/h_2$ = 2	4	6	8	10
1:.01:.1	0.932	0.690	0.431	0.246	0.138
:1/3	0.932	0.691	0.434	0.250	0.145
:1	0.932	0.691	0.435	0.252	0.150
:3	0.932	0.691	0.436	0.253	0.152
:10	0.932	0.691	0.436	0.254	0.155
1:.1:.01	0.925	0.719	0.480	0.293	0.176
:1/3	0.945	0.753	0.543	0.398	0.310
:1	0.950	0.760	0.560	0.422	0.350
:3	0.955	0.767	0.574	0.455	0.393
:10	0.958	0.772	0.584	0.472	0.422
:100	0.959	0.775	0.588	0.481	0.436
1:1/3:.01	0.920	0.765	0.575	0.405	0.280
:.1	0.935	0.790	0.621	0.473	0.369
:1	0.966	0.853	0.726	0.674	0.660
:3	0.972	0.877	0.785	0.780	0.816
:10	0.976	0.888	0.810	0.815	0.875
:100	0.980	0.900	0.840	0.850	0.950
1:3:.01	1.020	1.100	1.170	1.170	1.115
:.1	1.02	1.11	1.210	1.230	1.175
:1/3	1.03	1.130	1.230	1.280	1.250
:1	1.04	1.165	1.320	1.430	1.475
:10	1.05	1.30	1.63	1.91	2.21
:100	1.06	1.41	1.79	2.22	2.69
1:10:.01	1.050	1.290	1.580	1.835	1.980
:.1	1.06	1.30	1.60	1.85	1.99
:1/3	1.06	1.31	1.62	1.88	2.00
:1	1.07	1.315	1.65	1.965	2.125
:3	1.07	1.34	1.73	2.075	2.34
:100	1.090	1.43	1.92	2.45	3.03
1:100:.1	1.04	1.40	1.91	2.47	3.00
:1/3	1.04	1.40	1.91	2.47	3.00
:1	1.04	1.40	1.91	2.48	3.01
:3	1.05	1.43	1.92	2.50	3.02
:100	1.06	1.44	1.96	2.60	3.15

TABLE VIII

Part 2. $h_1 = 4$, $h_2 = 8$, Concluded

$\rho_1 : \rho_2 : \rho_3$	$8a/h_2$ = 15	20	25	30	40
1:.01:.1	0.056	0.0496	0.0540	0.0588	0.0665
:1/3	0.0665	0.068	0.077	0.0875	0.105
:1	0.0720	0.0775	0.090	0.103	0.130
:3	0.0742	0.0810	0.0960	0.112	0.143
:10	0.0748	0.0823	0.0978	0.114	0.147
1:.1:.01	0.0670	0.0345	0.0213	0.0152	0.0111
:1/3	0.236	0.239	0.261	0.278	0.301
:1	0.342	0.400	0.458	0.510	0.600
:3	0.415	0.510	0.618	0.720	0.910
:10	0.455	0.575	0.720	0.858	1.12
:100	0.475	0.618	0.765	0.920	1.24
1:1/3:.01	0.111	0.0480	0.0242	0.0162	0.0108
:.1	0.210	0.154	0.134	0.122	0.111
:1	0.700	0.745	0.795	0.830	0.890
:3	1.02	1.21	1.37	1.51	1.74
:10	1.20	1.53	1.84	2.13	2.68
:100	1.32	1.74	2.16	2.60	3.45
1:3:.01	0.820	0.455	0.250	0.148	
:.1	0.905	0.595	0.385	0.262	0.140
:1/3	1.03	0.800	0.610	0.495	0.390
:1	1.42	1.31	1.21	1.15	1.10
:10	2.97	3.62	4.20	4.70	5.50
:100	3.80	4.95	6.15	7.30	9.60
1:10:.01	1.94	1.71	1.42	1.11	0.565
:.1	1.99	1.78	1.51	1.23	0.720
:1/3	2.06	1.88	1.64	1.36	0.860
:1	2.31	2.27	2.12	1.92	1.43
:3	2.84	3.16	3.35	3.41	3.30
:100	4.50	5.95	7.40	8.80	11.6
1:100:.1	4.14	5.00	5.62	6.00	6.40
:1/3	4.14	5.00	5.62	6.05	6.50
:1	4.19	5.08	5.72	6.20	6.60
:3	4.25	5.25	6.00	6.55	7.05
:10	4.50	5.70	6.70	7.55	8.70

TABLE VIII

Part 3. $h_1 = 2$, $h_2 = 8$

$\rho_1 : \rho_2 : \rho_3$	$8a/h_2$ = 2	4	6	8	10
1:.01:.1	0.690	0.252	0.088	0.040	0.0295
:1/3	0.691	0.259	0.088	0.047	0.0340
:1	0.692	0.262	0.102	0.052	0.0365
:3	0.693	0.264	0.105	0.054	0.0380
:10	0.693	0.265	0.106	0.055	0.0385
1:.1:.01	0.725	0.325	0.166	0.102	0.0695
:1/3	0.736	0.350	0.206	0.162	0.156
:1	0.740	0.361	0.229	0.192	0.196
:3	0.744	0.370	0.245	0.219	0.228
:10	0.746	0.376	0.251	0.227	0.238
:100	0.748	0.378	0.253	0.232	0.245
1:1/3:.01	0.805	0.508	0.335	0.233	0.166
:.1	0.820	0.540	0.381	0.290	0.235
:1	0.840	0.570	0.490	0.484	0.500
:3	0.848	0.590	0.533	0.553	0.605
:10	0.853	0.600	0.545	0.581	0.661
:100	0.855	0.610	0.560	0.610	0.703
1:3:.01	1.185	1.510	1.625	1.585	1.46
:.1	1.190	1.520	1.635	1.608	1.493
:1/3	1.195	1.540	1.680	1.695	1.620
:1	1.200	1.570	1.770	1.870	1.895
:10	1.210	1.630	2.130	2.530	2.92
:100	1.235	1.730	2.33	2.95	3.55
1:10:.01	1.36	2.125	2.72	3.070	3.135
:.1	1.36	2.13	2.74	3.09	3.23
:1/3	1.37	2.15	2.77	3.11	3.26
:1	1.37	2.16	2.80	3.18	3.45
:3	1.38	2.19	2.94	3.45	3.76
:100	1.42	2.34	3.31	4.32	5.39
1:100:.1	1.41	2.55	3.65	4.68	5.65
:1/3	1.41	2.55	3.67	4.70	5.70
:1	1.42	2.57	3.70	4.75	5.72
:3	1.42	2.59	3.76	4.82	5.85
:10	1.47	2.65	3.86	5.00	6.18

TABLE VIII

Part 3. $h_1 = 2$, $h_2 = 8$ Concluded

$\rho_1 : \rho_2 : \rho_3$	$8a/h_2$ = 15	20	25	30	40
1:0.01:.1	0.0311	0.0362	0.0410	0.0459	0.0545
:1/3	0.0368	0.0442	0.0529	0.0610	0.0775
:1	0.0388	0.0475	0.0575	0.0670	0.0870
:3	0.0400	0.0495	0.0605	0.0715	0.0930
:10	0.0405	0.0502	0.0612	0.0725	0.0960
1:.1:.01	0.0348	0.0220	0.0160	0.0130	0.0102
:1/3	0.176	0.202	0.225	0.242	0.267
:1	0.250	0.314	0.370	0.422	0.505
:3	0.296	0.380	0.462	0.540	0.685
:10	0.322	0.421	0.525	0.630	0.825
:100	0.329	0.432	0.540	0.655	0.880
1:1/3:.01	0.068	0.030	0.0185	0.0140	0.0107
:.1	0.166	0.138	0.124	0.115	0.106
:1	0.565	0.640	0.705	0.758	0.820
:3	0.780	0.960	1.12	1.26	1.51
:10	0.920	1.19	1.44	1.69	2.14
:100	1.03	1.37	1.70	2.03	2.67
1:3:.01	0.970	0.555	0.325	0.205	0.100
:.1	1.04	0.650	0.420	0.283	0.152
:1/3	1.28	0.890	0.650	0.515	0.400
:1	1.75	1.55	1.38	1.27	1.14
:10	3.78	4.46	5.10	5.60	6.39
:100	5.10	6.60	8.15	9.63	12.6
1:10:.01	2.97	2.53	1.93	1.32	0.608
:.1	3.03	2.57	1.96	1.42	0.760
:1/3	3.19	2.75	2.18	1.64	0.950
:1	3.54	3.25	2.74	2.23	1.48
:3	4.10	4.09	4.00	3.87	3.64
:100	7.75	10.0	12.2	14.2	18.0
1:100:.1	7.60	9.00	9.90	10.4	10.8
:1/3	7.70	9.10	10.0	10.5	11.1
:1	7.85	9.43	10.5	11.2	11.8
:3	8.15	10.2	11.9	13.2	15.1
:10	8.80	11.3	13.5	15.2	17.7

deviate somewhat from the corresponding three-layer curve, and this deviation will be greatest where the two approximating curves intersect, as at a maximum or minimum in the field curve. However, the preparation of such curves, besides being a laborious task, involves the problem of representing graphically curves with a greater number of variables. In the two layer case the curves contain three unknowns, ρ_1, ρ_2, and h, and can all be plotted on a single sheet with ρ_2/ρ_1 and a/h or L/h as coordinates and $k = \frac{\rho_2-\rho_1}{\rho_2+\rho_1}$ as a parameter. In the three layer case there are five unknowns, ρ_1, ρ_2, ρ_3, h_1, and h_2, so that the curves must be plotted by groups for special cases in which the number of variables is reduced by specifying ratios between some of them. This is exemplified in Table VIII where values of ρ_a/ρ_1 are listed for various ratios of the three resistivities (with $\rho_1=1$) and various values of $8\ a/h_2$ for a single value of the ratio h_1/h_2. This data is taken from Wetzel and McMurry's article A Set of Curves to Assist in the Interpretation of the Three Layer Resistivity Problem where it occurs as Tables II, and III, and IV.(a) This is the only systematic set of tables published so far as the writer is aware. Curves from this data plot the log of ρ_a/ρ_1 against that of $8\ a/h_2$ for a given ratio of h_1/h_2 and of $\rho_1(=1)/\rho_2/\rho_3$. It is suggested in the article that these curves be grouped in families with a single value of $\rho_1/\rho_2/\rho_3$ for values of h/h_2 of $\frac{1}{4}$, $\frac{1}{2}$, and 3/4 on a single sheet of graph paper together with the two limiting two layer curves for the cases $h_1/h_2 = 0/4$ and 4/4. This is illustrated by Figure 33 which shows the field curve obtained at Test Point #1 near Victorville superimposed on the family which two layer approximation shows to be the closest fit. The awkwardness of using 3-layer curves becomes apparent when it is noted that 14 sets of these curve families are needed to include only those field curves which contain a minimum of apparent resistivity. The field curve is compared by superposition to families of master curves until one is found which includes a curve of the size and shape of the field curve. Then the field curve is fitted into its place in this family by eye until its shape and size are intermediate to those of the master curves between which it falls. The position relative to the other master curves gives the ratio h/h_2; the value of abscissa of the field curve opposite the master curve ordinate $8a/h_2 = 8$ gives the value of h_2; and the intersect on the field ordinate determines ρ_1 as in the two-layer case. ρ_2 and ρ_3 are then determined from the resistivity ratio of the family of master curves. This method at present is not strictly one of superposition because there are master curves for so few values of h_1/h_2 that most field curves fall between them rather than on them, and the matching involves extensive visual interpolation. Further, the field conditions do not often exactly correspond with any of the sets of resistivity ratios assumed in the master curves, and in the absence of a close fit with one of the master curves there is often no way to tell to which of various families the field curve is most closely related, or to determine the value of h_1/h_2.

(a) Geophysics, Vol. II, #4, p. 329. October 1937.

(2) The Paletca method The Paletca curves for all values of k are assymptotic at very small values of L/h to the L/h axis where the apparent resistivity is equal to that of the upper layer. At very large values of L/h they are assymptotic to the abscissa along which the apparent resistivity equals that of the lower layer. Between these two assymptotic portions of each curve is a connecting segment in which the apparent resistivity varies continuously from the resistivity of the upper layer to that of the lower. In the following discussion this connecting segment is called a "link". The link contains at each end a point of inflection which will be called a "turning point". The values of L/h at which the turning points occur are determined mainly by the depth to the interface between the two layers, and somewhat by the ratio of the resistivities. The greater the difference in the resistivity ratio or the larger the absolute value of the reflection factor k, the sooner the effect of the second layer on the apparent resistivity is noticed and the smaller is the value of L/h at which the first turning point occurs, and the larger the value of L/h for the second turning point. The steepness of the link increases with the absolute value of k in spite of the increased L/h interval between the turning points because of a greater increase of the ρ_a/ρ_1 intercept between apparent resistivity values of ρ_1 and ρ_2. Field curves of more than two layers are interpreted by assuming them to be made up of a number of two layer curves. If a third layer is present at sufficient depth,

the apparent resistivity may very nearly reach its assymptotic value before the effect of the third layer is noticeable. Further increase in L/h values will cause a third turning point in the field curve followed by a second link turning through a fourth turning point into a third assymptotic portion where the apparent resistivity is very nearly that of the third layer. If the second layer is thin, the apparent resistivity may not approach its resistivity assymptotically before the effect of the third layer becomes pronounced, and if the second layer is too thin, its effect on the apparent resistivity may be negligible so that its presence isn't noted. A field curve with n distinct links represents the presence of n + 1 layers of distinctly different resistivities and of thicknesses shown by experience to be from 5% to 10% at least of their depth.

In outline the procedure of interpreting the field curves is very simple. Each successive link of the curve is fitted with one of the Paletca curves. From the fit of the first link is determined the surface resistivity ρ_1, the depth h, to the top of the second layer, and from the values of ρ_1 and the k of the Paletca curve, the resistivity of the second layer ρ_2 as in the two layer case. From the second fit are determined the effective resistivity ρ' of the first two layers, the depth h_2 to the top of the third layer, and the resistivity ρ_3 of the third layer. The third fit gives the effective resistivity ρ'' of the first three layers, h_3 the depth to the

top of the fourth layer, and ρ_4 the resistivity of the fourth layer, and so on. If each link of the curve was sufficiently long to include both turning points there would be no ambiguity in the fit, but in practise the links are usually short so that they may be fitted to parts of links of Paletca curves for several values of k, and there is doubt as to whether it belongs to a certain portion of one curve, or to a less steep portion of a steeper curve. The different fits will give different values of the depths and resistivities. The following arbitrary rule is of assistance in determing the most likely of the possible fits. If the slope of the link is steep ($|k| > 0.5$) the most likely depth is that closest to 3/8 the value of L at the bend where the presence of the layer below the interface starts to make itself felt. By "bend" is meant the small portion of the field curve which contains two turning points at the meeting of two successive links. If the slope is small, ($|k| \leq .5$) the most likely interface depth is that closest to 3/8 the value of L at the middle of the link which is being interpreted. Joints on the field curve links close to the turning points should not be trusted because they may deviate considerably from theoretical two layer curves. It may happen that links are represented by only two points so that they will fit the Paletca curves in many places. In this case only an approximate solution is possible. A depth to the interface can be approximated by the rule given above, and the field curve moved over the Paletca curves, with the value of L equal to the approximate depth

Figure 32. Example VI, Paletca method: interpretation of ρ_a, L curve from Test Point 60.1 near Victorville.

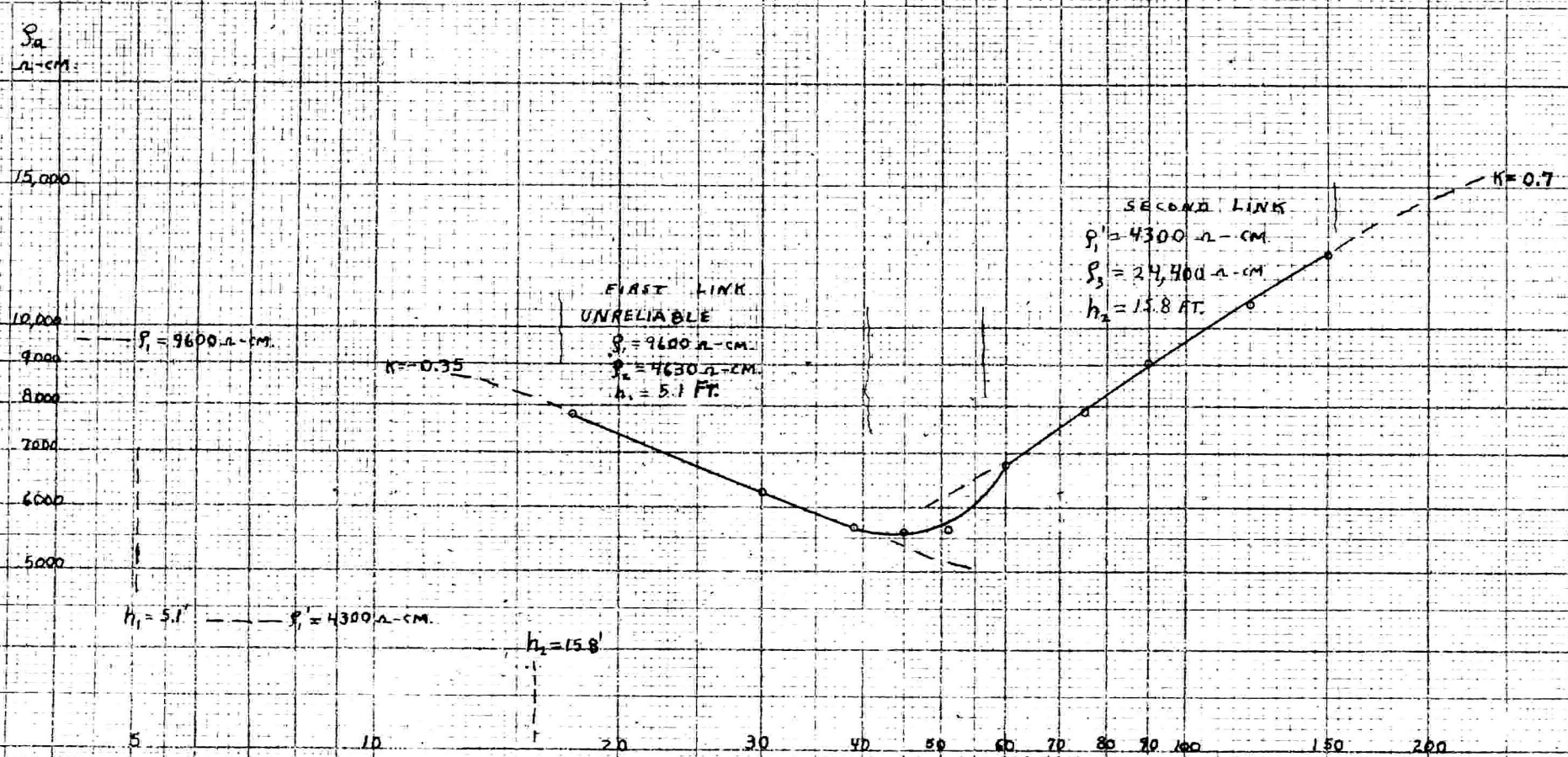

kept on the L/h = 1 ordinate, until the slopes of the curves are the same and thus determine an approximate value of k and of the resistivities.

A valuable check on the depths and resistivities determined is furnished by the application of Hummel's formula:

$$\frac{h_m}{\rho^{m-1}} = \frac{h_1}{\rho_1} + \frac{h_2 - h_1}{\rho_2} + \cdots\cdots + \frac{h_m - h_{m-1}}{\rho_m}$$

There will be n-1 of these equations in the case of n links or n+1 layers. Although they are approximate, they hold quite closely. If the two members of an equation differ by a two to one ratio after numerical values have been substituted, the nature of the inequality is helpful in deciding which depths or resistivities are probably too large or too small. If the members differ by ratios of five or ten to one, it may be advisable to change the interpretation.

The procedure is illustrated in the following examples.

Example VI. The curve obtained at Test Point #1 near Victorville is shown in Figure 32. The first link is unreliable because the point for which L = 18 feet may be affected by the finite size of the electrodes, and because the points at L values of 39, 45, and 51 feet are close to the turning point and appreciably influenced by the third layer. Only one good fit was obtained using the first three points, and this gives the values $k_1 = -0.35$, $\rho_1 = 9600$ ohm-centimeters, $h_1 = 5.1$ feet and ρ_2 is then computed to be 4630 ohm-centimeters.

The second link is more reliable. All five points fit quite closely Paletca curves for two values of k.

1. $k_2 = 0.7$, $\rho' = 4300$ ohm-cm. , $h_2 = 15.8$ feet
2. $k_2 = 0.8$, $\rho' = 2200$ ohm-cm. , $h_2 = 7$ feet

Since k is large, the best value of h_2 may be taken as that nearest 3/8 the value of L at the bend, or 3/8 of 45 feet which is 16.9 feet. The first fit is therefore the more probable and from this ρ_3 is computed to be 24,400 ohm-centimeters.

A break in the slope of the second link can be seen at L = 90 feet. If this is interpreted as indicating the presence

Figure 33. Example VI, Paletca method: Dashed line is ρ_a, L curve from Test Point no. 1 near Victorville fitted into the appropriate set of Wetzel-McMurry 3-layer master curves by the values of ρ_1 and h_2 determined from the Paletca curves.

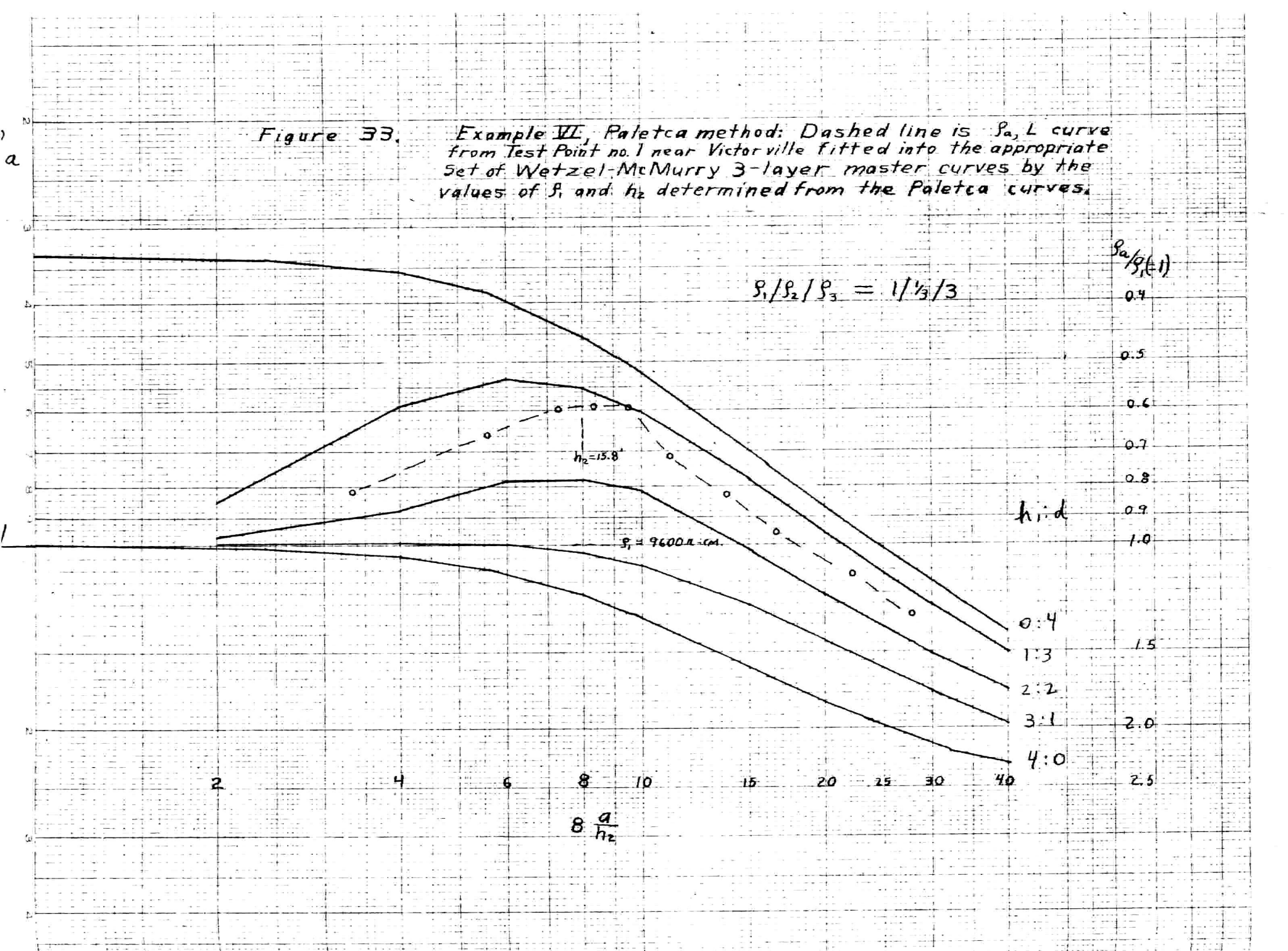

of a fourth layer, each sublink can be interpreted separately but this is poor practise. In the first place, a change in the apparent resistivity at the 90 foot spacing of 1%, which is well within the range of error of field measurements would remove the break entirely. Secondly, if the break is real, it is so slight that the ratio of resistivities above and below the interface is nearly unity and the discontinuity is not important. Thirdly, in this case it replaces one reliable 5 point link with two less reliable 3 point links. However, if the link is subdivided and the best fit chosen by the three-eighths rule, the depth h_2 is found to be about 17 feet, and a third layer 17 feet thick of 37000 ohm-centimeter resistivity to overlie a basement of 39000 ohm-centimeters. The difference in the resistivity determined for the basement in the two interpretations illustrates the difficulty of accurately determining the resistivity of the lower layer when k is large. When |k| is near 1.0, an error in determining the effective upper resistivity is multiplied many times in computing that of the lower layer, and also an error in determining k has greatest effect when k is nearly plus or minus one.

Application of Hummel's formula

$$\frac{h_2}{\rho'} = \frac{h_1}{\rho_1} + \frac{h_2 - h_1}{\rho_2} \quad \text{OR} \quad \frac{15.8}{4300} = \frac{5.1}{9600} + \frac{10.7}{4630}$$

results in the slight inequality 0.00368 = 0.00285 which indicates that the three layer interpretation is sufficiently good. Taking the values h_1 = 5.1 feet, h_2 = 15.8 feet, ρ_1 = 9600 ohm-cm., ρ_2 = 4630 ohm-cm., and ρ_3 = 24,400 ohm-cm., we find $\rho_1/\rho_2/\rho_3 = 1/0.482/2.54$ and can compare the curve with the theoretical three-layer family for 1/(1/3)/3. Figure 33 shows the field curve fitted into the family, oriented by the values of h_2 and ρ_1 determined by the Paletca method. It shows an excellent agreement in shape and size with the master curves, and in the indicated ratio of h_1/d ($d = h_2 - h_1$) which agrees well with the Paletca figure of 1.3/2.7. The maximum deviation from the theoretical curves is seen at the bend.

The value for h_2 of 15.8 feet agrees very well with the 16 feet measured with a steel tape in an adjacent road cut.

Example VII. Curve 3 shown in Figure 34 contains too few points to be reliable. The first three points, corresponding to L values of 30, 60, and 120 feet , may indicate the presence of three layers above the basement. It might also be that the apparent resistivity at the 30 foot spacing is too small from the effect of watering the electrodes, or that the 60 foot value is large because of irregularities in the top surface of the granite. For simplicity we will assume a three layer solution, ignoring the value at the 30 foot spread. The slope of the link between the 60 and 120 foot points is small so the depth to the second layer is about (3/8 x 80) 30 feet. Moving the field curve until the link fits one of the Paletca curves with the L = 30 feet ordinate placed over that for L/h = 1, we find an approximate value $k_1 = -0.35$.

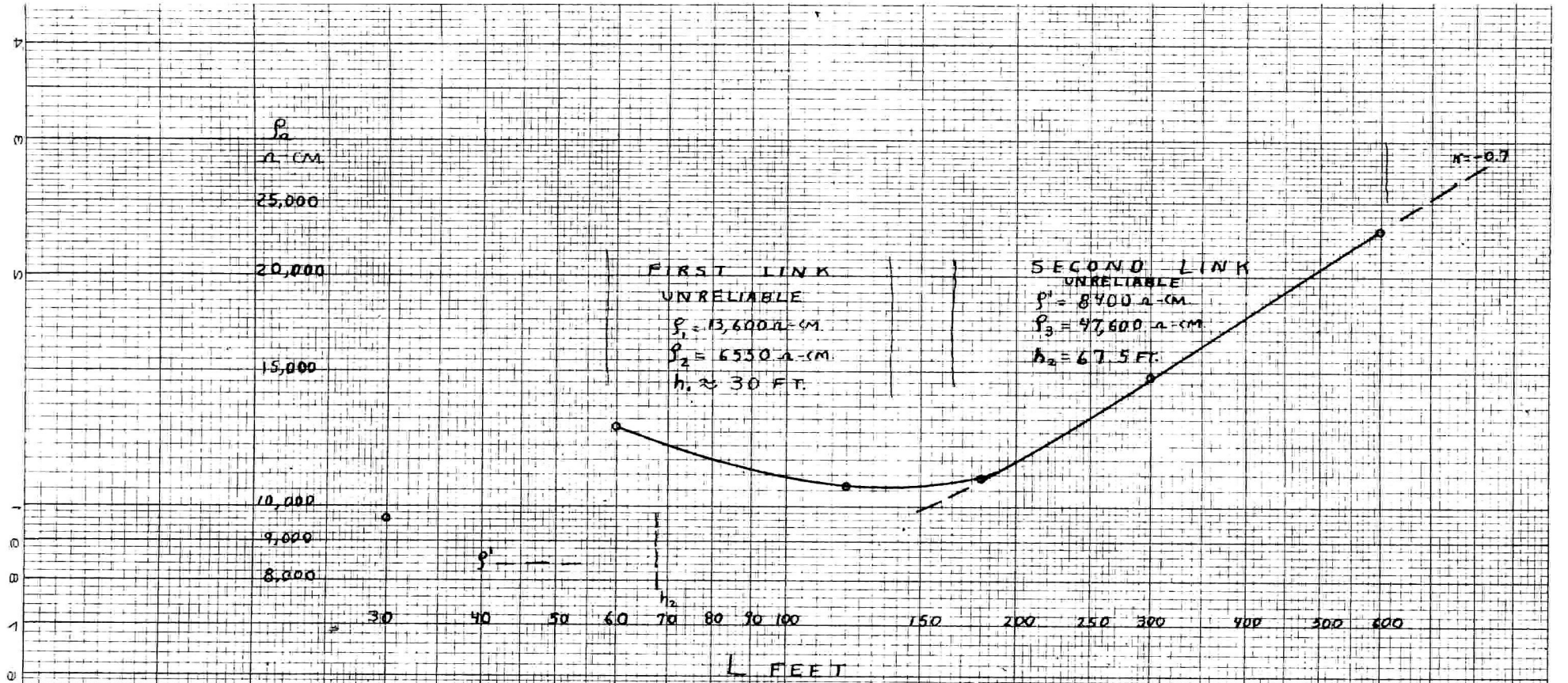

Figure 34. Example VII, Paletca method: interpretation of ρ_a, L data. Curve B, obtained near Victorville, California.

ρ_1 is 13,600 and ρ_2 6550 ohm-centimeters. The second link is more satisfactory, but still not very reliable because it has only three points of which one is near the bend. This link fits best at $k_2 = 0.7$, $\rho' = 8400$ ohm-cm., $\rho_3 = 47{,}600$ ohm-cm., $h_2 = 67.5'$. This value of h is 3/8 of 180 and that value of L is near the bend in the field curve so that h_2 is of the right order of magnitude. Application of Hummel's rule gives 0.0083=0.0079 which shows the fit is all right. For further check the curve was compared to the closest corresponding three-layer family which again is 1/(1/3)/3. In this case the fit determined by the Paleteca values didn't check so well, but this is not surprising when it is remembered that the resistivity ratios are somewhat different, that the values for ρ_1 and h_1 cannot be considered reliable, and that h_2 may easily be in error by 10%. When an attempt was made to fit the curve to the three-layer family independently, it was found that the master curves are so far apart that there is a considerable range of values of h_2 and ρ_1 for which a fit can be made. Certainly the failure to agree with the three layer curves is not sufficient reason to change the interpretation.

Example VIII. Curve 4 is illustrated in Figure 35. The first link fits very nicely for the five points from L = 30 to 105 feet, giving the values $k_1 = -0.3$, $\rho_1 = 19{,}200$ ohm-cm., $\rho_2 = 10{,}330$ ohm-cm. and $h_1 = 12$ feet. Interpretation of the middle part of the curve is hazardous. There is apparently a third layer of low resistivity above the granite, but there are too few points on this link. Of the three, those at L = 105 feet and L = 225 feet are on turning points, and the former is also included in the first link. The slope of the link between the points L = 225 and L = 300 feet is steeper than is possible if the layers are horizontal. To get a tentative solution, the point at the 225 foot spacing was ignored, and h_2 was taken as 40 feet (3/8 x 105). Using this value of h_2, k_2 was found to be -0.7, and ρ' to be 15000 ohm-centimeters. The last part of the curve appears to break in slope at the 450 foot spacing, but the break is too small to bother with. Within the limits of error in determining apparent resistivity, the third link fits nicely for $k_3 = 0.8$, $\rho'' = 5500$, $h_2 = 58$ feet. This value of h corresponds to L = 155 feet at the bend , which is not unreasonable when the point at the 225 foot spacing is cast out. Substituting the values in Hummel's formula gives for the first two layers 0.00267 = 0.00333, and for the first three layers 0.01053 = 0.01012 which is surprisingly good agreement. However, the interpretation should not be considered reliable.

Example IX. Curve 5 taken near Victorville is shown in Figure 36. Here the first link is unreliable because there are only two points sufficiently far from the bend. K appears to be large, but since the value of L at the first turning point is not known, the three-eighths rule cannot be applied. However the second link is more reliable. It fits the Paleteca curve

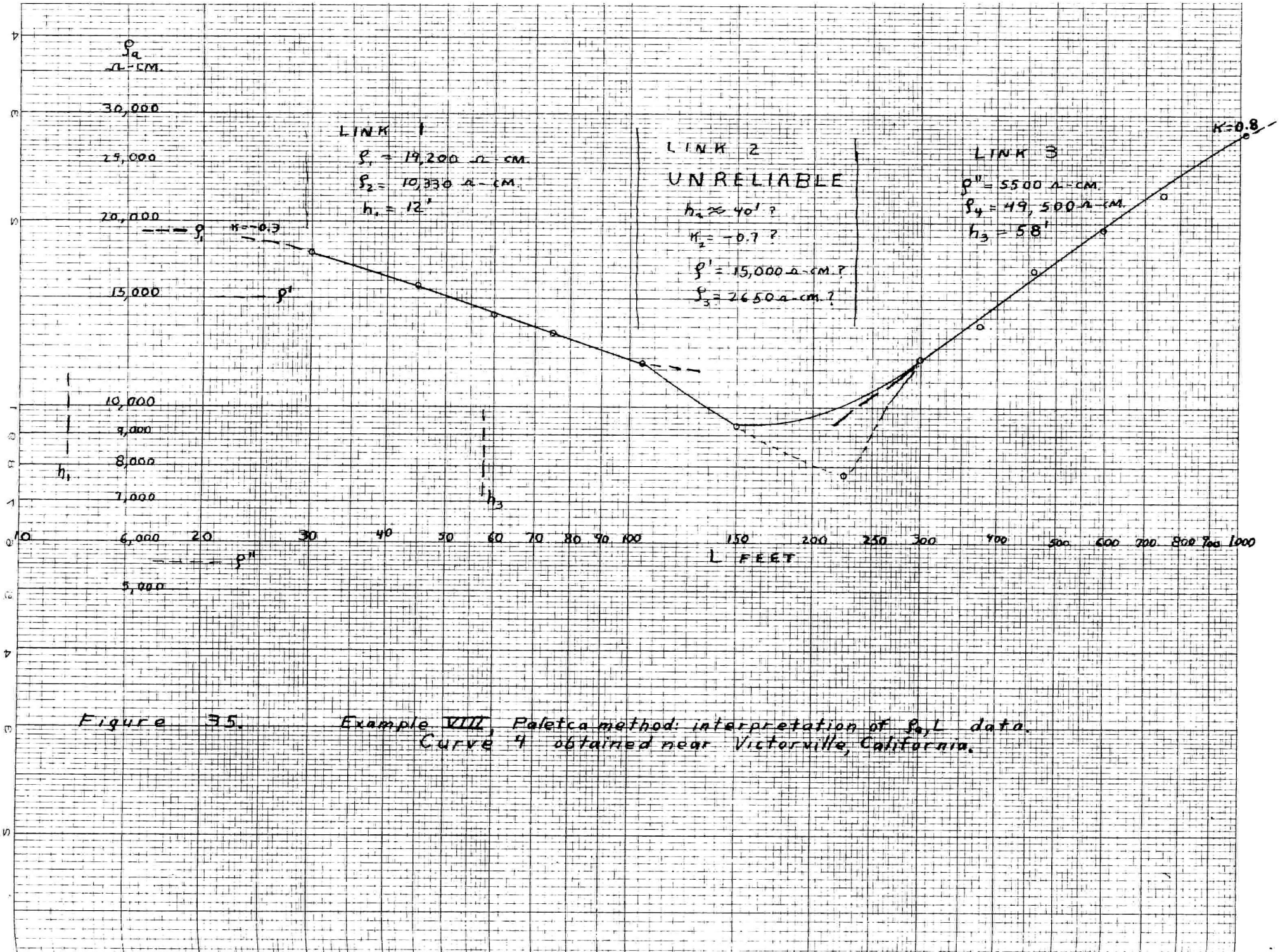

Figure 35. Example VIII, Poletca method: interpretation of ρ_a, L data. Curve 4 obtained near Victorville, California.

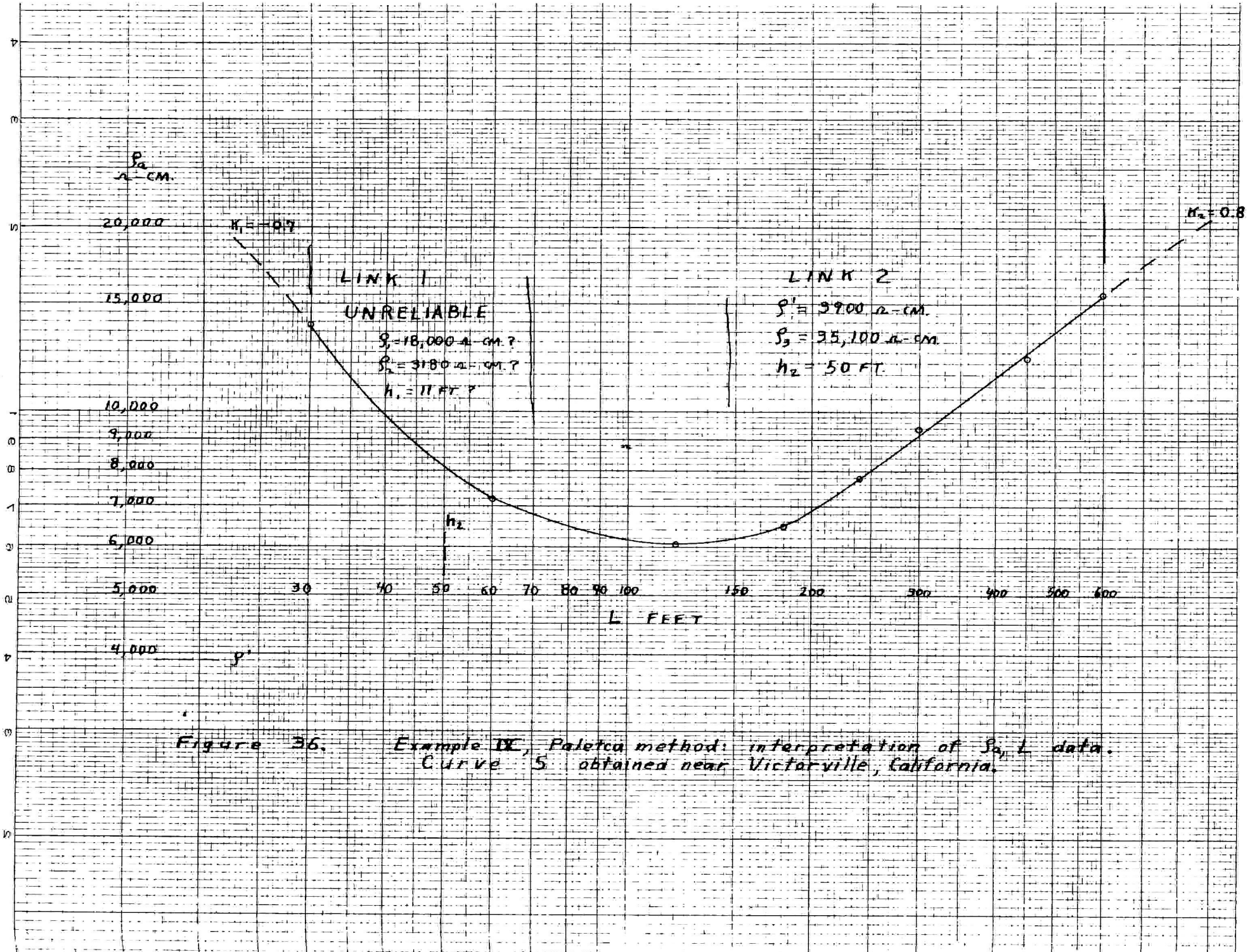

Figure 36. Example IX, Paletca method: interpretation of ρ_a, L data. Curve 5 obtained near Victorville, California.

for k=0.8 quite well for values of h_2 from 50 to 73 feet. Of these the lower limit is closest to the 45 feet given by the three-eighths rule. As a check, seven possible fits of the first two points of the first link were tried with three possible fits of the second link in different combinations to see which agreed best with Hummel's formula. The fits giving the decidedly closest check (0.01282=0.01328) are ρ_1 = 18000 a-cm, h_1 = 11 feet, k_1 = -0.7, ρ_2 = 3180 ohm-cm., and ρ' = 3900 ohm-cm., h_2 = 50 feet, k_2 = 0.8, ρ_3 = 35,100 ohm-cm.

Two comments may be made on these examples. First, they show the supreme importance of having reliable field curves. To ensure good values, the data should be plotted on logarithmic paper in the field, and any ambiguities removed by repeating observations or taking intermediate spacings. Second, it should be noted that the depths and resistivities are expressed in more precise numbers than is justified by the accuracy of the method. Even with good data, and careful use of the Paletca curves, an error of 10% may be expected in the depth determinations. The exact values were given to enable the reader to see the fit which appeared best to the writer. It is usual for interpretations to vary a few percent according to the individual.

The methods of interpreting the apparent resistivity-electrode separation curves discussed in this chapter all assume that the layers are horizontal. If links steeper than the Paletca curves for k equals plus or minus one are found, and if there is no error in the field measurements, some other distribution of resistivities is indicated. Some idea of the nature of the irregularity may be had by running depth profiles in several azimuths about a common spread center.

For layers with dips of less than thirty degrees, satisfactory results can be obtained if the line of electrodes is kept parallel to the strike of the beds. For steeper dips it is advisable to discard the use of depth profiles and use surface traverse profiles with a constant electrode separation and a moving spread center.

Bibliography

The following list of references is intended to enable the reader more easily to find some of the more important papers on direct current measurement of earth resistivity. As only a small part of the total literature could be included, preference was given to sources most apt to be available, and to articles in English. Contributions to interpretation of resistivity data, and descriptions of the main types of apparatus are quite completely covered, and discussions of applications to particular areas, while only a small part of the whole, are representative.

For a more exhaustive list the reader is advised to consult the Geophysical Abstracts published monthly by the U.S. Bureau of Mines through June 1936, and indexes of leading mining, engineering, petroleum, and geological periodicals.

Barus, Carl, On the electrical activity of ore bodies: U. S. Geol. Survey Mon. III (Becker, G. F., Geology of the Comstock lode) Chapter X, pp. 309 - 367, 1882.

Broughton Edge, A. B. and Laby, T. H., Principles and practice of geophysical prospecting (report of Imperial Geophysical Experimental Survey), Cambridge University Press, 1931.

Bruckshaw, J. M. and Dixey, F., Ground water investigations by geophysical methods: Mining Magazine, Vol. 50, No. 2 pp. 73 - 84, and No. 3., pp. 147 - 154, Feb. and Mar. 1934.

Crosby, I. B. and Leonardon, E. G., Electrical prospecting applied to foundation problems: A. I. M. E. Geophysical Prospecting 1929, pp. 199 - 211.

Ehrenburg, D. O. and Watson, R. J., Mathematical theory of electrical flow in stratified media with horizontal, homogeneous, and isotropic layers: A. I. M. E. Geophysical Prospecting 1932, pp. 423 - 438.

Eve, A. S. and Keys, D. A., Applied geophysics, 3d. ed., Chapter 3, Cambridge University Press, 1938.

Evjen, H. M., Depth factors and resolving power of electrical measurements: Geophysics, Vol. 3, No. 2, pp. 78 - 95, March 1938.

Fritsch, Volker, Der Einfluss des Wassergehaltes auf den Widerstand geologischer Leiter: Elektrotechnische Zeitschrift, 58 Jahrg., Heft 12, (Vol. 58, Pt I) pp. 319 - 320, Berlin, March 25, 1937.

Gilchrist, L., Geophysical investigations made in 1930: Canada Geol. Survey, Mem. 170 Pt. II, pp. 65 - 98, 1932.

Gish, O. H. and Rooney, W. J., Measurement of resistivity of large masses of undisturbed earth: Terr. Mag. and Atmosph. Electricity, Vol. XXX, pp. 161 - 188, 1925.

Hawkins, R. H., Application of resistivity methods to Northern Ontario lignite deposits: A. I. M. E. Geophysical Prospecting 1934, pp. 76 - 120.

Hedstrom, Helmar, Electrical prospecting for auriferous quartz veins and reefs: Mining Magazine, Vol. 46, No. 4, pp. 201 - 213, April 1932.

Hopper, R. H. and Jakosky, J. J., The effects of moisture on the direct current resistivities of oil sands and rocks: Geophysics, Vol. 2, No. 1, pp. 33 - 55, Jan. 1937.

Hotchkiss, W. O., Rooney, W. J., and Fisher, James, Earth resistivity measurements in the Lake Superior copper country: A. I. M. E. Geophysical Prospecting 1929, pp. 51 - 65.

Hubbert, M. K., Results of resistivity survey on various geologic structures in Illinois: A. I. M. E. Geophysical Prospecting 1934, pp. 9 - 29.

Hubbert, M. K. and Weller, J. M., Location of faults in Hardin County, Illinois, by the earth-resistivity method: A. I. M. E. Geophysical Prospecting 1934, pp. 40 - 47.

Hummel, J. N., A theoretical study of apparent resistivity in surface potential methods: A. I. M. E. Geophysical Prospecting 1932, pp.392 - 422.

Jakosky, J. J., Continuous electrical profiling: Geophysics Vol. 3, No. 2, pp. 130 - 153, March 1938.

Karcher, J. C. and McDermott, E., Deep electrical prospecting: A. A. P. G. Bull. Vol. 19, Pt. I, pp. 64 - 77, Jan. 1935.

Kurtenacher, K. S., Some practical applications of resistivity-measurements to highway problems: A. I. M. E. Geophysical Prospecting 1934, pp. 49 - 59.

Lancaster-Jones, E., The earth-resistivity method of electrical prospecting: Mining Magazine, Vol. 42, No. 6 pp. 352 - 355, and Vol. 43, No. 1, pp. 19 - 29, June and July 1930.

Lee, F. W., Measuring the variation of ground resistivity with a megger: U. S. Bur. Mines Tech. Paper 440, 1928.

Lee, F. W., Geophysical prospecting for underground waters in desert areas: U. S. Bur. Mines, Info. Circ. 6899, August 1936.

Lee, F. W. and Swartz, J. H., Resistivity measurements of oil bearing beds: U. S. Bur. Mines Tech. Paper 488, 1930.

Leonardon, E. G. and Kelly, S. F., Some applications of potential methods to structural studies: A. I. M. E. Geophysical Prospecting 1929, pp. 180 - 199.

Low, Bela, Kelly, S. F., and Creagmile, W. B., Applying the megger ground tester in electrical exploration: A. I. M. E. Geophysical Prospecting 1932, pp. 114 - 125.

Lugeon, M. and Schlumberger, C., The electrical study of dam formations, Mining Magazine, Vol. 48, No.6, pp. 340 - 345, June 1933.

Muskat, Morris, Potential distribution about an electrode on the surface of the earth: Physics, 4, pp. 129 - 147, 1933.

Ollendorf, Franz, Erdstrome, Berlin, Springer, 1928.

Pirson, S. J., Interpretation of three-layer resistivity curves: A. I. M. E. Geophysical Prospecting 1934, pp. 148 - 158.

Pirson, S. J., Effect of anisotropy on apparent resistivity curvescurves: A. A. P. G. Bull. Vol. 19, Pt. I, pp. 37-57, 1935.

Poldini, E., Geophysical exploration by spontaneous polarization methods: Mining Magazine, Vol. 59, No. 5 (Nov.) pp. 278 - 282, No. 6 (Dec.) pp. 347 - 352, 1938, and Vol. 60, No. 1, pp. 22 - 27, No. 2, pp. 90 - 94, Jan. and Feb. 1939.

Potter, E. V., Results of electrical resistivity and electrical induction measurements at Abana Mine, Quebec, Canada: U. S. Bur. Mines Tech. Paper 501, 1931.

Roman, Irwin, How to compute tables for determining electrical resistivity of underlying beds and their application to geophysical problems: U. S. Bur. Mines Tech. Paper 502, 44 pp., 1931.

Roman, Irwin, Some interpretations of earth resistivity data: A. I. M. E. Geophysical Prospecting 1934, pp. 183 - 197.

Rust, W. M., Jr., A historical review of electrical prospecting methods: Geophysics, Vol. 3, No. 1, pp. 1 - 6, January 1938.

Sayre, A. N. and Stephenson, E. L., The use of resistivity-methods in the location of salt-water bodies in the El Paso, Texas, area: Nat. Research Council, Am. Geophys. Union Trans. 1937, Pt. II, pp. 393 - 398.

Slichter, L. B., The interpretation of the resistivity prospecting method for horizontal structures: Physics, 4, pp. 307 - 322, 1933.

Schlumberger, C. and M., The method of the ground resistivity map and its practical applications: Canadian Min. and Met. Bull. 226, pp. 271 - 294, Feb. 1931.

Schlumberger, C. and M., and Leonardon, E. G., Electrical exploration of water covered areas: A. I. M. E. Geophysical Prospecting 1934, pp. 122 - 134.

Schlumberger, C. and M., and Leonardon, E. G., Some observations concerning electrical measurements in anisotropic media and their interpretation: A. I. M. E. Geophysical Prospecting 1934, pp. 159 - 181.

Schlumberger, C. and M., and Leonardon, E. G., Electrical coring; a method of determining bottom-hole data by electrical measurements: A. I. M. E. Geophysical Prospecting 1934, pp. 237 - 272.

Shepard, E. R., Subsurface exploration by earth-resistivity and seismic methods: Nat. Research Council, Am. Geophys. Union Trans. 1935, Pt. I, pp. 78 - 85.

Stefanesco, E., Schlumberger, M. and C., Sur la distribution electrique potentielle autour d'une prise de terre ponctuelle dans un terrain a couches horizontales, homogenes, et isotropes: Jour. de Physique et Radium, Serie VII, Tome I, No. 4, pp. 132 - 140, April 1930.

Sundberg, Karl, Effect of impregnating waters on electrical conductivity of soils and rocks: A. I. M. E. Geophysical Prospecting 1932, pp. 367 - 391.

Swartz, J. H., Artificial measurements upon artificial beds: U. S. Bur. Mines Info. Circ. 6445, 9 pp., Feb. 1931.

Swartz, J. H., Oil prospecting in Kentucky by resistivity methods: U. S. Bur. Mines Tech. Paper 521, 23 pp., 1932.

Tagg, G. F., The earth resistivity method of geophysical prospecting. Some theoretical considerations: Mining Magazine, Vol. 43, No. 3, pp. 150 - 158, Sept. 1930.

Tagg, G. F., Interpretation of resistivity measurements: A. I. M. E. Geophysical Prospecting 1934, pp. 135 - 145.

Tagg, G. F., Earth-resistivity surveying: Mining Magazine, Vol. 53, No. 3, pp. 148 - 154, Sept. 1935.

Watson, R. J., A contribution to the theory of the interpretation of resistivity measurements obtained from surface potential observations: A. I. M. E. Geophysical Prospecting 1934, pp. 201 - 232.

Watson, R. J., and Johnson, J. F., On the extension of two-layer methods of interpretation of earth resistivity data to three and more layers: Geophysics, Vol. 3, No. 1, pp. 7 - 21, January 1938.

Wenner, Frank, A method of measuring earth resistivity: U. S. Bur. Standards Bull. 258 (Vol. 12, No. 4), 1916.

Wetzel, W. W. and McMurry, H. V., A set of curves to assist in the interpretation of the three layer resistivity problem: Geophysics, Vol. 2, No. 4, pp. 329 - 341, Oct. 1937.

Plate I. Diagram of circuit used in measuring resistivity.

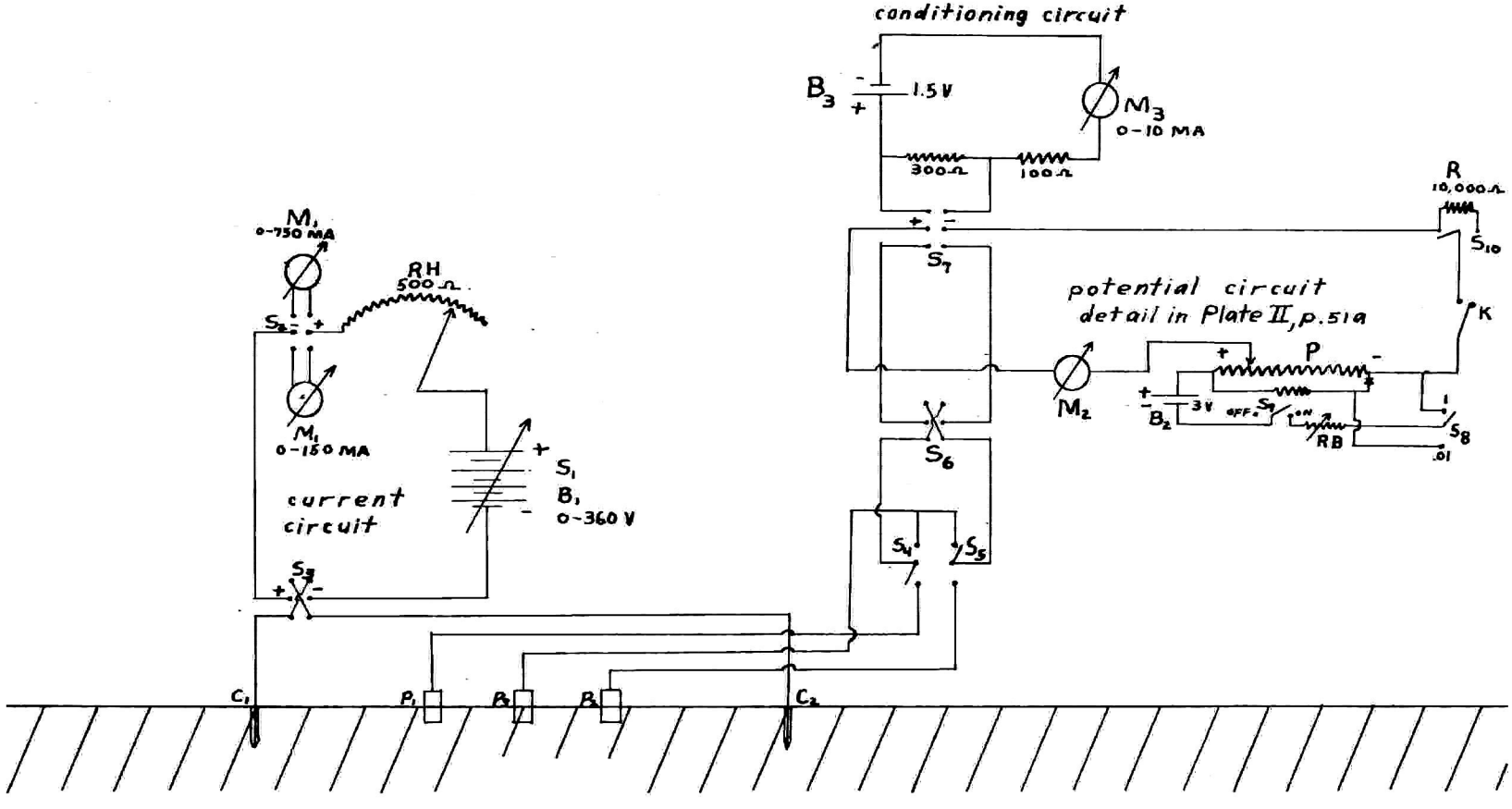

PLATE VII

DOOLITTLE – "EARTH RESISTIVITY"

$\left(\frac{S}{S_1}\right)$

"Paletca"

$\left(\log \frac{S}{S_1}, \log \frac{L}{h}\right)$

K = 1.0
K = 0.9
K = 0.8
K = 0.7
K = 0.6
K = 0.5
K = 0.4
K = 0.3
K = 0.2
K = 0.1
K = −0.1
K = −0.2
K = −0.3
K = −0.4
K = −0.5
K = −0.6
K = −0.7
K = −0.8
K = −0.9
K = −1.0

$\left(\frac{L}{h}\right)$

10 9 8 7 6 5 4 3 2 1 0.9 0.8 0.7 0.6 0.5 0.4 0.3 0.2 0.2 0.1

1 2 3 4 5 6 7 8 9 10 20 30 40 50 60 70 80 90 100 200 300 400

DOOLITTLE-RESISTIVITY

PLATE VIII

$\rho_1 > \rho_2$

$\frac{\rho_a}{\rho_1}$

K
1.0
0.975
0.95
0.925
0.9
0.875
0.85
0.825
0.8
0.775
0.75
0.725
0.7
0.675
0.65
0.625
0.6
0.575
0.55
0.525
0.5
0.475
0.45
0.425
0.4
0.375
0.35
0.325
0.3
0.275
0.25
0.225
0.2
0.175
0.15
0.125
0.1

0.003 0.004 0.005 0.006 0.007 0.008 0.009 0.01 0.02 0.03 0.04 0.05 0.06 0.07 0.08 0.09 0.1 0.2 0.3 0.4 0.5 0.6 0.7 0.8 0.9 1.0

0.1 0.2 0.3 0.4 0.5 0.6 0.7 0.8 0.9 1.0 2.0 3.0 4.0 5.0

$\frac{a}{h}$

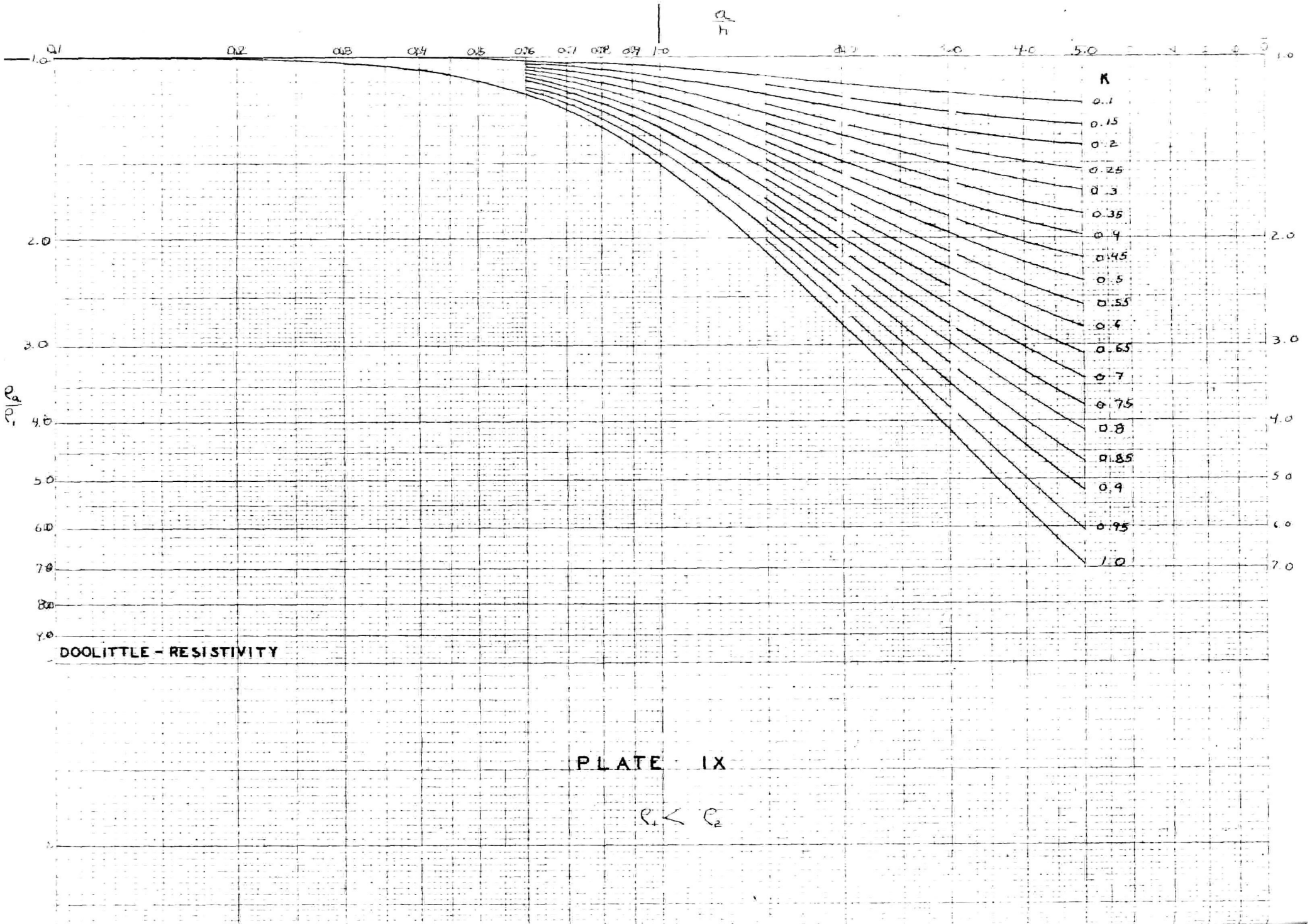

PLATE IX

$\rho_1 < \rho_2$